PROTOCOL

https://doi.org/10.1038/s41596-022-00796-2



1

Design and construction of a microfluidics workstation for high-throughput multi-wavelength fluorescence and transmittance activated droplet analysis and sorting

Jatin Panwar^{1,2,3}, Alexis Autour^{1,2,3} and Christoph A. Merten¹

Droplet microfluidics has revolutionized quantitative high-throughput bioassays and screening, especially in the field of single-cell analysis where applications include cell characterization, antibody discovery and directed evolution. However, droplet microfluidic platforms capable of phenotypic, fluorescence-based readouts and sorting are still mostly found in specialized labs, because their setup is complex. Complementary to conventional FACS, microfluidic droplet sorters allow the screening of cell libraries for secreted factors, or even for the effects of secreted or surface-displayed factors on a second cell type. Furthermore, they also enable PCR-activated droplet sorting for the isolation of genetic material harboring specific markers. In this protocol, we provide a detailed step-by-step guide for the construction of a high-throughput droplet analyzer and sorter, which can be accomplished in -45 working hours by nonspecialists. The resulting instrument is equipped with three lasers to excite the fluorophores in droplets and photosensors that acquire fluorescence signals in the blue (425-465 nm), green (505-545 nm) and red (580-630 nm) spectrum. This instrument also allows transmittance-activated droplet sorting by analyzing the brightfield light intensity transmitting through the droplets. The setup is validated by sorting droplets containing fluorescent beads at 200 Hz with 99.4% accuracy. We show results from an experiment where droplets hosting single cells were sorted on the basis of increased matrix metalloprotease activity as an application of our workstation in single-cell molecular biology, e.g., to analyze molecular determinants of cancer metastasis.

Introduction

Single-cell screening is an essential initial methodological step for answering many biological questions especially in genomic, transcriptomic or proteomic applications¹. Droplet microfluidics has emerged as reliable choice for single-cell assays^{2,3}, by allowing the generation of monodispersed droplets of small volumes (10⁻⁹-10⁻¹⁵ liters (ref. ⁴)) at high frequencies, reaching up to a few million droplets per hour (ref. 5). These sizes and rates of formation enable single-cell encapsulation with each droplet being its own compartment (comparable to a miniaturized microtiter plate well). By changing the droplet matrix, single cells can be encapsulated with other molecules/barcoded beads or even a second cell type (for probing interactions) making each droplet a microreactor and allowing high-throughput screening of these reactions. Such screening methods are commonly used in antibody or drug discovery experiments to sort cells secreting antibodies^{6,7} that either have inhibitory effects on enzymatic drug targets⁸ or bind to a second, co-encapsulated target cell⁹⁻¹². These methods can also be helpful in deciphering cellular heterogeneity for example by screening single cells with distinct cytokine secretion levels¹³. In the field of directed evolution, droplet sorting has enabled the selection of enzyme variants with 10-30 times higher catalytic activity¹⁴ and of aptamers with customized properties for imaging cellular RNAs^{15,16}. Other applications include microbiome studies to detect and sort rare microbes inside a population ^{17,18} and to discover new promiscuous enzymes ¹⁹. Overall, droplet-microfluidics-based single-cell screening gains remarkable momentum in the life science domain.

¹Institute of Bioengineering, School of Engineering, École Polytechnique Fédérale de Lausanne (EPFL), Lausanne, Switzerland. ²European Molecular Biology Laboratory (EMBL), Heidelberg, Germany. ³These authors contributed equally: Jatin Panwar, Alexis Autour. [⊠]e-mail: christoph.merten@epfl.ch

For screening, the droplet microfluidics workflows typically use quantitative readouts based on fluorescence, absorbance/transmittance or imaging signals to infer the droplet composition²⁰, along with high-speed real-time data processing algorithms that detect the 'droplets of interest' and sort them using electrokinetic, acoustophoretic or mechanical methods²¹. The most common configuration of these workflows includes multi-wavelength fluorescence analysis followed by positive dielectrophoretic force-induced droplet sorting, which has been used for a variety of applications^{8,10–12,18,22,23} (Table 1). A workstation capable of such analysis is an integrated network of optical, electrical and computational modules that work in unison to generate, acquire and process data for taking necessary decisions on droplet detection and sorting in real time (Fig. 1). The extent of interdisciplinary expertise required to construct a workstation capable of implementing such microfluidics workflows rarely exists in nonspecialized laboratories. Even though the growing popularity of microfluidics field has given rise to many new commercial manufacturing companies (e.g., Sphere Fluidics, BioRad, Elveflow, Fluidigm and Dolomite), their products do not allow the customization or flexibility (in terms of chip design, excitation wavelengths and other aspects) required by academic labs. Furthermore, no droplet-microfluidics workstation with multichannel fluorescence and transmission analysis is yet available commercially. Existing literature unfortunately does not provide an in-depth description for the construction of microfluidic workstations, but rather focuses on the application 8,10-12,18,22,23 (Table 1).

In our protocol, we intend to bridge this gap and to provide all relevant knowledge to the general scientific community. Our protocol focuses on the hardware, electrical and computational aspects of workstation construction and provides comprehensive instructions along with the resources (e.g., CAD/STL files for assembly parts, details of commercial parts, LabVIEW codes and software installations) to construct and use a workstation, capable of fluorescence- and transmittance-activated droplets sorting. Our approach uses in-house machined parts (CAD files provided) along with some commercially available parts to construct a robust setup. For example, we use machined aluminum blocks as laser supports (while also serving as heat sinks for the lasers) to ensure that the optical plane of the setup stays at a constant height of 9 cm above the surface of the breadboard, to match the height of the microscope's side port, eliminating the need for additional mirrors to guide laser beams to desired height.

For transmittance analysis, we share a method that uses 'droplet lensing induced transmittance amplification', based on the phenomenon that droplets passing through the field of view of a microscope act as physical lenses that converge the brightfield light on the photosensor, resulting in an amplification of the transmittance signal. Thus, contrary to other microfluidic methods for transmittance analysis that require fiberoptic waveguides embedded in the microfluidic device ^{24,25}, our method of transmittance analysis provides discernible transmittance signals using just the brightfield lamp, without the need for modifications of the fluorescence analysis setups or of the microfluidic device. The most important advantage of integrating transmittance analysis with fluorescence analysis is the label-free detection of droplets²⁴ that saves an additional fluorophore that is generally used only for droplet detection application¹⁴. This way, only the fluorescent labels that are essential to identify the phenotypic differences between the droplets are needed for the screening (Table 1).

Comparison with other methods

Phenotypic screening and sorting at single-cell level allows one to elicit and isolate specific functions of interest. Several methods have been developed to accomplish such applications; and each of these has advantages and limitations. This detailed protocol for building a complete droplet-based, phenotypic assay platform provides the flexibility to adapt the technology to custom applications, tailored microfluidic chips and the required overall functionality.

Currently, the leading method for high-throughput phenotypic single-cell analysis and sorting is fluorescence-activated cell sorting (FACS)²⁶. FACS enables high-throughput analysis and sorting of up to several thousand cells per second (~50 kHz), while measuring signals in separate channels for a variety of colours (typically ~5–10) (ref. ²⁷). The method relies on aqueous sheath fluid carrying fluorescently labeled cells that are sorted individually, using electrostatic deflection. Furthermore, the sorted cells can be seeded into microtiter plates for downstream applications. Nonetheless, conventional FACS screening can be performed only with solid particles such as cells. Therefore, it is typically not suited for the analysis of secreted factors or the effects of cell-cell interactions. To overcome these limitations, two specific methods have been implemented, enabling the combination

Table 1 Comparison of various droplet microfluidic pl	et microfluidic pl		he literature and their com	atforms described in the literature and their compatibility with the workstation described in the current protocol	rent protocol
Short experimental description (ref.)	Excitation lines (nm)	Emission lines (nm)	Throughput and droplet size (pL) ^a	Fluorescent assays (excitation/emission peaks in nm)	Compatibility
Current protocol	1: 405 nm 2: 473 nm 3: 561 nm or Brightfield	1: 445 ± 22.5 nm 2: 525 ± 22.5 nm 3: 605 ± 25 nm	100-200 Hz -140 pL	Ch1: Blue FluoSpheres (365/415 nm) Ch2: Dragon Green beads (480/520 nm) Ch3: transmittance for droplet detection (>580 nm) Ch2: MMP FRET Substrate XIV (494/521 nm) Ch3: transmittance for droplet detection (>580 nm)	∀ Z
Single antibody secreting cells screening Hybridoma screening ⁸	1: 488 nm	1: 520 nm	50 Hz 660 pL	Ch1: antibodies inhibiting ACE-1 enzyme activity, fluorogenic substrate - FITC (495/515 nm)	٩
Hybridoma enrichment ²²	1: 488 nm	1: 555 ± 22.5 nm 2: 572 ± 14 nm 3: 697 ± 37.5 nm	200 Hz 50 pL	Ch1: immuno-assay (antibodies DyLight 488 nm conjugated) with hybridomas (9E10) and beads	Ф
Cell pairing sorting ⁹	1: 405 nm 2: 488 nm 3: 561 nm	1: 450 nm 2: 521 nm 3: >610 nm	40 Hz 520 pL	Ch1: cell staining Calcein-violet staining (408/450 nm) Ch2: cell staining with Calcein-AM (495/515 nm)	q
Hybridoma screening targeting a coencapsulated cell sorting $^{\rm D}$	1: 405 nm 2: 488 nm 3: 561 nm	1: 450 nm 2: 521 nm 3: >610 nm	40 Hz 660 pL	Ch1: cell staining CellTrace violet (405/450 nm) Ch2: antibodies IgG Alexa 488 conjugated (490/525 nm)	Ф
Screening B cells binding to soluble antigens or bacteria $^{\rm II}$	1: 405 nm 2: 488 nm 3: 561 nm 4: 635 nm	1: 440 ± 20 nm 2: 525 ± 20 nm 3: 593 ± 23 nm 4: 708 ± 37.5 nm	NA 40-80 pL	Ch1: cell staining Calcein violet (405/450 nm) Ch2: Calcein AM Green (488 nm/520 nm) or antibodies IgG Alexa 488 (490/525 nm) Ch3: pHRodo Red AM Intracellular pH Indicator (560/585 nm) Ch4: AlexaFluor 647 (650/665 nm)	v
Screening antagonist antibodies from a monoclonal cell library ¹²	1: 405 nm 2: 488 nm 3: 561 nm 4: 635 nm	1: 440 ± 20 nm 2: 525 ± 20 nm 3: 593 ± 23 nm 4: 708 ± 37.5 nm	1,000-3,000 Hz 100 pL	Ch1: DY405 dye (400/420 nm) for droplets Ch2: GFP-expressing cell (488/507 nm) Ch3: Yellow CellTrace staining (546/579 nm) Ch4: Antibodies DyLight 650 conjugated (652/672)	v
Directed evolution					
Aldolase activity enhancement ¹⁴	1: 375 nm 2: 488 nm 3: 561 nm	1: 488 ± 10 nm 2: 520 ± 14 nm 3: 609 ± 28.5 nm	500-1,500 Hz 20 pL	Ch2: fluorogenic substrate (488/520 nm) Ch3: Kiton red dye (561/609 nm) for droplet	۵
RNA ribozyme activity-based enhancement ²³	1: 375 nm 2: 488 nm	1: 445 ± 22.5 nm 2: 525 ± 25 nm 3: 600 ± 18.5 nm	300 Hz 20 pL	Ch1: Coumarin dye (387/410 nm) Ch2: Atto488/EvaGreen dye (492/516 nm) Ch3: TexasRed dye (586/603 nm) for droplet	۵
Enzyme screening					
Screening for hydrolases from environmental samples ¹⁹	1: 488 nm	1: 520 nm	2,000 Hz 2-8 pL	Ch1: fluorogenic substrate (488/520 nm)	٩

antroughput is represented in Hz as the number of droplets analyzed per second. Note that throughput highly depends on the architecture of the microfluidic chip rather than on the platform/workstation on which the analysis is done. bWorkstation described in this protocol needs an additional laser and a PMT to adapt to this application (the compatible control software is provided in Supplementary Software 2).

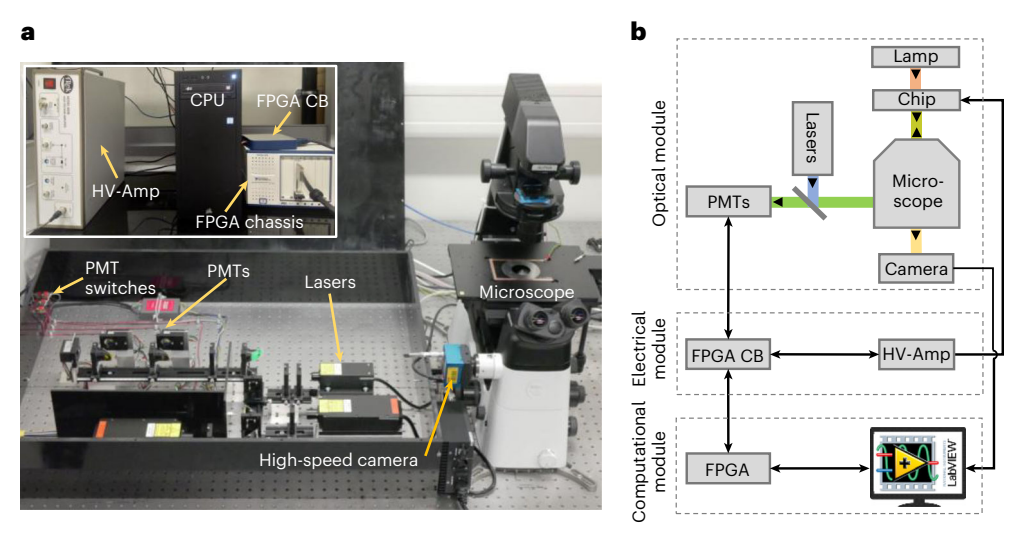


Fig. 1 | Workstation overview. a, Image of the complete workstation showing the microscope with the black box that covers the optical setup and electrical wirings on the breadboard. Inset: image of high-voltage amplifier (HV-Amp), CPU, FPGA connector block (CB) and FPGA chassis (that holds the FPGA card), all kept below the breadboard. **b**, Block diagram of the complete workstation setup with optical, electrical and computational modules. The microfluidic chip is excited by the lasers and the subsequent emission (and transmission from the brightfield lamp) is collected by the PMTs. The data from PMTs are acquired by the FPGA via an FPGA connector block (CB) and analyzed using a LabVIEW interface to detect and sort droplets according to user-defined criteria. Upon successful detection, the FPGA generates a trigger pulse to the high-voltage amplifier, which is used to sort the droplets. The brightfield lamp allows to image the microfluidic chip through a high-speed camera. The whole operation is monitored using a LabVIEW-based interface.

of droplet compartmentalization with FACS sorting. The first method makes use of double emulsions (water-in-oil-in-water droplets) where the carrier phase (water) is compatible with FACS sorting at frequencies of up to 10–15 kHz (ref. ²⁸). The second method involves hydrogel-based emulsions²⁹. In this scenario, with an intermediate step of polymerization of gel in droplets, the oil (carrier phase) of the droplets can be removed and exchanged with FACS sheath fluid for screening^{29,30}. Despite the advantages of combining droplet compartmentalization and high-throughput FACS, double emulsions are prone to droplet merging and also impede complex workflows, especially for droplet manipulation steps such as controlled fusion or pico-injection^{28,31}. These limitations are also valid for hydrogel beads, whose pore size has to be optimized additionally for any given application to prevent analytes of interest from diffusing out of the gel³².

To make fully microfluidic solutions (rather than using FACS instruments for droplet sorting) accessible to the wider public, commercial solutions are emerging. For example, the fully integrated CytoMine platform from Sphere Fluidics enables the screening of large cell libraries (>100,000 variants) at the single-cell level³³. In addition to sorting, individual droplets fulfilling a predefined selection criterion can be seeded into microtiter plates for downstream analysis of recovered cells. However, the setup comprises only one laser line (488 nm) and is therefore not compatible with multiplexed readouts as described in Table 1. Furthermore, it requires the use of chips with predefined geometries and functionalities, which do not provide the flexibility required in academic labs. Lastly, commercial solutions are quite expensive (compared with the setup described here, about five times higher hardware costs) and also create dependencies on specific consumables such as costly disposable chips.

Complementary to commercial solutions, several other academic laboratories have employed droplet microfluidic platforms to perform a broad range of phenotypic assays with varying droplet size and throughput. Their applications include the screening of antibody-secreting single cells, directed evolution and even the screening of environmental samples in metagenomics approaches^{8,10-12,18,22,23} (Table 1). However, the corresponding publications do not provide an adequate description to reconstruct the screening platform that was used. Herein, our in-depth protocol provides a comprehensive step-by-step blueprint to build and operate a droplet-based microfluidics platform that is compatible with these applications (for details on compatibility, see Table 1). Moreover, as we are providing a detailed protocol for a modular and expandable workstation, we anticipate that thoroughly following the protocol would train any researcher well

enough to modify or expand the setup for applications that require different lasers or even new lasers with additional detection channels^{11,12}. To further aid this, we also provide a LabVIEW program that is compatible with such modifications (Supplementary Software 1 and 2) and the housing of the workstation is made large enough to include new optics and lasers (Fig. 1a). All these modifications can also be validated using the same experiment as discussed in this protocol. In addition to fluorescence-induced droplet analysis, our workstation is also capable of transmittance-induced droplet detection. Transmittance (or absorbance) signals provide a label-free quantification method that expands the scope of droplet analysis with a throughput similar to that of fluorescence analysis^{24,34}. Taken together, the platform described here offers maximum flexibility in terms of possible applications and furthermore allows customization and expansion by the user.

Limitations of the protocol

Some limitations of our protocol are the ones that are inherent to any fluorescence-based droplet screening platform ^{10,11,22,35}. The most common among them are possible molecular exchange between droplets (especially for strongly hydrophobic and fluorinated compounds) and droplet coalescence during incubation before sorting ³⁶. While molecular exchange limits the use of certain small molecules (mainly fluorescent dyes like Coumarin and Rhodamine derivates that can be essential for some chemical screens in droplets), it also leads to droplet polydispersity ^{36–38}. Even though the use of specific surfactants may prevent both to a certain extent, they are compromised during long-term incubations ³⁹. Another limitation is the crosstalk between separate fluorescence channels during simultaneous signal acquisition, due to the overlap between emission and excitation spectra of fluorescent probes ⁴⁰. Our setup tries to reduce this crosstalk by using additional bandpass filters to limit the range of emission spectra gathered by the respective photosensors. However, a complete prevention of crosstalk is unavoidable ⁴¹.

Another limitation of the protocol and the resulting workstation is that it can process maximally three signal channels at a time, as it uses only three photosensors. In other words, the workstation can either work with three-channel fluorescence signal acquisition or two-channel fluorescence and one-channel transmittance signal acquisition. Nevertheless, if required, the workstations can be expanded to accommodate additional channels that can be operated using complementary software provided in the resource (Supplementary Software 1 and 2).

A common drawback of all the microfluidics technology that relies on dielectrophoretic force to sort droplets is that it is challenging to find the perfect set parameters for ideal dielectrophoretic field strength within the channel for efficient sorting ⁴². These parameters are the amplitude, frequency and duration of the high-voltage pulse that generates the dielectrophoretic field, as well as the delay between the droplet detection and pulse trigger. Moreover, as these parameters are sensitive to flow rates and droplet sizes, the ideal parameter values for one flow condition may not work as efficiently in another condition. Our workstation inherits the same drawback. Even though we suggest an optimum range of these parameters (Step 183), it is likely that a certain number of trial-and-error experiments are required to get close to 100% sorting efficiency.

Overview of the protocol

In this protocol, we describe the construction of a microfluidic workstation capable of multiplexed fluorescence- and transmittance-activated sorting of droplets (Fig. 1a). The complete workstation comprises optical, electrical and computational modules for data acquisition, data processing and the user interface necessary for droplet sorting (Fig. 1b). All these modules require customized setups to assemble various hardware and software components. In the following sections, we discuss these setups and the associated protocols in detail, to eventually build the workstation using the suggested materials. We also provide the resources necessary to develop and operate the workstation, including the CAD files for hardware machining, 3D printing and microfluidic chip fabrication along with the LabVIEW program for process control. Furthermore, we point the reader to external service companies that could probably manufacture all in-house parts based on our provided design files. In addition to machined and 3D printed parts, a few commercially available components are also modified to fit the setup perfectly. All such machined/3D printed/modified parts have to be prepared before starting the protocol. We have divided the protocol into four parts: (i) assembly layout, (ii) electrical connections, (iii) optical setup and (iv) computational setup.

Assembly layout (Steps 1-29)

We start by assembling the basic skeleton and prepare various components such as PMTs, dichroic mirrors and microscope for installation. All these components, however, are sensitive to physical vibrations and even a slight perturbation in their orientation can impair the optical alignment. Therefore, the setup requires a robust and sufficiently vibration-free support with minimal moving parts. For this reason, the setup is mounted on a breadboard placed on vibration-dampening rubber feet and aluminum blocks are used to support the lasers and other parts (Extended Data Fig. 1). The precisely machined aluminum blocks ensure that the optical plane of the setup stays at a constant height of 9 cm above the surface of the breadboard, to match the height of the microscope's side port. These aluminum blocks also serve as heat sinks for the lasers.

We also roughly mount the microscope on breadboard for initial assembly. We use the left side port of the microscope both for excitation as well as to collect emission signals; therefore, we have to make provisions to split this path so that a fraction of the emission signal can be simultaneously captured by a camera. To allow this, the microscope is pre-equipped with a prism in its side port turret. This prism reflects 80% of the incident ray and transmits the rest. This ensures that 20% of the incident light is directed to the upper side port where a high-speed camera is mounted. Note that this secondary emission beam also contains a considerable fraction of the excitation beam that may saturate the emission signals as read by the camera and would potentially be a hazard if observed via eyepiece. To avoid this, an additional triple band pass filter is placed in the path of this secondary emission beam (F9 in Fig. 2).

Electrical connections (Steps 30-68)

The workstation setup requires a considerable amount of wiring for power supply to the photomultiplier tubes (PMTs) and for the data communication with the computer. Therefore, it is essential to follow a systematic and clean approach for convenient installation, repairs or upgrades. For robust wire connections, the ends of all the wires are crimped and a consistent color code is followed throughout the protocol, especially for the power supply and data communication to avoid misconnections. The subsequent wiring procedure for the power and data communication is described in Steps 30–55. The communication between PMTs and the computational setup for data acquisition is interfaced by a connection block (Fig. 1b). The connection block has multiple pins that are numbered (corresponding to various input/output channels used by the computer) to which the wires are connected as per the pin assignment presented in Table 2. The high-voltage amplifier used to generate the dielectrophoretic force²² for sorting the droplets is also connected to the connection block. Lastly, the breadboard is grounded to provide safety in case of any unwanted contact or leakage of high voltage from the amplifiers or other electrical components mounted on the board. The high-voltage connections and grounding are described in Steps 56–68.

Optical alignment (Steps 69-131)

The primary role of the optical setup is to explicitly excite different fluorophores in the droplets and direct the subsequent emission, or transmission in case of transmittance-based sorting, toward the photosensors (Fig. 2). For excitation, the setup aligns three lasers using an array of dichroic mirrors. The three lasers emit at wavelengths of 405 nm, 473 nm and 561 nm, corresponding to the excitation spectra of fluorophores widely used in bioanalysis, such as cascade blue excited at 405 nm, green fluorescent protein (GFP) or fluorescein (FITC) excited at 473 nm and mCherry protein or Rhodamine Red excited at 561 nm. The combined laser beam is then guided to pass through the microscope's objective lens and intercept the device perpendicularly, where it is focused to create a detection zone. The fluorophores in the droplets get excited as they cross the detection zone and their subsequent fluorescence emission is collected by the objective and is directed outward the same side port. The emission setup then distributes the emission from the droplets in three channels using an array of optical filters and dichroic mirrors (Fig. 2). The emission is eventually collected by the corresponding PMTs that work as photosensors and signal amplifiers. Additional bandpass filters with a narrow bandwidth of 45-50 nm are placed in front of each PMT, reducing the effect of spectral overlap in the emission spectra of the fluorescent dyes and thus, reducing the crosstalk between the three different fluorescence channels. A longpass filter is placed in front of the brightfield lamp to block the wavelengths detected by the PMTs. This filter allows to simultaneously image the setup with a camera without interfering with the fluorescent signals. We first perform the emission light alignment (Steps 69-89) that fixes the position of the microscope on the breadboard, and then the lasers are aligned to complete the optical setup (Steps 89-131).

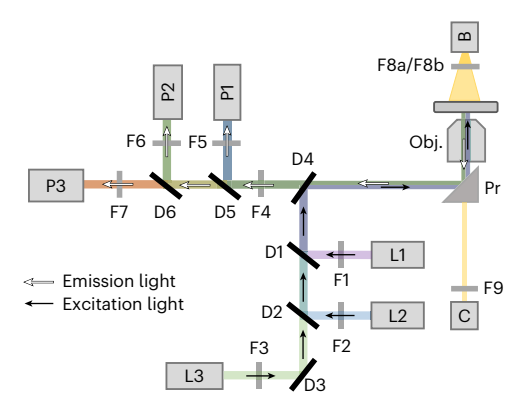


Fig. 2 | Ray diagram. Illustration of the optical path from lasers (L) to PMTs (P) via optical filters (F), dichroic mirrors (D), prism (Pr), brightfield lamp (B) and a high-speed camera (C). During experiment, the chip will be placed on the microscope stage over the objective (Obj.) Lasers: L1, 405 nm; L2, 473 nm; L3, 561 nm. PMTs: P1 and P2, H111903-20; P3, H111903-20. Optical filters: F1, 405/10 nm; F2, 488/6 nm; F3, 563/9 nm; F4 and F9, 405/473/561 nm triple band notch filter; F5, 445/45 nm; F6, 525/45 nm; F7, 605/50 bandpass; F8a, 561 nm longpass; F8b, 633 nm longpass. Dichroic mirrors: D1, 409 nm beam-splitter; D2, 488 nm beam-splitter; D3, full reflective mirror; D4, 403/497/574 triple beam-splitter; D5, 484 nm beam-splitter; D6, 552 nm beam-splitter. Prism: Pr, T-BP E20 L80. Objective lens: Obj, 40× with a working distance of 0.66 mm.

Table 2 | Coordinates of screw positions of all components mounted on the breadboard following the coordinate system defined in Fig. 5a and Extended Data Fig. 2

Component	Coordinates of screw positions (x,y)		
Support block for rail A	(24,11)	(25,11)	
Support block for rail B	(24,6)	(25,6)	
Support block for rail C	(17,3)	(18,3)	
Support block for rail D	(38,14)	(39,14)	
Support block for rail E	(21,26)	(21,25)	
Support block for rail F	(21,7)	(21,8)	
Support block (left) for rail G	(6,14)	(7,14)	
Support block (right) for rail G	(13,14)	(14,14)	
Laser support block L1	(27,13)	(31,13)	
	(27,9)	(31,9)	
Laser support block L2	(28,8)	(32,8)	
	(28,4)	(32,4)	
Laser support block L3	(10,5)	(14,5)	
	(10,1)	(14,1)	
PMT P1	(15,17)		
PMT P2	(9,17)		
PMT P3	(4,15)		
PMT power supply	Positioned along (8,24)	Positioned along (8,24) to (13,28)	
Eight- and three-pin connectors	Positioned along (2,10)	Positioned along (2,10) to (17,10)	

Computational setup (Steps 132-149)

Fluorescence and transmittance activated droplet sorting requires real-time analysis of voltage signals from multiple PMTs, which in turn demands a computational infrastructure with high sampling rates (>50 kHz) and multiparameter parallel processing that is beyond the capacity of desktop computers. To overcome this, the system's capacity is expanded by integrating a field programmable gate array (FPGA) module. A step-by-step guide for FPGA module installation and PC communication can be found online (https://www.ni.com/pdf/manuals/378000b.pdf). After the installation as per Steps 132–145, the connector block is connected to the inlet port of the FPGA module. As the high-speed data acquisition and processing is performed by the FPGA, no high-end computer configuration is

needed. However, the computer should have enough processing power to accommodate the Lab-VIEW 2016 (or higher) runtime environment for running the user interface and displaying live data from the FPGA as well as from a high-speed camera. In addition, we installed a PCI express card on the PC motherboard that communicates with the external FPGA setup. A detailed procedure to install the FPGA card is described in Steps 132–146.

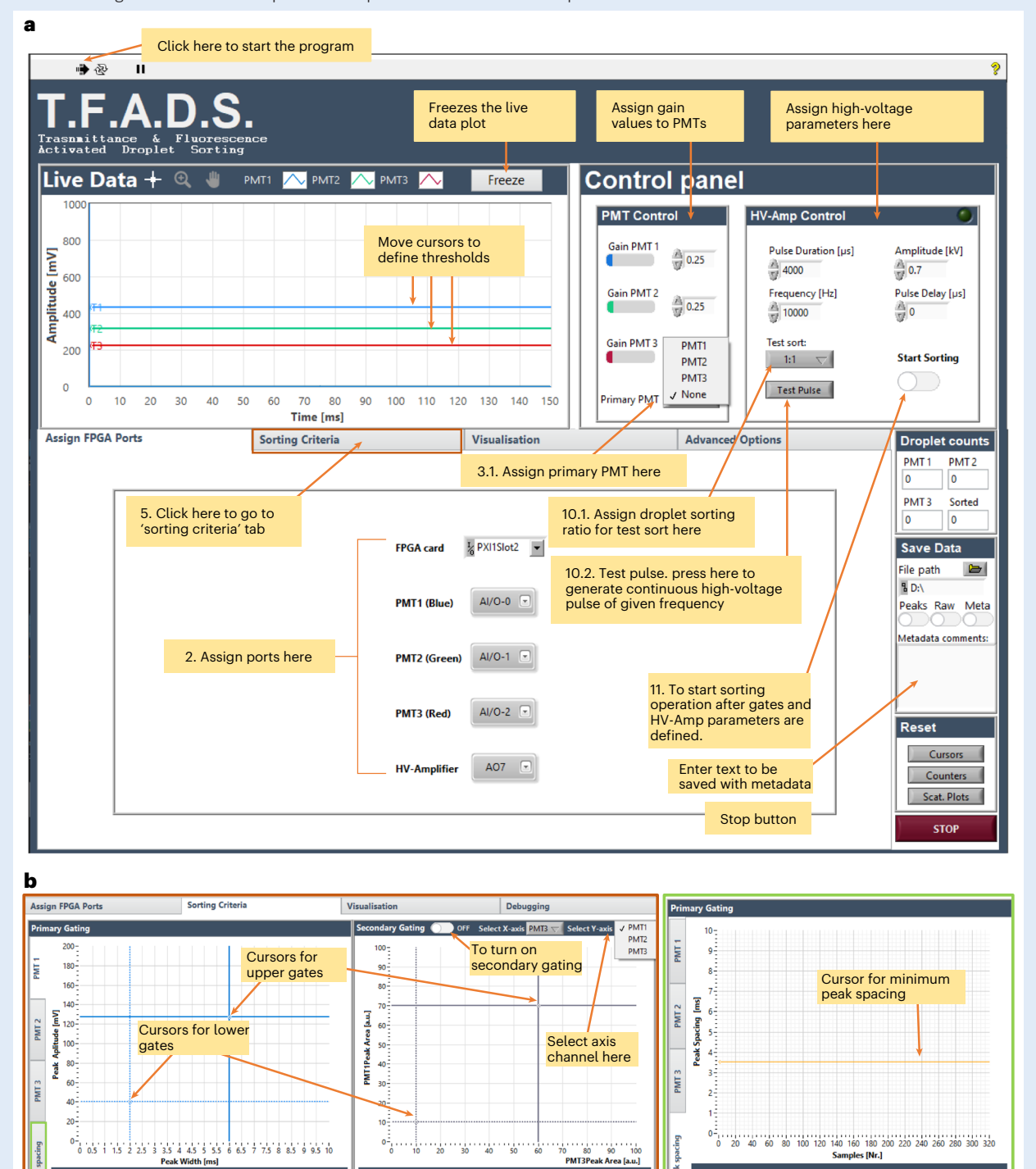
A custom-made program called 'Transmittance and Fluorescence Activated Droplet Sorting or TFADS' is designed in LabVIEW FPGA Module development environment to control the sorting process (Supplementary Software 1). TFADS' algorithm first acquires voltage signals simultaneously from maximally three PMTs that can be assigned to analog input (AI) ports of the FPGA at a rate of 20 MHz (Supplementary Fig. 1). These raw signals are then offset corrected to bring the baseline of all signals close to zero and filtered to discard high-frequency noise (Supplementary Fig. 2). The processed signals can be visualized on the TFADS interface where a threshold can be set to define 'droplet' signals. A complete description of TAFDS user interface is provided in Box 1. On the FPGA end, the filtered signals are checked against the corresponding thresholds. Each continuous signal that traversed into and out of the threshold is considered as a peak that indicates a droplet passing in and out of the detection zone. The FPGA then calculates the peak amplitude, peak width, peak area and the delay between two consecutive peaks (peak spacing). All the calculated parameters are then sent to TFADS, where the user defines the upper and lower limits of peak amplitude, peak width and peak area for each PMT signal. A minimum value of spacing between the peaks is also defined, which helps in getting rid of closely spaced droplets (for example, in case of undesired satellite droplets). A droplet is considered for sorting if it passes all the gates and at its detection. Then a signal is sent to the highvoltage amplifier via FPGA to generate a pulse of user-defined delay, frequency, amplitude and duration that eventually produces the dielectrophoretic force within the microchannels to sort the detected droplet (for TFADS operation, see Box 1).

The algorithm also provides an optional subcase—'Primary PMT mode'—that allows assignment of one of three PMTs as primary. In this mode, the algorithm considers that a droplet is detected in each channel if the droplet is recognized in the primary PMT channel, as per the primary PMT threshold. Note that peak width will be defined only by the primary PMT and thus its values will be same for each PMT. This mode is preferred for experiments where the droplet detection signal is high and consistent in one of the PMT channels while the other signals have high noise and/or variability that makes thresholding and peak detection difficult¹⁰. In such a case, the PMT with consistent signal is assigned as the primary PMT, which allows the processing of signals from the other PMTs without an assigned threshold. Primary PMT mode is also useful when the droplets host multiple particles (cells, beads, etc.). In this mode, the PMT pools all signal intensities from all encapsulated particles as the resulting overall droplet signal. Another interesting application of primary PMT mode is when negative selection or the selection of nonfluorescent entity is required. In this case, the algorithm has to identify and sort the droplets where the entity of interest is missing, which can be made possible by assigning the PMT that provides the signals for droplet detection as the primary PMT. It is to be noted that, for such complex experiments, it is essential to have a biocompatible and inert fluorescent dye dedicated exclusively for droplet detection. Alternatively, our workstation also allows to use droplet transmittance as a readout signal to allow label-free droplet detection.

Transmittance readout is based on principals of refraction of light, where the aqueous droplets (e.g., hosting phosphate-buffered saline or similar aqueous medium) with a high refractive index (~1.33) suspended in fluorinated oil (HFE 7500) with a lower refractive index (~1.28), act as convex lenses (Fig. 3). As a result, when a droplet passes through the field of view of the microscope's objective lens, it converges the overhead brightfield light close to the front focal plane of the objective lens⁴³. Note that, due to the lack of curvature in the PDMS and glass substrates, their effect on the refraction of light is negligible. The objective lens further focuses this transmitted light close to the back focal plane of the microscope. An aperture placed downstream the back focal plane selectively allows this focused transmitted light to pass and to eventually fall on a photosensor (PMT). The photosensor thus detects an increase in the optical signals each time a droplet passes through the detection zone. The optical setup for fluorescence data acquisition and the associated computational architecture that is presented in this protocol is inherently aligned for such a transmittance signal acquisition. The optical path makes sure that the objective lens gathers most of the converged light, while the body of the dichroic mirror mount kept in front of PMT acts as aperture to allow only the transmitted light signals to be acquired by the PMT (Fig. 3). Similar to the fluorescence signals, transmittance signals received from the PMT are also processed for baseline correction, by identifying the low-frequency (<1 Hz) components to measure the offset and then subtracting the measured offset from the signals. The baseline of transmittance signals is thus matched with the baseline of

Box 1 | Quick guide to TFADS operation

TFADS is a custom-made LabVIEW interface that allows the user to analyze the droplets and to control the sorting operation. This interface complements the algorithm discussed in the 'sorting operation' section by providing it with the values for physical inputs (e.g., FPGA ports, PMT gain values and high-voltage amplifier control parameters) and sorting criteria (e.g., thresholding, gating and triggering). The interface has various tabs and windows that are explained in detail below. TFADS operation is also demonstrated in Supplementary Video 4 for a test experiment that aims to sort the green fluorescent droplets from a pool of non-fluorescent droplets.



王 澳 約

To zoom and drag on

the scatter plot

Click to open 'peak

spacing' tab

◆ 田図園

For manual entry of

cursor values

♦ 田河豚

Box 1 | Quick guide to TFADS operation (Continued)

Assign FPGA ports tab: The interface has to be configured once by assigning correct ports for hardware communication, i.e., three input/output ports for the PMTs (input port allows data acquisition from PMT and the corresponding output port provides gain voltage to the same PMT) and one output for triggering the high-voltage amplifier. As per the connection box configuration of our FPGA setup, these ports are AI/O-0 for PMT1 (to acquire the fluorescence signals in 445 ± 22.5 nm range), AI/O-1 for PMT2 (to acquire the fluorescence signals in 525 ± 22.5 nm range), AI/O-2 for PMT3 (to acquire the fluorescence or transmittance signals above 561 nm) and AO-7 for triggering a high-voltage amplifier.

Live data window: The interface has a live-data feed showing various plots of fluorescence signals from the assigned PMTs as per their respective colors (blue for PMT1, green for PMT2 and red for PMT3). When the fluorescent droplets pass over the detection zone in the microfluidic chip, the fluorescence signals on the live feed appear as peaks in the respective color plots. Separate cursors are then used to define the thresholds for each signal and every time the signal crosses this threshold, the program considers it as a droplet signal for that particular channel.

Sorting criteria tab: This tab provides upper and lower limits of droplet parameters to the algorithm as sorting criteria, similar to FACS gating strategies. The tab has two windows called primary gating and secondary gating. There are four plots in the primary gating window; three of these plots corresponds to the individuals PMTs and are used to provide upper and lower gates for peak amplitude and peak width using the two cursors. The fourth plot, named 'Peak spacing', is used to define the minimum spacing between consecutive droplet peaks that can be considered for sorting. When two droplets are close to each other, the algorithm uses this minimum spacing to avoid droplet fusion due to high-voltage pulse or co-sorting of undesired droplets along with the positive droplet. The secondary gating window is optional and can be turned on using the toggle. The plot in the secondary gating window shows the peak area and the cursors here can be used to define the upper and lower limits of peak area for the selected PMT. These plots collectively define the sorting criteria that the algorithm would use to define droplets of interest.

PMT control window: This window allows the user to control PMT gain values and to define the primary PMT if needed. If the peaks are not distinguishable from the noise in the live data feed, the gain values of the PMTs can adjusted to improve the signal intensities (between 0.25 V and 0.6 V). Alternatively, if the signal from a PMT is too noisy to define a threshold, any other PMT with consistent signal can be assigned as primary PMT. **Visualization tab:** To further refine the sorting conditions, the visualization tab provides various options to visualize the droplet signals in various combinations of parameters (peak amplitude, peak width and peak area for each PMT). Even though this option does not allow thresholding, we envisage that a proper visualization of the signal may result in additional critical insights over efficient droplet selection.

HV-Amp control window: To configure HV-amp trigger signal, four parameters are defined in the 'HV-Amp control' window by the user. These parameters are pulse delay, pulse duration, pulse amplitude and pulse frequency.

The pulse delay is the timespan after which the high-voltage amplifier is triggered to generate a high-voltage pulse after the detection of the droplet to be sorted. The pulse delay is required to sort the correct droplet when there is a distance between the detection zone and the sorting junction. In such case, a low pulse delay may result in the sorting of the droplet preceding the droplet of interest while a long pulse delay may result in sorting the droplet that follows the droplet of interest. Typically, the pulse delay is kept between 0 ms and 20 ms.

The pulse duration is the duration for which the high-voltage amplifier provides the pulse to generate the electric field for droplet sorting. Its value should be high enough that the droplet of interest is moved to the collection channel and low enough that the following droplet is not dragged along. Therefore, the pulse duration is kept lower than the average temporal spacing between the droplet peaks, which can be estimated using the minimum peak spacing plot.

The pulse amplitude is the amplitude of the high-voltage pulse that defines the strength of the dielectrophoretic force induced at the sorting junction for droplet sorting. A low amplitude may not generate enough force to move the droplet, while a high amplitude may result in droplet breaking. The pulse amplitude is usually kept between 0.5 kV and 1.2 kV.

The pulse frequency defines the frequency of the high-voltage pulse. Its value depends upon the dielectric properties of the oil and droplet fluids⁵⁴. While the above-mentioned parameters are highly sensitive to experiment conditions such as droplet size, fluid flow rates and microchannel dimensions and thus have to be optimized for every setup separately; the pulse frequency is not a sensitive parameter, and its value is usually kept constant at 10 kHz for all sorting operations.

The 'start sorting' button initiates the sorting process by triggering the high-voltage amplifier (with user defined parameters) each time a droplet passes the sorting criteria.

The 'test pulse' button sends a continuous pulse (of user-defined amplitude and frequency) to the high-voltage amplifier each time it is pressed. It is mainly used to validate proper connection between the FPGA, the HV-amp and the microfluidic chip, and also to adjust the flow rates for efficient sorting When the experiment is set up and all the droplets are going to the waste channel, pressing the test pulse button should result in the deflection of all the droplets toward the collection channel, indicating proper electrical connection and efficient flow rate distribution between collection and waste channel of the microfluidic chip.

The 'test sort' button provides options to sort fractions of the detected droplets for test purposes. The 1:1 test sort will trigger the high-voltage amplifier every time a droplet passes the sorting criteria, while a 1:3 test sort will trigger on every third droplet that passes the criteria (Supplementary Video 7). To test the sorting efficiency of the setup with the chosen HV amp parameters, the test sort is assigned to a particular sorting ratio and the start sorting toggle is turned on. The sorting efficiency is then checked optically via the high-speed camera. If the sorting efficiency is suboptimal, the high-voltage parameters can be adjusted accordingly (e.g., if droplets are not deflected completely to the collection channel, voltage amplitude can be increased, or if more than individual droplets are sorted, the pulse duration can be decreased).

Droplet counts window: Shows the number of droplets detected in each PMT channel, as well as the number of sorted droplets. **Save data window:** Allows the user to save the live-data and peaks data form all PMTs, as well as the metadata along with the user comments. The metadata file registers the current state of the interface including PMT gains, high-voltage amplifier parameters, thresholding and gating positions. **Reset window:** Resets the cursor positions, droplet counts and scatter plots. The cursors in the sorting criteria tab are reset back to a lower gate at (0,0) and an upper gate at (50,50); the droplet counts are reset to zero, and the scatter plots are refreshed.

fluorescence signals in real time, enabling the integration of transmittance analysis with existing droplet fluorescence quantification technology for 'transmittance- and fluorescence-activated droplet sorting'. Steps 147–149 describe the procedure to install TFADS on PC.

Workstation setup validation (Steps 150-201)

Once the installation of the workstation is complete, it needs to be verified to make sure the connections are working as expected. We conduct a quick experiment using fluorescent slides to check that the PMTs are acquiring the expected signals and are correctly communicating with the FPGA module

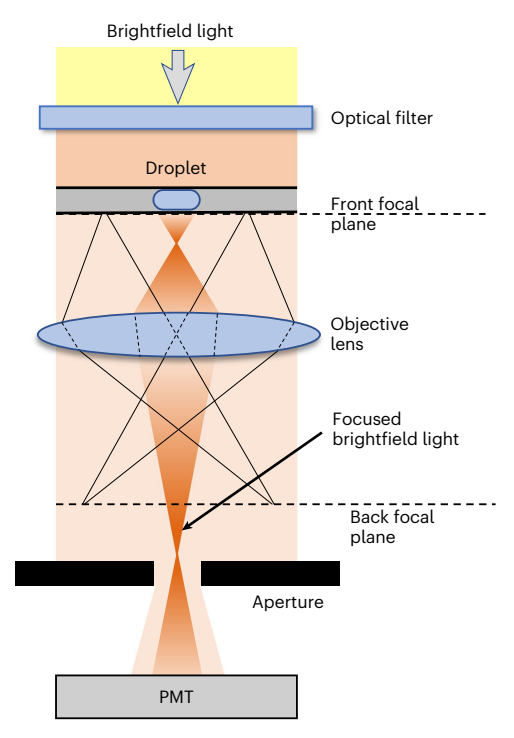


Fig. 3 | Droplet lensing. Ray diagram illustrating the lensing effect caused by an aqueous droplet suspended in HFE 7500 oil as it passes over the objective lens.

(Steps 150–161). We also provide a typical workflow to conduct any fluorescence- and/or transmittance-activated droplet sorting experiment (Steps 162–201). General practices such as microfluidic chip placement, electrode connections and flow initiations are described in Steps 162–174 toward a final aim of sorting the droplets of interest in Steps 175–201. For the sorting experiments, we used a microfluidic chip that has a flow-focusing geometry for droplet generation upstream of a droplet sorting junction, where the droplets are directed either toward the collection channel or toward the waste channel (Fig. 4a). The collection channel has an excess length (twice the length of the waste channel) to provide additional fluid flow resistance (Fig. 4a and Supplementary Video 5). As a result of the higher resistance, the droplets are inherently driven toward the waste channel unless the sorting is triggered by activating the electric field via the electrodes (Steps 171–174) (ref. 22). Other alternatives exist in the literature, such as chip designs using a second oil inlet before the separation junction to induce biased oil flow and to facilitate droplet flow in the waste channel 44.45.

The droplet sorting is based on the principal of dielectrophoresis, where, in a non-uniform electric field, a dielectric particle (i.e. the aqueous droplet) suspended in a medium with higher dielectric constant (i.e., the oil) experiences a net force ($F_{\rm DEP}$) toward the region of higher electric field density 42,46 (Fig. 4b). The droplets traveling through the sorting junction are pulled toward the collection channel due to this net force upon activation of the electrodes via a high-voltage pulse (Fig. 4c and Supplementary Video 6). The strength and timing of this high-voltage pulse are optimized for an efficient sorting by controlling the amplitude, frequency, duration and delay of the pulse using TFADS as explained in Steps 184–194 and Box 1. This section further defines the steps to select the droplets of interest by defining sorting criteria in TFADS where the upper and lower limits of the fluorescence and transmittance signals of the droplet of interest are defined (Steps 195–196 and Box 1). These sorting criteria are usually defined by the user's discretion when a cluster of droplets of interest is distinctly observable in the signal distribution readout during the live experiment, similar to a FACS procedure (Steps 195–196 and Box 1). In cases where a distinct cluster is not observed, more stringent criteria can be defined to reduce the false positives in the collection channel at the expanse of more true negatives in the waste channel. Whenever a new droplet passes these criteria, TFADS generates the high-voltage pulse that eventually sorts the droplet.

Example applications

In 'Anticipated results', we illustrate the application of the workstation developed by this protocol through various experiments. We first conduct characterization experiments to demonstrate that our

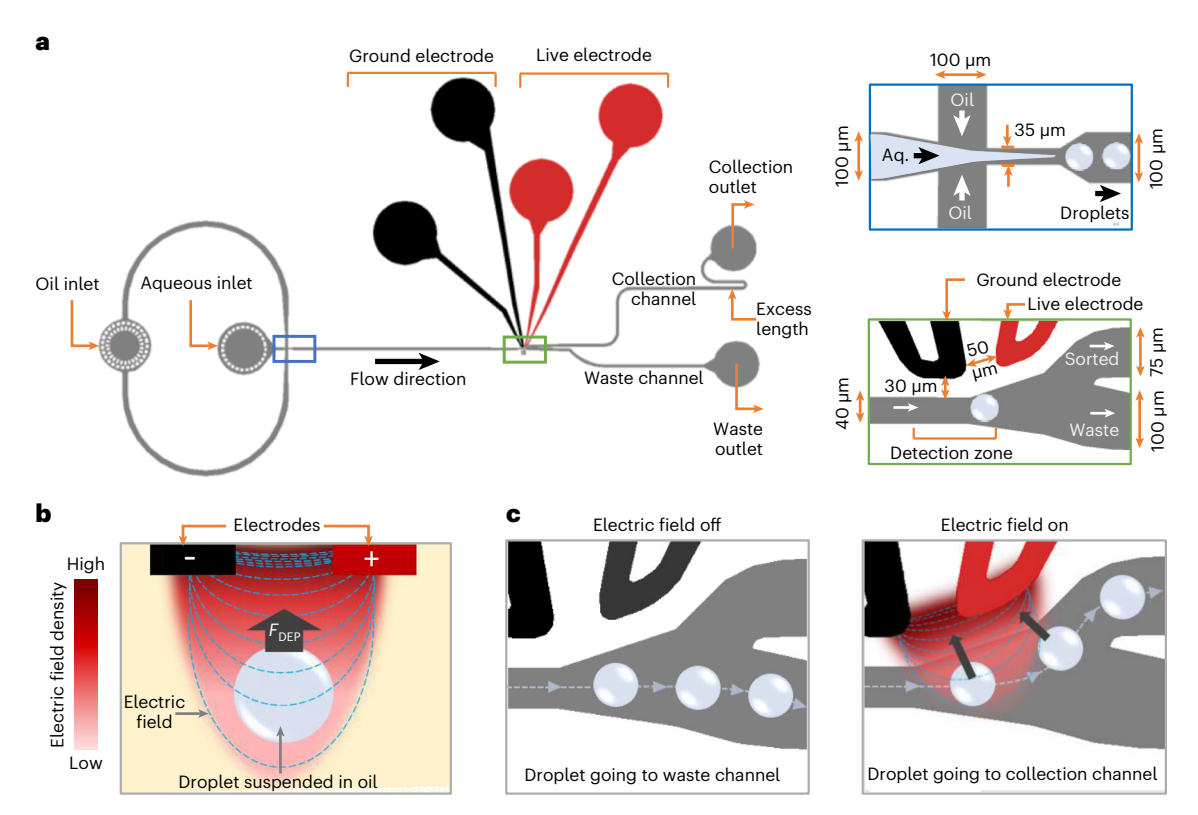


Fig. 4 | Droplet sorting chip. a, Sorting chip design depicting the inlets for oil and aqueous phase, outlets for waste and sorted droplet collection. The channels for casting live (red) and ground electrodes (black) are also shown. Inset: dimensions of the flow focusing junction and the sorting junction. The microfluidic channels have a height of 50 μm. **b**, Principle of dielectrophoresis where a droplet suspended in oil experiences a net force (F_{DEP}) toward the region with higher electric field density. **c**, Schematic of the sorting junction. In absence of any electric field, all droplets flow toward the waste channel, which has a lower hydrodynamic resistance. When the electric field is switched on, droplets are pulled toward the collection channel.

transmittance analysis is capable of label-free droplet detection and then calculate its sensitivity and limit of detection. We then conduct an experiment to sort droplets that contain fluorescent beads as a training exercise to familiarize users with the basics of droplet screening experiments. Finally, we demonstrate a real-world application with complete microfluidic workflow for 'single-cell high-throughput droplet sorting' by screening droplets hosting single cells and sorting only those droplets in which the encapsulated cell shows high enzymatic activity.

Materials

Biological materials

- HT-1080 fibrosarcoma cell line (DSMZ, cat. no. ACC 315, RRID: CVCL_0317)
- HELA carcinoma cell line (DSMZ, cat. no. ACC 57, RRID: CVCL_0030) !CAUTION The cell lines used in your research should be regularly checked to ensure that they are authentic and are not infected with mycoplasma.

Reagents

▲ CRITICAL The main part of this procedure is the construction and setup of the equipment. The reagents that are specific to the construction are divided into the three categories listed below:

Reagents used in the main procedure

- PicoSurf (5% (wt/wt) in Novec 7500, SphereFluidics, cat. no. C022)
- Novec 7500 oil (3M, cat. no. 98-0212-2928-5) ! CAUTION Causes respiratory, skin and eye irritation. Wear appropriate personal protective equipment and avoid direct contact.
- Fluorescein sodium salt (Sigma, cat. no.46960)
- Phosphate-buffered saline (PBS) pH 7.4 1× (Gibco, cat. no. 10010-015)

Reagents used for mold and microfluidic chip fabrication

▲ CRITICAL The mold and chip fabrication procedures are described in Box 2.

- SU-8 2035 photoresist (Kayaku Advanced Materials (MicroChem), cat. no. SU-8 2035)
 !CAUTION Photoresist is toxic and flammable; always handle it under a chemical hood in accordance with the local cleanroom safety guidelines.
- Propylene glycol monomethyl ether acetate (Sigma-Aldrich, cat. no. 484431) **!CAUTION** The solvent is flamable; handle it by following the safety guidelines of the cleanroom facility.
- Isopropanol (Sigma-Aldrich, cat. no. 278475) ! CAUTION The solvent is flammable.
- Poly(dimethyl siloxane) (PDMS; Dow Corning, Sylgard 184)
- Aquapel (PPG Industries, cat. no. 47100) ! CAUTION Aquapel is toxic and must be handled under chemical hood. Wear appropriate safety equipment.

Reagents used in the example experiments

- FluoShperes polystyrene 10 µm blue fluorescent (365/415) (Thermo Fisher Scientific, cat. no. F8829)
- PolyStyrene/DVB (480,520), Dragon Green (Bangs Laboratories, cat. no. FSDG007)
- 0.25% trypsin-EDTA 1× (Gibco, cat. no. 25200-056)
- DMEM medium (Gibco, cat. no. 41965-039)
- Fetal bovine serum (FBS; Sigma, cat. no. F7524)
- Penicillin-streptomycin (Gibco, cat. no. 15140-122)
- FreeStyle 293 Expression Medium (Gibco, cat. no. 12338018)
- 10% Pluronic F-68 (Gibco, cat. no. 24040-032)
- CellTrace Blue stain (Invitrogen, cat. no. C34574)
- CytoTell Red 590 (AAT Bioquest, cat. no. 22261)
- 520 MMP FRET substrate XIV (Anaspec, cat. no. AS-60581)
- Dimethyl sulfoxide (DMSO; Sigma, cat. no. D5879)
- Trypan blue stain, 0.4% (Invitrogen, cat. no. T10282)

Reagent setup

Reagents setup used in the main procedure

1% Picosurf working solution

Dilute the 5% PicoSurf surfactant to 1% into Novec 7500 oil (vol/vol). Prepare 2 mL solution for one experiment. Store at room temperature (RT, ~23 °C) and protect from light. Working solution is stable for up to 3 months.

Fluorescein working solution

Add 0.37 mg of fluorescein to 1 mL of PBS for preparing a 1 mM stock solution. Dilute 1 μ L of fluorescein stock solution in 1 mL PBS to have 1 μ M fluorescein working solution. Fluorescein solution is light sensitive and has to be protected from light. It can then be stored ~1 year at RT.

Reagents setup used for example experiments

The reagent preparation (including cells and fluorescent beads) that are used to show example results is included in Box 3.

Equipment

Optics support parts

- Breadboard, NEXUS Optical Breadboard 1,500 × 750 × 60 mm (Thorlabs, cat. no. B-SP0004)
 !CAUTION Heavy objects can cause muscle strain or back injury. Use lifting aids and proper lifting techniques when moving the breadboard.
- Passive vibration isolator blocks, silicone stopper, qty: 4 (VWR, cat. no. 217-9524)
- Dichroic mounts, mirror adjustment insert 30, qty: 6 (Qioptiq Photonics, cat. no. G063-730-000)
- Filter holder 30 mm, H 30, qty: 6 (Qioptiq Photonics, cat. no. G061-225-000)
- Clamping fork, 1.75" counterbored slot, qty: 4 (Thorlabs, cat. no. CF175)
- Fluorescent slides (Thorlabs, cat. no. FSK5)

Machined parts

The following parts can be machined in any academic or commercial (e.g., emachineshop.com, protolabs.co.uk) machine shops. Details such as materials, tolerances and threading are provided in the engineering drawing files associated with the CAD files.

Box 2 | Quick guide on microfluidic chip fabrication

Complementary information on the procedure below can also be found in literature for microfluidic chip fabrication including photolithography, PDMS casting, fabrication of electrodes and surface coating²². Alternatively, the chips can be ordered from commercial companies (e.g., fivephoton.com, microfluidic ChipShop) using the design files in Supplementary Data 10.

Cleanroom equipment

- High-frequency plasma cleaner for silicon wafer (Tepla 300)
- Manual coater (Sawatec LSM250)
- Hot plates (IKA)
- UV mask aligner (Süss MJB4)
- Surface activation plasma cleaner for bonding (Harrick Plasma)
- Vacuum dessicator (Nalgene, cat. no. 5311-0250)

Procedure

(A) Vacuum pump (Laboport N840.3FT.18) photolithography—mold fabrication Timing 2 h

- ▲ CRITICAL All the photolithography steps should be performed in a cleanroom in accordance with the local safety guidelines of your facility.
- 1 Order a flexible photomask (e.g., from Selba S.A, Switzerland) with 25,400 dpi from the chip CAD file provided in Supplementary Data 10.
- 2 Heat up hot plates to 65 °C and 95 °C.
 - !CAUTION The high temperature can cause burn.
- 3 Clean the silicon wafer with an air gun, keep it for 30 min at 95 °C and let it cool down to RT. Alternatively, use a high-frequency plasma cleaner with the recommended procedure.
- 4 Place the clean silicon wafer on the spin-coater and pour ~10 g of SU-8 2035 photoresist on the wafer.
 - ▲ CRITICAL STEP Pour the photoresist slowly and hold the container close to the wafer to avoid bubbles.
- 5 Spin-coat to reach the desired thickness of 50 μm using a three-step spinning program: First, spin at 500 rpm for 5 s, followed by a high-speed step of ~1,750 rpm for 30 s and finish with a last step of 500 rpm for 5 s. The acceleration between every speed change is kept at 100 rpm/s except for the high-speed step where the acceleration was 300 rpm/s.
 - ▲ CRITICAL STEP For further information on the spin-coating parameters, refer to the SU8 manufacturer's datasheet at https://kayakuam.com/products/su-8-photoresists/.
- 6 Soft bake the coated silicon wafer at 65 °C for 2 min followed by 7 min at 95 °C.
- 7 Place the soft-baked mold on UV mask aligner with the printed photomask.
- 8 Expose the silicon wafer to UV light following the SU-8 manufacturer's instructions. Typically, we recommend an exposure for -8 s with a 20 mW/cm² lamp power for a thickness of 50 μm.
- 9 Bake the mold at 65 °C for 1 min and then 7 min at 95 °C.
- 10 Develop the mold by diving it into propylene glycol monomethyl ether acetate bath for 5 min.
- 11 Wash it with isopropanol and dry with an air gun. If white precipitate is observed during isopropanol treatment, repeat Steps 10 and 11 until the non-UV-exposed SU-8 is completely removed.

(B) Soft photolithography-PDMS casting • Timing 24 h

▲ CRITICAL All the soft photolithography steps should be performed in clean environments to diminish dust and particles that could clog the microfluidic device. If a professional clean room is not available, this work can alternatively be performed under a laminar flow hood.

- 1 Weigh 1 g of crosslinker for 10 g of PDMS (w/w) and blend the mixture using a disposable fork
- 2 Place the PDMS mixture in the vacuum chamber and degas until no bubbles are visible. The procedure typically takes -10-15 min For the remaining bubbles, if needed, remove them gently with an air blower.
- 3 Pour the PDMS mix onto the silicon wafer.
- 4 Degas the mold containing the PDMS mixture in vacuum chamber to remove the last air bubbles.
- 5 Cure at 60 °C for 4 h.
 - **PAUSE POINT** The mold can be left overnight in the incubator.
- 6 When the PMDS is solid, delimit the outline of the chip using a scalpel and cut gently to peel off the PDMS.
 - ▲ CRITICAL STEP The silicon wafer is fragile and can break or scratch easily. Avoid pressing excessively when cutting on SU-8 pattern.
- 7 Punch holes for all the fluid inlets and outlets with a 0.75 mm punch and use the 0.5 mm punch for the electrode's inlet and outlets.
- 8 Remove the PDMS residuals using tape and an air gun.
 - ▲ CRITICAL STEP Cleaning step is important to avoid PDMS residuals that could clog the channels during the experiment.

(C) Glass or ITO glass-PDMS bonding • Timing 1 h

- 1 Clean the microscope glass with water and isopropanol. If ITO is used, check the ITO face using a multimeter set in continuity-test mode and label the conductive face with a marker.
- 2 Place the chip and glass in the plasma oven and run the recommended program for glass-PDMS bonding according to your plasma oven manufacturer.
 - ▲ CRITICAL STEP The PDMS with the chip design imprint must be pointed upward. For the ITO glasses, the nonconductive side must be pointed upward during the plasma treatment. The conductive side is needed only for electrical grounding during droplet sorting experiment (Step 161)
 - ▲ CRITICAL STEP An efficient bonding is required, otherwise delamination can occur.
- 3 Bond the nonconductive side of the glass side to the microchannel side of the PDMS.
- 4 Put the bonded chip in the incubator for 2 min at 60 °C.

(D) Manufacturing of electrodes • Timing 30 min

- 1 Turn on the hot plate and set the temperature at 95 °C.
 - !CAUTION The high temperature can cause burn.
- 2 Put the chip on the hotplate and wait for 10 min so that the chip reaches the hot plate's temperature.
- 3 Use tweezers to insert short fragments of Indium alloy wire (-1 cm) into the electrode channel until it is completely filled.
 - !CAUTION Electrode fabrication must be done in a well-ventilated environment or under a chemical hood.
- 4 Insert a ~5 cm electrode wire in which both ends have been previously stripped of 0.5 cm.
- 5 Turn off the hot plate. Remove the chip and let it cool down to RT (check if the connections made are effective using the multimeter set in continuity-test mode).
 - ▲ CRITICAL STEP The connection must be done properly to perform a sorting experiment. If necessary, remove the electrode cable and repeat the process starting from step 3.

Box 2 | Quick guide on microfluidic chip fabrication (Continued)

(E) Water-repellent treatment • Timing 15 min

- 1 Fill a 5 mL syringe with Aquapel, connect a piece of tubing on the needle and fix a 0.45 μm filter between the syringe and the needle.

 !CAUTION The Aquapel procedure must be performed under a chemical hood, and appropriate laboratory clothing and safety glasses must be used.
- 2 Flush the channels with Aquapel from the oil inlet until the liquid comes out from all the outlets and wait for 30 seconds.
- 3 Fill a 5 mL syringe with Novec 7500 oil with a tubing on the needle and wash the channel with the oil.
- 4 Remove the excess of oil by flushing air into the channel with the help of empty syringe with a needle capped with a piece of tubing.

Box 3 | Quick guide to sample preparation for droplet analysis and sorting experiments

In this section we describe how to prepare cultured cells for analysis and sorting. We use the HT-1080 fibrosarcoma cell line (RRID: $CVCL_0317$) and HELA carcinoma cell line (RRID: $CVCL_0030$) as examples. Cell cultures follow conventional cell cultivation procedures for adherent cells. Briefly, cells should be maintained at 37 °C and 5% CO_2 using DMEM supplemented with 10% FBS (vol/vol) with a confluency below 70-80%. Every manipulation of cells should be done in a sterile environment using a biosafety cabinet. Other cells can also be used as long as they meet their appropriate culture and manipulation conditions to guarantee a high cell viability while complying with the relevant local regulations.

!CAUTION The cell lines used in your research should be regularly checked to ensure that they are authentic and are not infected with mycoplasma

Additional wet lab equipment

- Tissue culture biosafety cabinet
- 5% CO₂ cell culture incubator operated at 37 °C (Thermo Fisher Scientific, cat. no. 51030287)
- Centrifuge Heraeus multifuge X1R (Thermo Fisher Scientific, cat. no. 75004210)
- Automatic cell counter (Countess II, Thermo Fisher Scientific, cat. no. AMQAX1000)
- Spectrophotometer Varioskan Lux (Termo Fisher Scientific)

Reagent setup

Fluorescein working solution

Add 0.37 mg of fluorescein to 1 mL of PBS for preparing a 1 mM stock solution. Dilute 1 μ L of fluorescein stock solution in 1 mL PBS to have 1 μ M fluorescein working solution. Fluorescein solution is light sensitive and has to be protected from light. It can then be stored ~1 year at RT.

1% Picosurf working solution

Dilute the 5% PicoSurf surfactant to 1% into Novec 7500 oil (vol/vol). Prepare 2 mL solution for one experiment. Store at RT and protect from light. Working solution is stable for up to 3 months.

Trypan blue working solution

Prepare a dilution series of trypan blue. Dilute 250 μ L trypan blue stain (0.4% stock solution) into 1,750 μ L of PBS to obtain a starting concentration of 0.05%. Then prepare further twofold serial dilutions in PBS to yield the concentration of 0.025%, 0.0125%, 0.00625% and 0.003125% with final volume of 2 mL for each solution. In addition, include a blank (only PBS) and an intermediate concentration of 0.0375% by mixing 1 mL each of 0.05% and 0.025% solutions. The working solutions are stable for months at RT.

Complete DMEM medium

Supplement DMEM medium with 10% (vol/vol) FBS and 1% (vol/vol) penicillin-streptomycin. This solution is stable for a couple of months at $4 \, ^{\circ}\text{C}$.

520 MMP FRET substrate XIV stock solution

To prepare 1 mM stock solution, resuspend 0.1 mg powder in 52 μ L DMSO and protect the solution from light. The reagent can be stored at -20 °C for several months; avoid repeated freezing and thawing cycles.

CellTrace Blue stain and CytoTell Red 590 working solution

Prepare the stock solutions into DMSO (wt/vol) according to the manufacturer's instructions. The reagent can be stored at -20 °C for weeks. Avoid repeated freezing and thawing cycles.

Procedure

(A) Trypan blue droplet transmittance analysis • Timing ~1 h

- 1 Measure OD at 600 nm on spectrophotometer for the trypan blue dilution series.
- 2 Insert 20 cm PTFE tubing onto eight 27 G needles using tweezer.
- 3 Load one 3 mL syringe with the 1% surfactant working solution, set up a needle capped with a tubing piece and mount it on syringe pump.
- 4 Load 1 mL PBS in one 3 mL syringe, place a needle with tubing and mount the syringe on second syringe pump.
- 5 Insert the tubing into the corresponding inlets of the sorting chip (Supplementary Data 10 and Supplementary Fig. 5) and start the pumps with flow rates of 300 μL/h for the oil and 150 μL/h for the aqueous solution.
- 6 Slowly increase the oil flow by 50 μL/h (every ~1 min) to reach a final flow rate of 500 μL/h.
- 7 Slowly decrease the aqueous by 50 μ L/h (every ~1 min) to reach a final flow rate of 50 μ L/h.
- 8 Measure the transmittance signal at the detection zone (Fig. 16c) using PMT3 only, and record the data (Box 1).
- 9 Stop the pumps. Gently unplug the aqueous tubing from the chip and remove the aqueous syringe from the pump.
- 10 Load a new syringe with a new trypan blue concentration starting with the lowest and repeat the procedure from step 4.

(B) Fluorescent bead encapsulation • Timing ~2 h

- 1 Add 20 μ L of Dragon Green fluorescent beads and 150 μ L FluoShperes blue fluorescent beads to 830 μ L PBS. The volume indicated is to reach an average occupancy of ~0.1 per droplet ($\lambda = 0.1$).
 - ▲ CRITICAL STEP For having a homogeneous bead suspension, vortex for 30 s before pipetting. The indicated pipetted volumes are dependent on your initial bead concentration. It is highly recommended to measure your beads concentration (e.g., using a cell counter chamber) to confirm a ratio of green to blue beads of ~1:3 with an average of 0.1 beads per droplet volume.
- 2 Insert 20 cm PTFE tubing onto two 27 G needles using tweezer.
- 3 Remove the syringe plunger and add a magnetic stirrer into one syringe. Insert back the plunger.
- 4 Fill the syringe containing the magnetic stirrer with the aqueous bead mixture and a second syringe with the 1% surfactant working solution.
- 5 Place the needle capped with the PTFE tubing onto the syringes and mount these syringes onto separate syringe pumps.

 CRITICAL STEP Remove the air bubbles from the syringe by holding it vertically (needle facing up), gently taping and pushing the plunger of the syringe before placing the needle.

Box 3 | Quick guide to sample preparation for droplet analysis and sorting experiments (Continued)

- 6 Place the magnetic stirrer close to the syringe containing the bead solution and the stirrer. Set the speed to 500 rpm for having a constant resuspension of the solution.
- 7 Plug the tubing into the sorting chip with on-chip droplet generator (Supplementary Data 10) and start the pumps with an initial flow rate of 600 µL/h for the oil mix and 200 µL/h for the aqueous bead suspension, so that the two flows are visible on the camera.
- 8 Slowly increase the oil flow rate by 200 μ L/h (every ~1 min), to reach a final flow rate value of 1,450 μ L/h.
- 9 Slowly decrease the aqueous flow rate by ~30 µL/h (every ~1 min), to reach a final aqueous flow rate of 90 µL/h.
- !CAUTION For efficient droplet collection, we recommend sorting at least 3,000 droplets and using a cell counter chamber for droplet imaging.

(C) Cell staining • Timing ~1 h

- 1 Use cells at 70% confluency on the flask, remove the complete DMEM medium and wash twice with PBS.
- 2 Add ~0.3 mL trypsin-EDTA per 10 cm² of flask and incubate for ~5 min at 37 °C 5% CO₂.
- 3 Add two volumes of complete DMEM medium prewarmed at 37 °C and transfer the detached cells into a 15 mL conical tube.
- 4 Centrifuge the cells at 200q for 5 min.
- 5 Discard the supernatant and suspend the cells in 2 mL PBS, prewarmed at 37 °C.
- 6 Add 4 µL CytoTell Red 590 (500×) for HT-1080 cells, and 4 µL CellTrace Blue stain (5 mM) for HeLa cells.
- 7 Incubate for 20 min at 37 °C in a 5% CO₂ atmosphere.
- 8 Resuspend the cells in 10 mL of prewarmed complete DMEM medium and incubate for 10 min at 37 °C in a 5% CO₂ atmosphere.
- 9 Pellet cells at 200q for 5 min and wash them in FreeStyle 293 Expression Medium. Repeat once.
- 10 Suspend the cells in 1 mL FreeStyle 293 Expression Medium precooled at 4 °C and count the cells with an automatic cell counter. This should result in an average cell occupancy of -0.1 per droplet volume (-140 pL), with a ratio of one HT-1080 cell to five Hela cells.

 !CAUTION Since those cells are adherent and tend to aggregate, a low occupancy is suggested as well as passing the cells through a cellular strainer (40 µm) before loading into a syringe. Pluronic F-68 can be added to a final concentration of 0.2% (vol/vol) to diminish the aggregation formation.
- 11 Add 5 μ L 520 MMP FRET substrate XIV (1 mM) to 1 mL FreeStyle 293 Expression Medium.

(D) Emulsion production • Timing ~2 h

- 1 Load the cell mixture into a 3 mL needle-free syringe (Supplementary Fig. 8) with a magnetic stirrer, the MMP substrate in FreeStyle 293 Expression into a 1 mL syringe, and the 2 mL of 1% PicoSurf surfactant in Novec 7500 oil into a 3 mL syringe.
- 2 Mount the three syringes onto three different syringe pumps and place the magnetic stirrer onto the cell-loaded syringe.
- 3 Plug the tubing into the droplet generator chip (Supplementary Data 10) and start the pump with an initial flow rate of 1,500 μL/h for the oil mix and 400 μL/h for the aqueous samples (MMP substrate and cell suspension).
- 4 Once the flows are stabilized and droplets generated, increase the oil flow rate to a value of 2,100 μ L/h and decrease the aqueous flow rates to 375 μ L/h. Once the flow rates are reached and the droplets generated, plug a tubing and collect into Falcon tube (Supplementary Video 9).
- 5 Incubate the collected emulsion in the closed tube at 37 °C for 30 min.
- 6 Incubate the emulsion at 4 °C for 5 min to stop the enzymatic reaction.
- 7 Remove the plunger and transfer the emulsion into the needle-free syringe (Supplementary Fig. 9). Hold the tubing and the syringe tube at the same level. Pour the emulsion into the syringe tube and re-insert the plunger (Supplementary Fig. 9).

(E) Emulsion reinjection • Timing ~4 h

- 1 Mount and connect the syringe containing 1% PicoSurfacant in Novec 7500 oil and the syringe with the emulsion to the droplet reinjection and sorting chip (Supplementary Data 10).
 - ▲ CRITICAL STEP Keep the emulsion syringe at ~4 °C using ice packs to stop the enzymatic reaction.
- 2 Set a flow rate of 120 µL/h for the emulsion syringe and 400 µL for the oil syringe with the surfactant.
- 3 Once the emulsion starts to stack, increase gradually (every -3 min by 100 μ L/h) the oil flow rate to reach a flow rate of 900 μ L/h.
- 4 Decrease slowly (every ~3 min by 20 μ L/h) the emulsion flow rate to reach 50-60 μ L/h.
 - Flat rail, FLS 40-1000, qty: 2 (Qioptiq Photonics, cat. no. G061-361-000, cut into five pieces of 10-cm-long rails and one piece each of 30-cm-long and 40-cm-long rails)
 - Rail clamp, Rider FLR 4020, qty: 10 (Qioptiq Photonics, cat. no. G061-372-000, modified as per the design file in Supplementary Data 1)
 - Filter holder 25 mm, H 25, qty: 10 (Qioptiq Photonics, cat. no. G065-061-000, 3 are modified as per the design file in Supplementary Data 2)
 - Rail support block, qty: 8 (CAD files in Supplementary Data 3)
 - Laser support block, M series (CAD files in Supplementary Data 4)
 - Laser support block, FN series, qty: 2 (CAD files in Supplementary Data 4)
 - PMT mount, support plate and base plate, qty: 3 each (CAD files in Supplementary Data 5)
 - Black box (CAD files for all the parts in Supplementary Data 6)

3D printed parts

 \triangle CRITICAL 3D prints can be taken from any 3D printer that can print with rigid materials such as acrylonitrile butadiene styrene or polylactic acid with a resolution of at least 500 μ m. Alternatively, commercial 3D printing services (e.g. hubs.com, sculpteo.com) can also provide 3D prints using the provided STL files.

- Target disk, 3D printed (STL files in Supplementary Data 7)
- Aperture disk, 3D printed (STL files in Supplementary Data 8)
- Filter rim, 3D printed (STL files in Supplementary Data 9)

Optical filters

!CAUTION Wear gloves while handling optical filters and dichroic mirrors to avoid fingerprints.

- F1: 405/10 BrightLine HC (AHF, cat. no. F39-404)
- F2: 488/6 BrightLine HC (AHF, cat. no. F37-488)
- F3: 563/9 BrightLine HC (AHF, cat. no. F37-563)
- F4 and F9: Triple Line Laser Rejectionband ZET405 / 473/561 NF, qty: 2 (AHF, cat. no. F67-405)
- F5: 445/45 BrightLine HC (AHF, cat. no. F37-446)
- F6: 525/45 BrightLine HC (AHF, cat. no. F37-521)
- F7: 605/50 ET Bandpass (AHF, cat. no. F49-605)
- F8a: 633 LP Edge Basic Longpass (AHF, cat. no. F76-631)
- F8b: 561 LP Edge Basic Longpass (AHF, cat. no. F76-561)
- ND: neutral density filter ND 1.0 (10%T), qty: 2 (AHF, cat. no. F06-125)

Mirrors

- D1: full-reflective mirror 98.5% UV-NIR (AHF, cat. no. F21-025)
- D2: dichroic mirror, Beamsplitter HC BS R488 (AHF, cat. no. F38-488)
- D3: dichroic mirror, Beamsplitter HC BS 409 (AHF, cat. no. F38-409)
- D4: dichroic mirror, HC Triple-Beamsplitter 403/497/574 (AHF, cat. no. F68-412)
- D5: dichroic mirror, Beamsplitter HC BS 484 (AHF, cat. no. F38-484)
- D6: dichroic mirror, Beamsplitter HC BS 552 (AHF, cat. no. F38-552)

Lasers

! CAUTION Exposure to laser radiation can cause injuries to eye and skin. Use protective equipment such as safety glasses, ND filters and laser viewing cards when lasers are on.

- Laser viewing card, VIS/NIR Detector (Thorlabs, cat. no. VRC2)
- Laser safety glasses (Thorlabs, cat. nos. LG2 and LG3 and Offenhäuser, cat. no. RR09)
- L1: 405 nm M Series 50 mW Laser System, CW (Changchun Dragon Lasers Co., cat. no. 405M50)
- L2: 473 nm FN Series 100 mW Laser System, CW (Changchun Dragon Lasers Co., cat. no. 473FN100)
- L3: 561 nm FN Series 50 mW Laser System, CW (Changchun Dragon Lasers Co., cat. no. 561FN50)

PMTs

- P1 and P2: medium dynamic range photosensor module with PMT, qty: 2 (Hamamatsu Photonics, cat. no. H11903-210)
- P3: high-dynamic-range photosensor module with PMT (Hamamatsu Photonics, cat. no. H11903-20)
- PMT power supply, ±15 V direct current (DC), 30 W, 1A (Traco Power, cat. no. TMP 30215C)
- PMT switches, dual circuit toggle swdtch, 2A, qty: 3 (RND Lab, cat. no. 210-00669)

Camera

• Camera (C), CAMMINI MotionBLITZ EoSens mini1 (Mikrotron, cat. no. 109724)

Microscope

- Ti2-U inverted microscope (Nikon, cat. no. MEA54200) ! CAUTION No rubber feet should be installed under the microscope's body.
- TI2-T-BC tube with C-Mount (Nikon, cat. no. MQF52056)
- C-DA C-mount adapter (Nikon, cat. no. MBF11300)
- TI2-D-PD eyepiece arm (Nikon, cat. no. MEB52340)
- TI2-D-LHLED LED lamp housing (Nikon, cat. no. MAK10110)
- TC-C-TC manual system condenser (Nikon, cat. no. MAK99000)
- T-C ELWD front condenser (Nikon, cat. no. MEE59920)
- TC-S-SR right hand cross table (Nikon, cat. no. MEL51005)
- CFI S-Fluor 20×/0.75/1.00 objective (Nikon, cat. no. MEP51316)
- CFI P-Fluor 40×/0.75/0.66 objective (Nikon, cat. no. MRH00401)
- PRISME T-BP E20 L80 (Nikon, cat. no. MED59040)

Computer hardware

• FPGA card, PXIe-7856R, R Series multifunction input and output (I/O) module, Kintex-7 160T (National Instruments, cat. no. 784145-01)

• PXI Chassis, NI PXIe-1073 with integrated MXIe controller, five slots for peripherals (National Instruments, cat. no. 781161-01)

- PCIe card, PCIe-8361 with driver CD and 3 m cable (National Instruments, cat. no. 779504-01)
- FPGA connector block, shielded I/O SCB-68 (National Instruments, cat. no. 776844-01)
- FPGA cable, shielded cable SHC68-68-RDIO for DIO connectors of 7831R boards, 68-pole. Type D to 68-pole. VHDCI, 1 m cable (National Instruments, cat. no. 191667-01)
- Computer (64-bit Windows-10 personal computer with a 3.00 GHz Intel core i7-9700F processor with 32 GB RAM with two ethernet ports and spare PCIe slot)
- High-voltage amplifier, TREK 623B-H-CE (ACAL Bfi, cat. no. TRE-20-00247) !CAUTION High-voltage safety rules should be followed and the amplifier should be kept turned off unless specified to turn on. The instrument should not be turned on without proper grounding. The current (limited to 0.05 Amp) can cause shock, respiratory arrest, severe muscle contractions and other adverse effects.

Computer software

All the software from National Instruments (NI) can be downloaded from www.ni.com.

- NI PXI Platform Services (19.5 or higher, provided with PCIe card, National Instruments)
- Ni System Driver Set (April-2019 or higher, provided with FPGA card, National Instruments)
- LabVIEW 2016 or higher (Full or run-time Engine, 32-bit, National Instruments)
- LabVIEW Real-Time Module (2016 or higher, 32-bit, National Instruments)
- LabVIEW FPGA Module (2016 or higher, 32-bit, National Instruments)
- NI R series Multifunction RIO Device drivers (version 19.1, 32-bit, National Instruments) **! CAUTION** The version of NI RIO drivers should match the version used for developing the application, i.e., version 19.1.
- TFADS application (custom-made software, provided in Supplementary Software 1; another version of the same software to accommodate four-laser/four-PMT upgrade is provided in Supplementary Software 2; for updates, check www.epfl.ch/labs/lbmm/downloads/)
- MotionBlitz Director2 (Camera software, Mikrotron, cat. no. 200670)

Microfluidic chips

Microfluidic chips can either be fabricated in the clean room or be ordered from commercial suppliers (e.g., darwin-microfluidics.com, fivephoton.com) using the provided design files.

- Microfluidic chip for alignment (CAD files in Supplementary Data 10)
- Microfluidic chip for droplet sorting (CAD files in Supplementary Data 10)
- Microfluidic chip for droplet generation (CAD files in Supplementary Data 10)
- Silicon wafer, 4 inches (Siltronix)
- Microscope slide $50 \times 75 \text{ mm} \times 1 \text{ mm}$ (Thermo Fisher Scientific, cat. no. 15326395)
- Indium tin oxide (ITO)-coated glass slide 50 mm × 70 mm × 1.1 mm (Diamond Coatings Ltd, Float Glass with 8–12 Ohm/m² ITO coating)
- Electrode wires (0.5 mm diameter solid core, RS Pro, cat.no. 712-5311)
- Indium alloy wire (Indium Corporation of America, solid solder wire of diameter 0.5 mm containing 51% In, 32% Bi and 16.5% Sn) **!CAUTION** All soldering procedure must be done with appropriate safety with an adequate ventilation. The resulting smoke is toxic.
- Biopsy punch 0.75 mm (ProSciTech Pty Ltd, cat. no. T983-07)
- Biopsy punch 0.5 mm (ProSciTech Pty Ltd, cat. no. T983-05)
- Filter syringe membrane (Millex, cat. no. SLHP033RS)

Other equipment

- Screws, head cap (M6: 1.6 cm and 5 cm; M5: 1.6 cm; M4: 1 cm; M3: 1 cm; M2.5: 0.6 cm and 1.6 cm)
- Insulated multicore wire (American Wire Gauge: 12 to 14)
- Eight- and three-pin connectors (12 pole terminal strip cut into eight- and three-pin sections, RND Lab, cat. no. 205-01062)
- Ribbon cable, $10 \times 0.08 \text{ mm}^2$ (3M, cat. no. 3302/10)
- Wire stripper (e.g., Proskit, cat. no. CP-080E)
- Wire crimping ferrules (e.g., Vogt, cat. no. 440005.47)
- Crimping pliers (e.g., RND Lab, cat. no. 550-00180)

- Copper tape, 5 mm wide (3M, cat. no. 1181 X 1/4")
- Epoxy adhesive (25 mL Loctite EA 3450)
- Allen key set, Hex ball-head (e.g., Wera, cat. no. 5022720001)
- Screwdriver Set, Phillips and slotted (Head size 1 to 3 mm)
- Soldering iron with standard soldering wire (e.g. Weller, cat. no. T0052923499) !CAUTION All soldering procedure must be done with appropriate safety with adequate ventilation. The resulting smoke is toxic.
- Multimeter (Fluke, cat. no. 115)
- Zip ties (lengths: 10 cm and 20 cm, generic)
- Alligator clip, insulated, qty: 2 (e.g. RND Lab, cat. no. 350-00045)

Materials for droplet-sorting experiment

- 27 G needle (BD Medical Microlance, cat. no. 302200)
- 1 mL, 3 mL or 5 mL Luer Lock Syringes (BD Plastipak, cat. no. 303175, 309658 or 309649)
- PTFE tubing, ~0.3 mm inner diameter, ~0.5 mm outer diameter (Adtech Polymer Engineering Ltd, cat. no. TW30)
- Syringe pump, qty: 2 (e.g., Harward Apparatus PhD Ultra, cat. no. 70-3007)
- Magnetic stirrer MR Hei-Mix S (Heidolph Instruments, cat. no. 503-02000-00)
- Magnetic stirrer 8 × 1.5-mm-long bar (VWR, cat. no. 442-0364)
- 15 mL conical centrifuge tubes (Falcon Corning, cat. no. 352096)
- Cell strainer 40 µm (Corning, cat. no. 352340)
- Cell counting chamber slides (Thermo Fisher Scientific, cat. no. C10228)

Procedure

Assembly layout

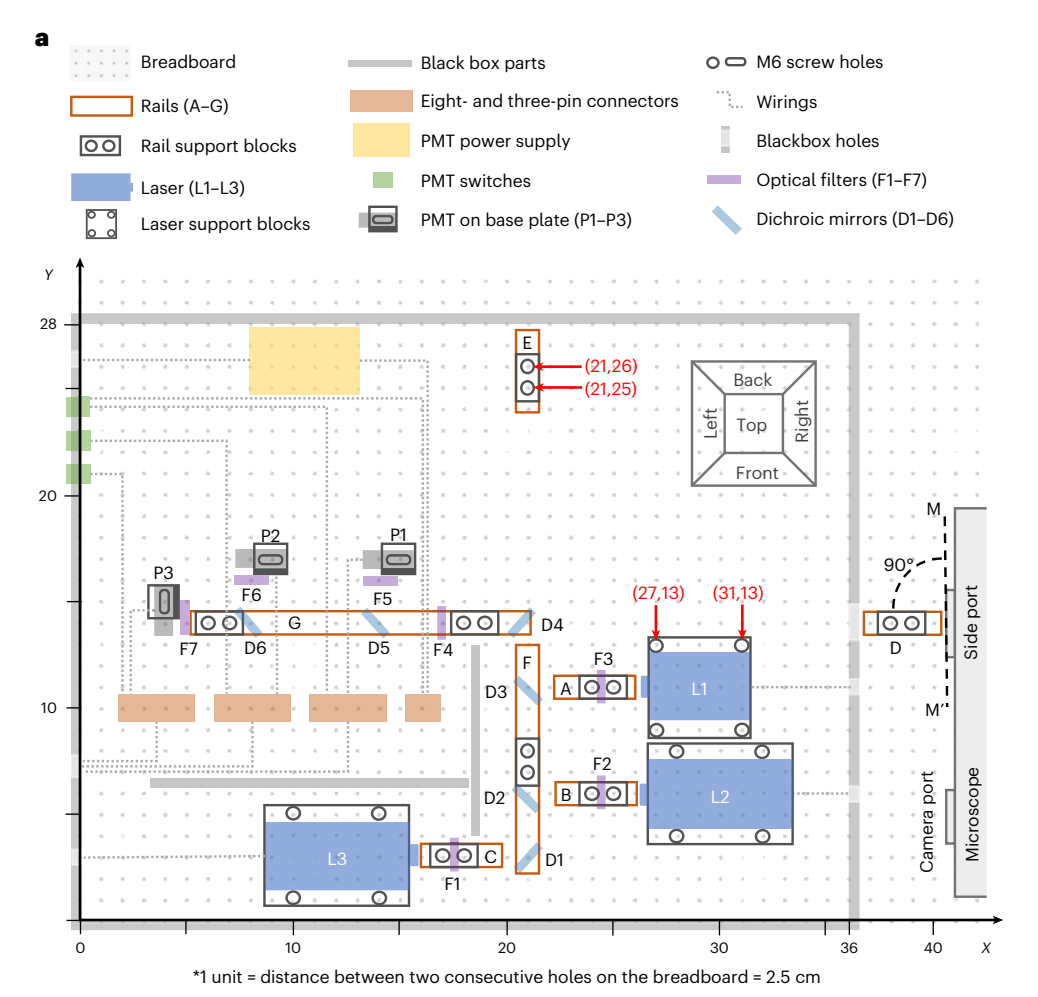
Breadboard installation Timing 1 h

▲ CRITICAL For the installation of the breadboard and all its components, we follow a strict and easy 'Lego-like' assembly protocol. As part of this, all threads on the breadboard are numbered with *X* and *Y* coordinates to assign unambiguous locations for the installation of optomechanical equipment (Fig. 5). This way readers only have to follow the individual steps below, and the components will automatically show a proper basic alignment, ready for fine tuning in later steps. (The following steps are also illustrated in an animation in Supplementary Video 1.)

- 1 Place the breadboard on four silicone stoppers on the host bench (Extended Data Fig. 1). The silicone stoppers work as passive vibration isolators.
- 2 Mark the periphery of the setup on the left of the breadboard leaving a margin of at least one breadboard hole from the left edge of the breadboard (Fig. 5a and Extended Data Fig. 2).
- 3 Mark the threads on the breadboard that are given the screw positions as per Table 2 and Fig. 5a. As an example, the coordinates for the screw positions of support blocks for rail E and laser L1 are highlighted in red color in the breadboard layout map (Fig. 5 and Extended Data Fig. 2).
- 4 Place the eight support blocks for rails and two support blocks for lasers at their respective positions and fix them on the breadboard using the 1.6 cm M6 screws (Fig. 5 and Table 2).
- 5 Place the three lasers L1 (405 nm), L2 (473 nm) and L3 (561 nm) on their respective support blocks and fix them using the 1.6 cm M6 (for L1) and 1.2 cm M3 (for L2 and L3) screws.
- 6 Connect the lasers to their respective control boxes, which are kept outside the setup's periphery.
- Take the commercially available rails that are precut into five pieces of 10-cm-long rails (rails A–E) and one piece each of 30 cm (rail F) and 40-cm-long rails (rail G). Note that a few millimeters variation is tolerated.
- 8 Fix the rails A-G at their respective positions on the support blocks using 1.6 cm M6 screws (Extended Data Fig. 3).

Mounting filters Timing 30 min

▲ CRITICAL The rails already installed on the breadboard in previous steps provide a robust and modular support to the optical filters and dichroic mirrors (Fig. 6). To mount the filters on the rails, the filters are first fixed into the filter holders. These filter holders are further fixed onto the rail clamps. The rail clamps are premachined as per the provided CAD drawing (Supplementary Data 1) to allow easy



b

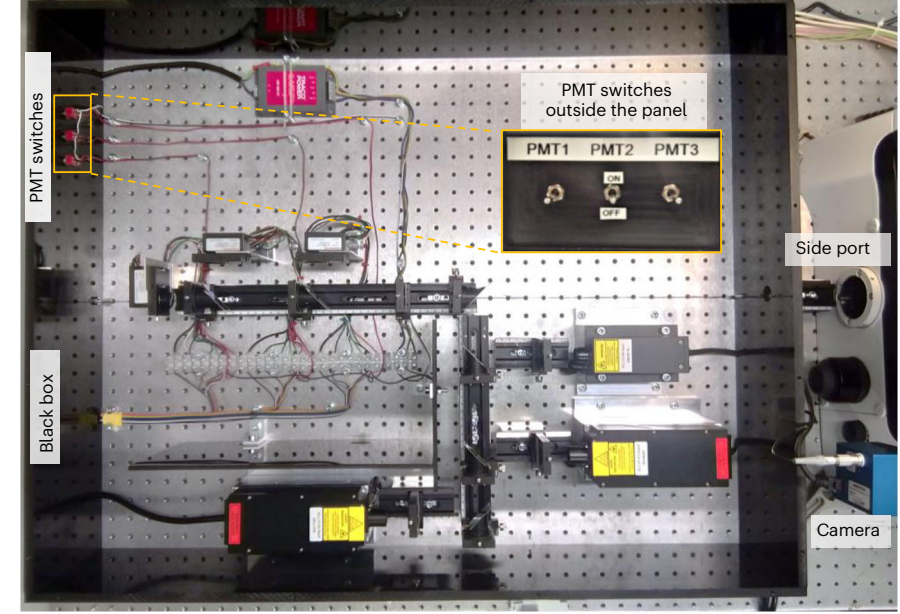


Fig. 5 | Breadboard layout. a, Map depicting the positions of the assembly components to be fixed on the breadboard at their respective coordinates. The black box (thick gray rectangle) defines the periphery of the assembly. The coordinate system has the origin at the left-bottom thread on the periphery and a single unit in the layout is equal to the distance between two holes (2.5 cm). As an example, the coordinates for the screw positions of support blocks for rail E and laser L1 are shown in red and detailed positioning is presented in Extended Data Fig. 2. The line M-M' represents the plane of the microscope's left side port that should make a 90° angle with rail D. **b**, Image of the finished assembly with every component corresponding to the map.

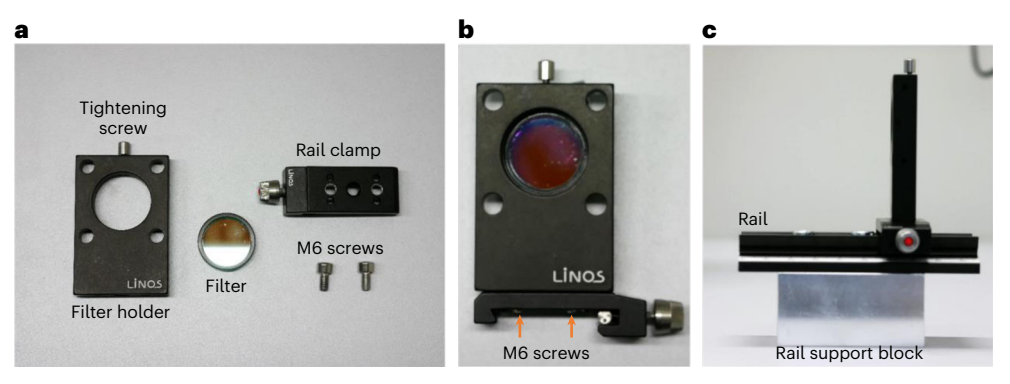


Fig. 6 | Filter holder assembly. a, The essential pieces to mount filters comprise a modified filter holder, a modified rail clamp, a filter and two 1.6 cm M6 screws. **b**, The filter is inserted into the filter holder and held by the tightening screw. Filter and holder mount are fixed and tightened on the rail clamp with the two screws. **c**, Filter holder with a dedicated filter is mounted on the rail/block support assembly thanks to the rail clamp.

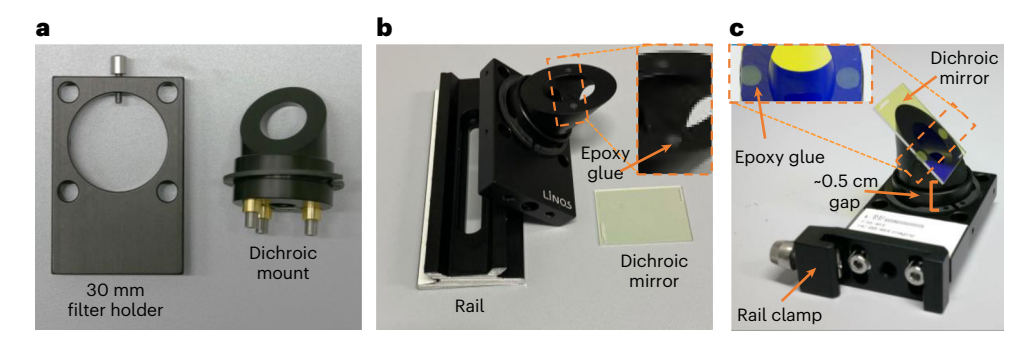


Fig. 7 | Dichroic mirror assembly. a, 30 mm filter holder and dichroic mount. b, The dichroic mount fixed in the 30 mm filter holder and placed beside a rail, to ensure that the flat surface stays horizontal while applying epoxy glue. Drops of epoxy glue on the flat surface are shown in the inset. c, The dichroic mount inserted into the filter holder with the dichroic mirror glued on the mount. The original sticker label of the filter bag is transferred to the filter mount for easy identification during maintenance and upgrading of the workstation.

sliding of the clamps and the filter holder along the rails. The following steps are highlighted in Supplementary Video 1.

- Place filters F1 to F4 in the unmodified 25 mm filter holders (Fig. 6a,b).

 ! CAUTION We advise to stick the filter label on the holder denoting the direction of the arrow on the filter rim as well.
 - !CAUTION Wear gloves while handling optical filters to avoid fingerprints.
- 10 Fix filter holders F1 to F4 on the modified rail clamps (modified as per CAD file in in Supplementary Data 1) using 1 cm M4 screws (Fig. 6b). The modification on the rail clamps helps in easier sliding of the clamp on the rail.
- 11 Clamp F1 to F3 on the rails A–C in front of lasers L1 to L3, respectively, and F4 near the right end of rail G (Fig. 6c). Refer to Fig. 5 for correct positioning.
 - ▲ CRITICAL STEP Make sure the arrow on the filter rim points along the direction of the beam passing through it as per Fig. 2.
- 12 Place filters F5 to F7 in modified 25 mm filter holders (modified as per CAD file in Supplementary Data 1). These filters will be used for PMT mounting in later steps.

Mounting dichroic mirrors Timing 24 h

▲ CRITICAL The dichroic mirrors also need to be mounted on dedicated mounts. For mounting, the dichroic mirrors are glued on commercially available mounts. This helps in easy manipulation of dichroic mirrors without interfering the path of the beam during alignment steps. (The following steps are also illustrated in an animation in Supplementary Video 1.)

13 Fix a dichroic mount in place of the filter in a 30 mm filter holder, such that the flat part of the dichroic mount is perpendicular to the horizontal plane when the holder is standing upright (Fig. 7).

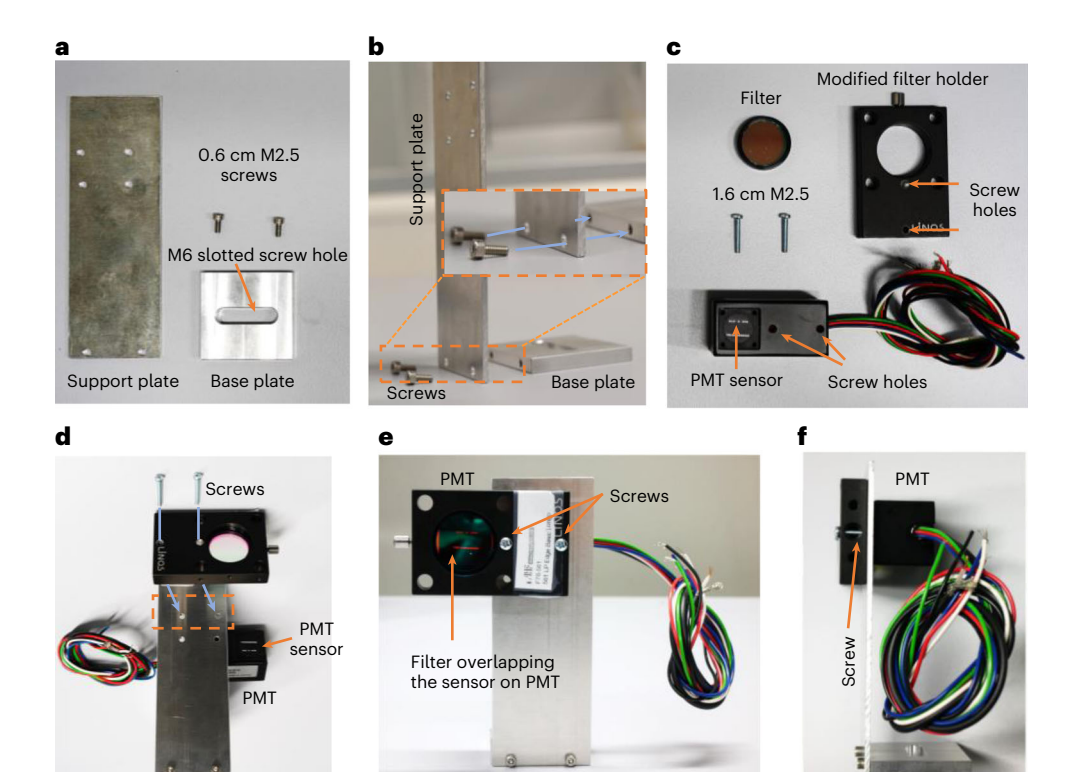


Fig. 8 | PMT mount assembly. a,b, PMT mount made by assembling the support plate (to hold the PMT) and the base plate (to be attached on the breadboard). **c**, Essential components required to mount PMT. **d**, Support plate sandwiched between filter holder and PMT to align the screw holes to fix the assembly. **e**, Front view of the finished PMT mount with the filter overlapping the PMT sensor that is behind it. **f**, Side view of PMT mount with the screws passing through the modifications made in the filter holder to tighten the assembly.

- 14 Mix a two-part epoxy glue and dispose a small drop (\sim 5 μ L) on the border of the flat side of the dichroic mount (Fig. 7b).
- 15 Gently lay the mirror D1 on the flat side of the holder, keeping a gap of ~0.5 cm from the holder base (Fig. 7b,c). The dichroic should be held horizontally while curing to avoid any slipping. Small corrections can still be done by eye to adjust the mirror position while the glue is hardening (within the first 15 min).

▲ CRITICAL STEP Make sure that the side of the dichroic with reflective coating (where the writings are readable) is facing outward while the nonreflective side is facing the mirror mount.

▲ CRITICAL STEP This step is irreversible and must be done with the utmost care to avoid any damage to the dichroic mirror. A small drop of glue should be used to avoid overflowing that may obstruct the optical path. The 0.5 cm gap is important to provide clearance during optical alignment.

!CAUTION Wear gloves while handling mirrors to avoid fingerprints.

16 Repeat Steps 13–15 to prepare mounts for dichroic mirrors D2 to D6 and fix all these mounts on modified rail clamps like in Step 10 and keep them aside.

Mounting PMTs • Timing 30 min

▲ CRITICAL The PMTs are mounted on the breadboard using custom made PMT mounts ('Materials' and Supplementary Data 5). These mounts are designed so that the center of the PMT sensor stays 9 cm above the breadboard to match the height of the emission light projected from the microscope (Fig. 8 and Supplementary Video 1). Furthermore, the baseplate of the mount has slotted holes to accommodate for the fine adjustments in the PMT's position on the breadboard.

- 17 Take a custom-made support plate and a base plate and join them at 90° angle using 0.6 cm M2.5 screws to assemble the PMT mount (Fig. 8a).
- 18 Take out the PMTs P1, P2 and P3 from their container box and carefully remove the safety sticker from the sensor on each PMT.

▲ CRITICAL STEP Note that the PMT H11903-20 that has a higher dynamic range and higher sensitivity to larger (>550 nm) wavelengths is assigned as P3 to gather red fluorescence.

- Hold P1 in its position at one side of the support plate (such that the screw holes of P1 overlaps the holes in the support plate) along with the modified filter holder with filter F5 on the other side, in a way that the filter covers the sensor of the PMT and fix them using 1.6 cm M2.5 screws (Fig. 8b,c). The modification of the filter holder provides two holes that overlaps with the screw positions on the PMT through the support plate (Fig. 8c).
- 20 Fix the P1- filter mount assembly on the breadboard at their respective position as per the map in Fig. 5 using 1.6 cm M6 screws.
- 21 Repeat Steps 19 and 20 for P2 and P3.
 - ▲ CRITICAL STEP Make sure that the P3 is positioned in front of the left end of rail G and the center of F7 is coinciding with the center of the rail. To ensure flexibility, the PMT base plate has slotted holes. The fine tuning of P3 position can be done during emission light alignment in Step 88.

Mounting microscope Timing 1 h

▲ CRITICAL The microscope's positioning is critical to the setup, because the emission light projected from its left side port has to perfectly align with rail G. In the following steps, the microscope is roughly placed at the desired position and the position will be fine-tuned during the emission light alignment procedure. A 3D-printed filter rim (STL file in Supplementary Data 9) is used to install an additional laser clean-up optical filter in the microscope's body that prevents the laser radiation from entering the eyepiece and camera (Supplementary Fig. 3 and Supplementary Video 1).

- 22 Place the microscope on the breadboard with its left side port opening toward the rail D (Fig. 5).
- 23 Adjust the microscope such that the plane of its left side port (i.e., line MM' in Fig. 5) is close to and at 90° angle to the rail D as seen from top and the side port's center aligns with the rail's center (Fig. 5).
 ! CAUTION Do not fix the microscope to the breadboard at this point as its position will be refined during alignment procedure.
- 24 Remove the top-front piece of the microscope that contains the eyepiece using suitable Allen keys. Also dismount the microscope stage to clear the access of the middle piece (Supplementary Fig. 3a).
- 25 Remove the middle-front piece of the microscope that also contains the side port for the camera. You should be able to see an ~3-cm-wide tube with a lens at its bottom (Supplementary Fig. 3a).
- 26 Place the filter F9 on the 3D-printed filter rim and place them both on the tube keeping the arrow on the filter pointing upward (Supplementary Fig. 3a,b).
- 27 Fix the middle-front piece, the stage and the top-front piece of the microscope in their respective positions.
- 28 Mount the camera in the upper left port of the microscope and connect it to the PC via provided ethernet cable.
- 29 Install the 'motion-blitz' software on the PC.

? TROUBLESHOOTING

Electrical connections

Power supply Timing 1 h

▲ CRITICAL The power supply is used to provide ±15 V DC to the PMTs. A single power supply unit is used to connect the PMTs in parallel via three switches to individually control the PMTs (Fig. 9). The wires are connected through modular connector units (termed three- and eight-pin connectors) that not only contribute to robust wiring but also provide easy access if any component needs to be replaced or upgraded in future.

▲ CRITICAL For robust wire connections, the ends of all the wires are secured using crimp ferrules and pliers (Extended Data Fig. 4).

- 30 Take a sufficiently long (2–3 m) power chord with the region-specific wall socket and strip 5 cm of cladding from its rear end to expose the three wires. Identify the wires as live, neutral and ground as per the country-specific color coding for public power supply. Strip and crimp the three wires (Extended Data Fig. 4).
- 31 Connect the live and neutral wires to the dedicated alternating current (AC) inlets in the ±15 V DC power supply. Also connect the ground wire to the common output terminal of the DC power supply (labeled as Com), this terminal serves as the common ground for all the components in the setup (Fig. 9a,b).

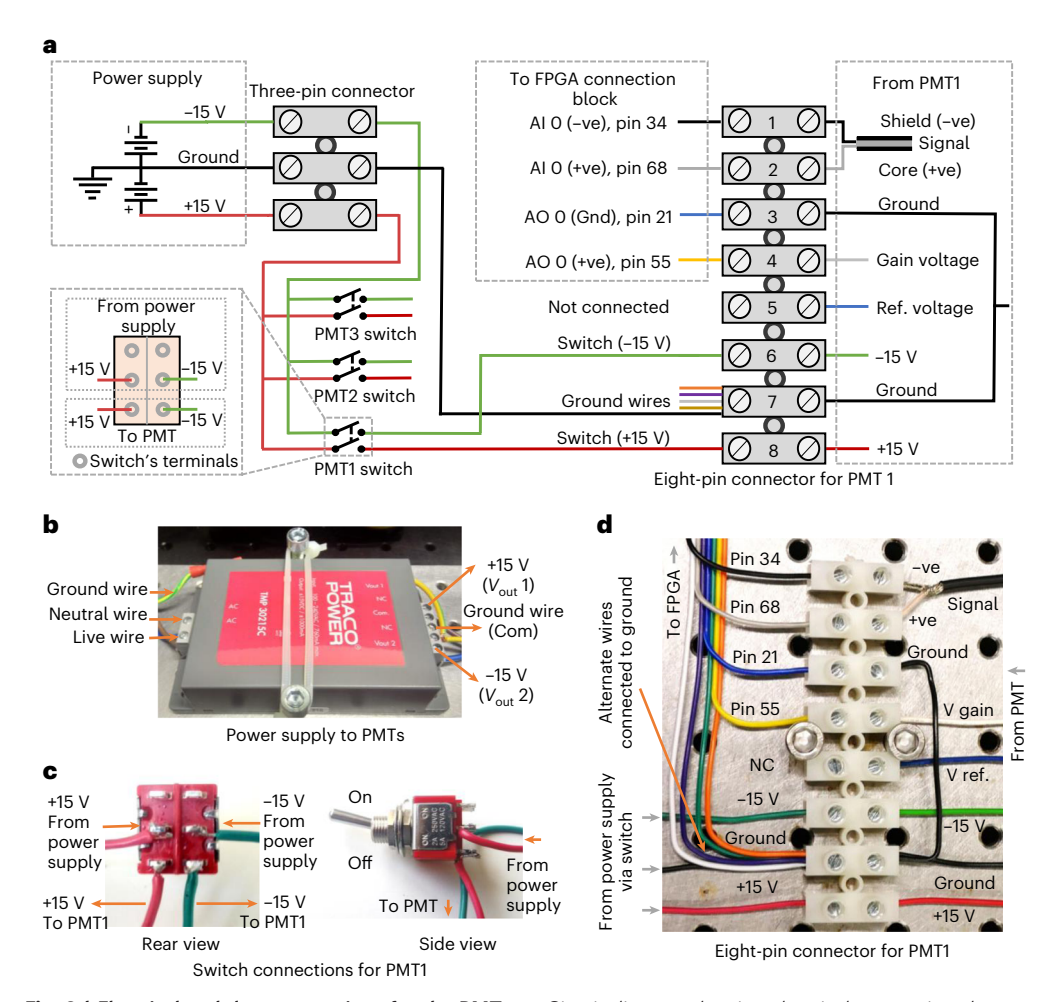


Fig. 9 | Electrical and data connections for the PMTs. a, Circuit diagram showing electrical connections between PMT1, the power supply and the FPGA connection block via eight- and three-pin connectors and dual circuit switches. The zoomed image of the switch shows the wire connections of the dual circuit switch terminals. The diagram follows the color code that resembles the color codes of PMT wires and a similar color code is followed coherently throughout the entire protocol. The numbers (1-8) assigned to individual pins of the eight-pin connector are also shown. **b**, Image of the PMTs' power supply with the incoming connections (live wire, neutral wire and ground wire) and outgoing connections (+15 V, -15 V and ground). **c**, Image of the dual circuit switch with the wiring for switch connections to PMT1 from the power supply as per the circuit diagram. **d**, Image of the eight-pin connector for PMT1 connected as per the circuit diagram.

- 32 Connect the positive (+15 V), negative (−15 V) and ground terminals from the DC power supply (labeled as V_{out} 1, V_{out} and Com, respectively) to a three-pin connector (Fig. 9a,b).

 ▲ CRITICAL STEP If the power supply has any LED, it will interfere with the signals during the
 - experiment and, thus, any such light source should be covered appropriately using several layers of a masking tape or black paint.
- 33 Connect the power chord to the mains supply and measure the voltage between the positive and negative terminals of the three-pin connector using a multimeter, it should read 30 V. Consequently, the voltage between positive terminal and ground, as well as between negative terminal and ground, should read +15 V and -15 V, respectively.
- 34 Tie the power supply, the three-pin connector and the three eight-pin connectors onto the breadboard on positions shown in Fig. 5, using zip ties and 5 cm M6 screws (Fig. 9b).
- 35 Take two differently colored wires and connect them to the positive and negative terminal of the three-pin connector.
- Take a dual circuit switch and solder the positive and negative wires from Step 35 on its middle pins as shown in Fig. 10. A dual circuit switch is preferred because it allows to control two power lines with a single switch.

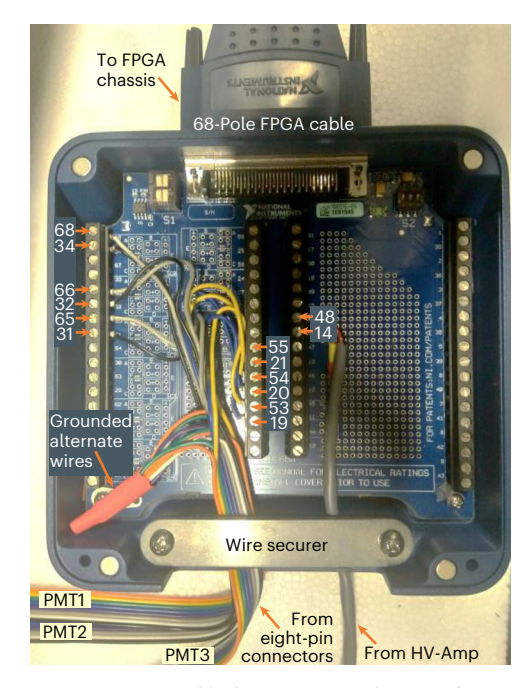


Fig. 10 | FPGA connections. FPGA connector block SCB-68A with wires from PMTs and HV-Amp (trigger), connected to their respective pin numbers. The grounded alternate wires from all three ribbon cables are bundled together using electrical insulation tape.

! CAUTION All soldering procedure must be done with appropriate safety procedure and equipment under a chemical hood or with an adequate ventilation in accordance to the local safety guidelines and laws. The resulting smoke is toxic.

- 37 Take two more wires of the same color as before and solder them to the respective side pins of the double circuit switch (Fig. 9a,c).
- 38 Measure the voltage across the wires taken in the above step; it should read 30 V when the switch is 'on' and 0 V when the switch is 'off'.
- 39 Label the switch as PMT1/blue and connect its positive output wire to the eighth pin of the eight-pin connector dedicated to PMT1. Similarly, connect the negative output to the sixth pin of the eight-pin connector (Fig. 9).
- 40 Connect two more double circuit switches (for PMT2 and PMT3) in parallel to the power supply of the first switch and repeat Steps 36–39 with the new switches.
- 41 Label the two switches as PMT2/green and PMT3/red and connect them to separate eight-pin connectors (B and C), dedicated to PMT2 and PMT3, respectively.
- 42 Connect every third and seventh pin of the three eight-pin connectors to the ground terminal of the three-pin connector (Fig. 9d).

PMT connections Timing 30 min

▲ CRITICAL Every PMT comes with eight wires out of which three are dedicated for power supply (+15 V DC, -15 V DC and ground), four are for data communication with FPGA card (positive signal, negative signal, gain voltage and ground) and one is left unconnected. In the following steps, the wires form all the three PMTs are connected to their respective eight-pin connectors that were mounted on the breadboard in Step 34.

- 43 Connect the positive and negative input voltage terminals of the PMT to the eighth and sixth terminals on their respective eight-pin connectors (Fig. 9a,d).
 - ▲ CRITICAL STEP The Hamamatsu PMTs follow a color coding where red wire is positive and green is negative. However, these conventions might vary and one should refer to the PMT datasheet to confirm terminal allocation.
- 44 Connect the positive (core wire of the thick black wire) and negative (cladding wire of the thick black wire) signal output terminal from the PMTs to the second and first pin of their respective eight-pin connectors (Extended Data Fig. 5). The signal output cable of the PMT is a coaxial cable with core as positive terminal and shielding wire as negative terminal (Fig. 9a,d).

Table 3 | Pin numbers of the FPGA connector block SCB-68A, assigned to represented functions and devices

Pin no.	Channel	Function	Device	Wire color ^a
68	AI 0	Positive signal	PMT1	Gray
34		Negative signal		Black
55	AO 0	Gain voltage		Yellow
21		Ground		Blue
66	Al 1	Positive signal	PMT2	Gray
32		Negative signal		Black
54	AO 1	Gain voltage		Yellow
20		Ground		Blue
65	Al 2	Positive signal	PMT3	Gray
31		Negative signal		Black
53	AO 2	Gain voltage		Yellow
19		Ground		Blue
48	AO 7	Trigger	High-voltage amplifier	Red
14		Ground		Black

^aThe wire color refers to the connections shown in Fig. 9d as per the color code followed in this protocol.

- 45 Connect the gain voltage input terminal (white wire) from the PMTs to the fourth pin of their respective eight-pin connectors (Fig. 9a,d).
- 46 Connect the ground terminal (black wire) for each PMTs into the ground terminal (seventh pin) of their respective eight-pin connector (Fig. 9a,d).
- 47 Connect the reference voltage terminal (blue wire) to the fifth pin of the eight-pin connector for each PMT (pin numbers on the eight-pin connector are shown in Fig. 9a). The reference voltage output is not used in our setup, and we are connecting this wire just to avoid free-hanging wires in the setup.

FPGA I/O connections Timing 1 h

▲ CRITICAL The FPGA is the brain of the workstation that communicates with the PMTs to provide gain voltage and gather data and also with the high-voltage amplifier to provide it the trigger signal when needed. The FPGA board used in this protocol (NI PXIe-7856R) comes with a dedicated connector block (SCB-68) that allows to connect wires for various I/O connections. These I/O connections are made in the following steps:

▲ CRITICAL As the FPGA connection block configuration may vary depending upon its model number and FPGA card used, the correct configuration has to be confirmed from the connector block's datasheet.

- 48 Take three ribbon cables of two meters each. These ribbon cables should have eight multicolored wires in each strip to provide a convenient color convention for all data connections.
- 49 Every alternate wire in each ribbon has to be grounded. This provides an electromagnetic shielding to the signal carrying wires and prevents interference noises from surroundings. For this, the alternate wires are crimped together and connected to the seventh pin of the eight-pin connector that was grounded in Step 42.
- 50 Two out of the four remaining wires for each PMT are for positive and negative signal acquisition and are inserted in the second and first pin of the eight-pin connector. These are to be connected to the AI ports of the FPGA connector block, SCB-68A (Table 3 and Fig. 10).
- 51 The other two wires provide the gain voltage and ground to the PMT and, thus, are connected to the fourth and third pin of the eight-pin connector. These will be connected to their respective analog output (AO) ports of the SCB-68A as per Table 3.
 - ▲ CRITICAL STEP A uniform color convention should be followed while assigning the terminals for each ribbon and the color should be noted.
- 52 For signal acquisition, connect the wires to the respective positive and negative terminals of AI 0 (pins 68 and 34), AI 1 (pins 66 and 32) and AI 2 (pins 65 and 31) for each PMT sequentially (Table 3 and Fig. 10).

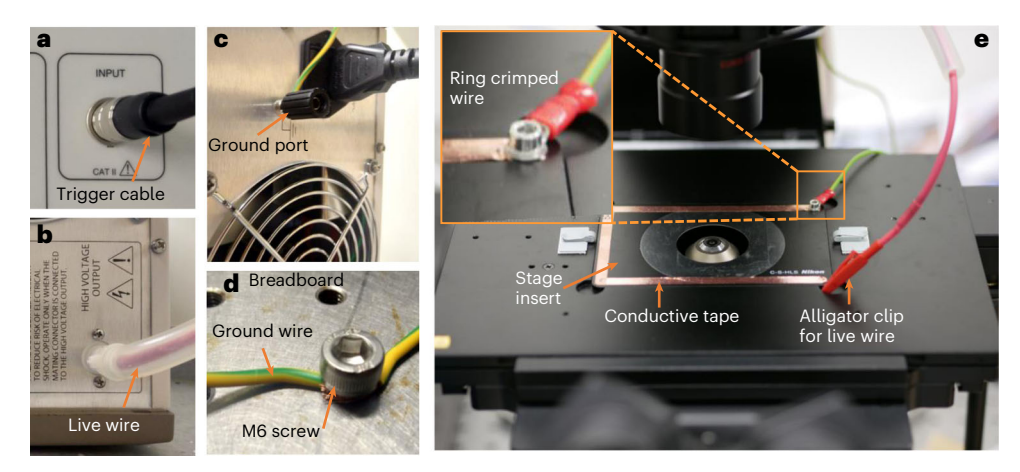


Fig. 11 | High-voltage amplifier connections and grounding. a, Trigger cable in its socket in the front panel of the amplifier. **b**, Live wire connected to its dedicated port on the back panel of the amplifier. **c**, Grounding wire in its port on the back panel of the amplifier. **d**, Grounding wire connected to the breadboard using an M6 screw. **e**, Conductive copper tape covering the periphery of the microscope stage insert. Grounding wire (from the breadboard) connected to the stage insert using crimp and screw (inset). The alligator clip is connected to the live wire from the high-voltage amplifier.

- 53 For the gain voltage, connect the wires to the respective positive and ground terminals of AO 0 (pins 55 and 21), AO 1 (pins 54 and 20) and AO 2 (pins 53 and 19) for each PMT sequentially (Table 3 and Fig. 10).
- 54 Tape the free end of the ground wires from Step 49 together and leave them disconnected inside the connection block (Fig. 10).
- 55 Label the ribbon cables to represent the respective PMT and also secure the cables tightly at the connector box end as well at the breadboard end using zip ties.

High-voltage amplifier connections Timing 30 min

▲ CRITICAL The high-voltage amplifier provides a high-voltage (0.5–1.5 kV) pulse to the microfluidic chip every time the FPGA sends it a trigger. The amplifier thus needs to be connected to the FPGA, as well as to the microfluidic chip. In the following steps, these connections are described:

!CAUTION High-voltage safety rules should be followed and the amplifier should be kept turned off unless specified to turn on. The current (limited to 0.05 Amp) can cause painful shock, respiratory arrest, severe muscle contractions and other adverse effects.

- 56 Connect the trigger cable provided with the high-voltage amplifier to its dedicated socket in the amplifier's front panel (Fig. 11a).
- 57 Connect the crimped signal wire (red) from the open end of the trigger cable to the positive terminal of the AO 7 (pin 48) (Table 3, Fig. 10 and Extended Data Fig. 4).
- 58 Connect the crimped ground wire (black) from the trigger cable to the ground terminal of AO 7 (pin 14) (Fig. 10 and Extended Data Fig. 4).
- 59 Secure the trigger cable on the connection block along with the ribbon cables (Fig. 10).
- Connect the thick red cable for power output provided with the amplifier to its port on the back panel (Fig. 11b). This wire works as the live wire that delivers the high voltage to the microfluidic chip.
- 61 Connect an insulated alligator clip on the other end of the thick red wire and secure the wire close to the microscope stage (Fig. 11e).

Electrical grounding • Timing 30 min

▲ CRITICAL Electrical grounding is an essential step to ensure safety of any electrical circuit. In our setup, grounding of the microfluidic chip used for droplet sorting is also needed²². In the following steps, we first ground the breadboard to ensure safety from any accidental connection between high voltage and the conductive breadboard. Then we ground the microscope stage so that the microfluidic chips kept on it will be grounded too.

!CAUTION Never turn on the high-voltage amplifier without finishing the following steps for grounding.

- 62 Take two thick multicore and insulated copper wires of 1 m each and connect ring crimps to the ends of both the wires.
- 63 Connect one end of a wire to the ground port located at the backside of the high-voltage amplifier (Fig. 11c).
- 64 Connect another end of the grounded wire along with one end of the other wire to the bread board using a 1.6 cm M6 screw (Fig. 11d).
- 65 Take 5-mm-wide conductive copper tape and stick it on the peripheries of the microscope stage insert as shown in Fig. 11e.
- 66 Make a whole in the copper tape that overlaps with the threaded whole in the top right of the stage insert (Fig. 11e).
- 67 Connect the crimped end of the second wire to the stage using a 1 cm M3 screw and a washer (Fig. 11e).
- 68 Take a multimeter in contact mode and contact one of its probes to the breadboard. Contact the other probe first to the copper tape on the stage and then to the grounding port of the high-voltage amplifier. The multimeter should make a beep sound in both cases, confirming proper grounding. **!CAUTION** Never switch on the high-voltage amplifier without checking the proper grounding as per the above step.

? TROUBLESHOOTING

Optical alignment

Emission light alignment Timing 1 h

▲ CRITICAL The workstation setup is now ready for optical alignment procedure. It starts by aligning the emission light projected from the side port of microscope with the rail G that will carry the optical setup to distribute emission signals form the microscope among three channels (blue: 425–465 nm; green: 505–545 nm and red: 580–630 nm) and direct these signals toward their respective PMT. 3D-printed aperture disk (Supplementary Data 8) is used to reduce the diameter of the emission beam so that its brightest (central) part can be overlapped with the PMT sensor for precise alignment. Emission light alignment also finalizes the position of the microscope on the bread board. The complete emission light alignment procedure is also demonstrated in an animation video (Supplementary Video 2, emission alignment).

- 69 Turn on the camera and the brightfield lamp of the microscope mounted with 40× objective lens. Increase the lamp's intensity to maximum and open its shutter completely.
- 70 The light from the lamp should come out through the left side port as a wide beam and can be viewed using any white sheet (Extended Data Fig. 6).

? TROUBLESHOOTING

71 This beam should pass through the filter F4 and should fall on PMT3 via filter F7 (Fig. 2). However, as the microscope is not perfectly positioned, the beam might not be colinear with the straight path defined by the filters.

? TROUBLESHOOTING

- 72 Gently move and tilt the microscope body in very small steps to make the emission beam coinciding as good as possible to the center of filter F7 while passing through the center of F4. This concludes the coarse alignment process, and the following steps describe fine tuning.
- 73 Fix the 3D-printed target and aperture discs on 25 mm filter holders and modified rail clamps (like the optical filters are mounted in Steps 9–10 and Fig. 5). The 3D-printed aperture and target discs already have indentations for gridlines. Marking these gridlines with a black pen is advised to ease the alignment process (Fig. 12a). We further recommend using a white material (polylactic acid) when 3D printing for better contrast during alignment.
- 74 Place the aperture and target discs on the left end of rail D and G, respectively (Fig. 12a).
- 75 Place the alignment chip on the microscope stage such that the alignment line appears horizontal on the camera. The alignment chip has a microfluidic channel that has to be filled with molten indium alloy to generate a thin alignment line (fabrication discussed in Box 2) (Extended Data Fig. 7).

 Δ CRITICAL STEP An empty microchannel in the alignment chip would also cast a discernible projection; however, the dark and opaque metal provides much better contrast that eases the alignment process. Alternatively, any other object with a thin (10–100 μm) line can pe placed on the microscope instead of an alignment chip.

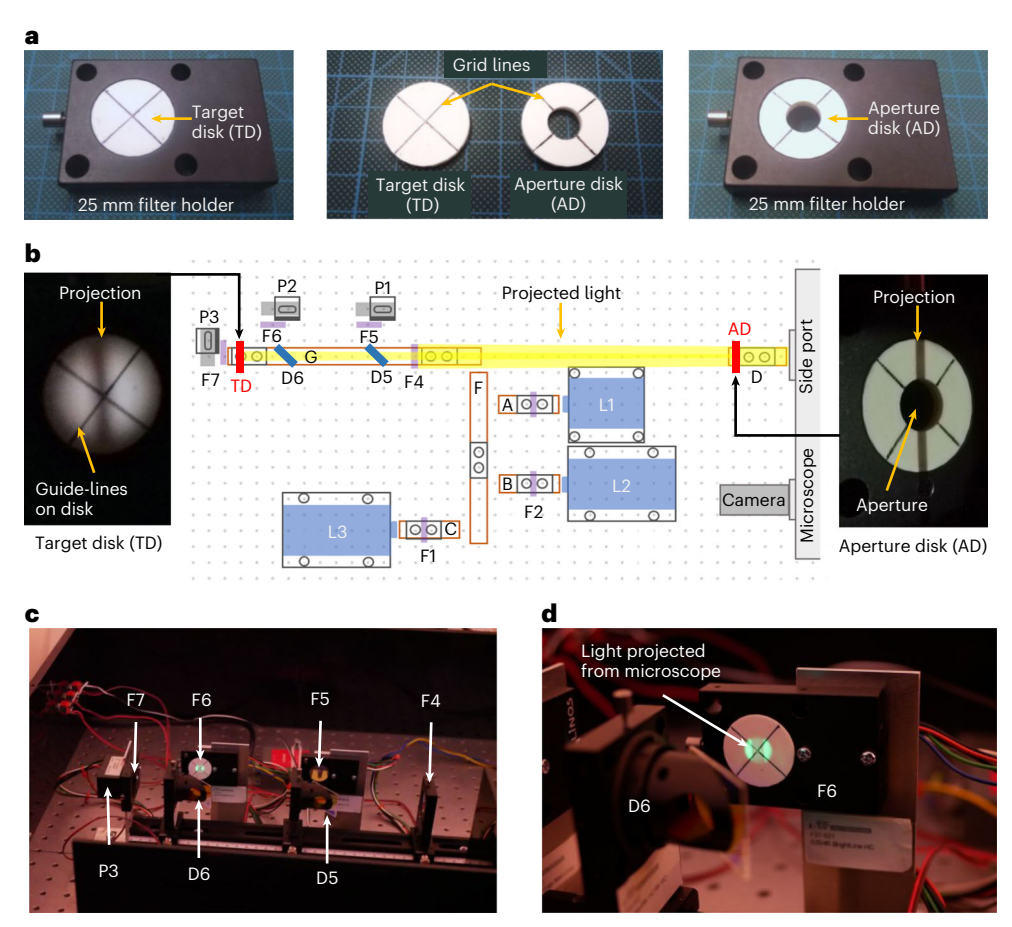


Fig. 12 | Emission light alignment. a, Target disk (TD) and aperture disk (AD) mounted in the 25 mm filter holders. Both disks are 3D printed in white material (polylactic acid) for a better contrast during alignment (.stl file in Supplementary Data 7 and 8). b, Positions of target disk holder and the aperture disk holder are shown along with the centered projections of the alignment line on the disks. The target disk and the aperture disk are used to observe and align the projection of the alignment line's image coming out from the microscope's side port. The image is sharper on the aperture disk as it is placed close to the back focal plane of the microscope. Similarly, the target disk shows the enlarged and blurred projection of the fraction of beam that passed through the aperture disk. The positions of dichroic mirrors (D5 and D6) are also shown. Note that the filters (F1-F7) are already installed in previous steps. c, Actual image of the finished emission assembly. d, Close-up of the filter F6 showing a perfectly aligned emission beam at the center of the filter. Note that the white disk is used in front of the filter only for better visualization of projected light; it is not part of the assembly. This alignment process is also demonstrated in Supplementary Video 3.

- 76 Mark the camera window using gridlines with horizontal and vertical spacing of 320 and 256 pixels, respectively (Extended Data Fig. 7).
- 77 Focus the image and center the electrode on the screen (Extended Data Fig. 7).
- 78 You should be able to see the physical projection (rotated by 90°) of this image on the aperture disk (Fig. 12b).
- Move the microscope front or back in very small steps to center the electrode projection on the aperture, such that the electrode image is crossing through the center of the hole in the disk (Fig. 12b).
- 80 Once the electrode image is centered on the aperture disk, the fraction of the image that is passing through the aperture has to be centered on the target disk. In case the microscope body (line MM') is making a perfect 90° angle with the rails, the image fraction should already be centered on the target disk.
- 81 An enlarged and 'out of focus' fraction of the electrode image should be visible on target disk if the microscope is aligned perfectly with rails in Step 79 (Fig. 12b). This projection can be improved by moving the focus knob of the microscope, if needed.
 - ? TROUBLESHOOTING

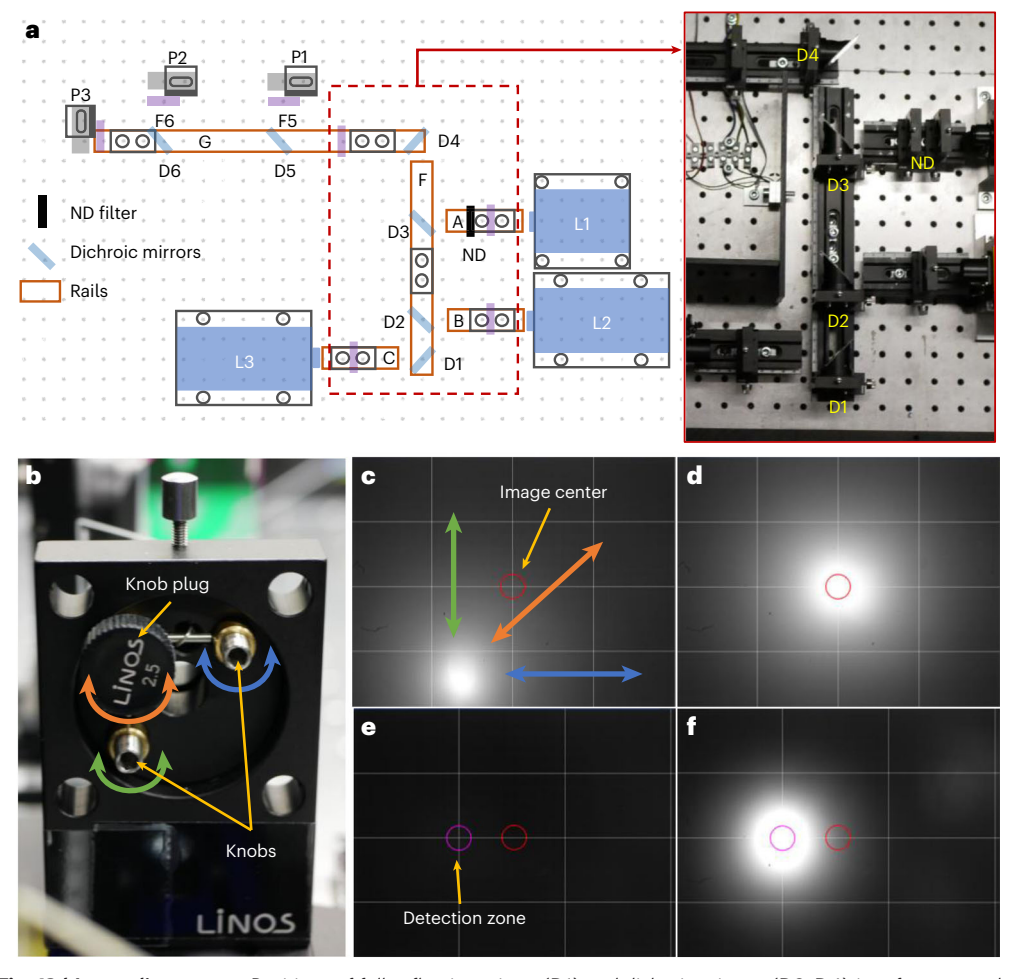


Fig. 13 | Laser alignment. a, Positions of full-reflective mirror (D1) and dichroic mirrors (D2-D4) in reference to the map. **b**, Knobs at the rear side of the dichroic mount. A single knob plug is used to rotate the knobs and is moved to a new knob when desired position of the laser spot is achieved. **c**, Fluorescent spot (on the fluorescent slide) visible (through the camera) at an arbitrary position through a 20× objective lens. The gridlines are set to a horizontal and vertical spacing of 320 and 256 pixels, respectively, and the red circle marks the center of the field of view. The arrows show the trajectory of the spot when the corresponding knob (color coded) is rotated. **d**, Fluorescent spot moved to the center of the field of view. **e**, The gridlines modified to a horizontal spacing of 420 pixels and a magenta circle placed at (420, 256) pixels denoting the detection zone through a 40× objective lens. **f**, Fluorescent spot moved to the magenta circle to coincide with the detection zone.

- 82 If the image is not centered on both discs, tilt the microscope in very small steps till the electrode image is centered on both discs.
- 83 Remove the target, aperture and microfluidic device from the stage and turn the objective turret to a blank position. This increases the brightness of the output beam to ease up the next alignment steps.
- 84 Place the aperture disk on the right end of the rail G.
- 85 Place the dichroic mount D5 on the rail G beside P1, such that the reflection from the dichroic is falling near the center of filter F5. Fix the rail clamp at this position (Fig. 12c,d).
- Adjust the tilt control knobs on the back of the dichroic mount D5 to move the reflected beam to the center of filter F5 (Figs. 12c,d and 13b).
- 87 Place the dichroic mount D6 on the rail G beside P2 and repeat Steps 85 and 86 (Fig. 12c,d).
- 88 Adjust the PMT3 holder position to center the transmitted beam on F7 (Supplementary Video 2). The beam also gets further cropped by the dichroic mounts and only a thin beam of ~5 mm diameter is allowed to fall on the PMTs. The fixed height of the assembly along with the alignment ensures that this thin beam carries the signals transmitted only through the detection region.
- 89 Remove aperture disk from the rail G, turn off the brightfield lamp and fix the microscope at this position permanently using four clamping forks (Extended Data Fig. 8).

Laser alignment Timing 3 h

▲ CRITICAL Once the microscope's position is fixed on the bread board, we can align the beams from lasers L1 to L3 so that they coincide at a specific point that defines the detection zone in the field of view of microscope with a 40× objective. The detection zone is made off-centered because for sorting applications with high-magnification objectives such as 40× it is preferable to align the lasers rather at one edge of the field of view (Fig. 15b). This allows one to have a bigger distance between the detection point and the sorting divider. If centered, it is often not possible to see if droplets end up in the collection channel. The complete laser alignment procedure is also demonstrated in an animation video (Supplementary Video 3, laser alignment).

!CAUTION Exposure to laser radiation can cause injuries to eye and skin. Use protective equipment such as laser viewing cards, safety glasses and ND filters when lasers are on.

- 90 Take two 25 mm filter holders fixed on the modified rail clamps (as used in Steps 9–10) and place an ND filter with 10% transmission in each of them.
- 91 Mount these ND filter holders on rail C in front of the laser L3. The ND filters make sure that the intensity of the laser beam used for alignment is less harmful.
- 92 Place the target disk on the far end of rail E.
- 93 Place the dichroic mount D1 (with the full-reflective mirror D1) on rail F in front of L3 and turn on the laser L3 (Fig. 13a).
- 94 Move D1 along the rail F till the laser beam incidents approximately at the center of the mounted dichroic. Fix the dichroic holder's rail clamp at this position. Use the laser viewing card to detect the laser beam and its incident point on the dichroic surface. The reflected laser beam should also be visible somewhere close to the target.
- 95 Adjust the tilt control knobs at the back of the dichroic mount to move the beam and bring it to coincide with the target's center (Fig. 13b).
- 96 Turn off the laser L3 and move the two ND filters from rail C to rail B.
- 97 Turn on laser L2 and repeat Steps 93-95 with dichroic mount D2.
- 98 Turn off the laser L2 and move the two ND filters from rail B to rail A.
- 99 Turn on laser L1 and repeat Steps 93-95 with dichroic mount D3.
- 100 Turn off laser L1 and remove the ND filters.
- 101 Move the target disk from rail E and fix it on the far end of rail D.
- 102 Place the dichroic mount D4 on rail G and turn on laser L1 (Fig. 13a).
- 103 Move D4 along the rail G until the L1 beam incidents approximately at the center of the mounted dichroic. Fix the dichroic holder's rail clamp at this position. The reflected laser beam should be visible close to the target disk again.
- 104 Adjust the tilt control knobs at the back of the dichroic mount D4 to move the beam and bring it to coincide with the target disc's center (Fig. 13b).
- 105 Turn off the laser L1 and move the two ND filters from rail A to rail B.
- 106 Turn on laser L2. The beam should be visible close to the target disc's center, and the tilt control knobs of D2 should be adjusted to move the beam exactly to the target disc's center.
- 107 Turn off the laser L2 and move the two ND filters from rail B to rail C.
- 108 Turn on laser L3 and repeat Step 106 with dichroic mount D1.
- 109 Remove the target from rail D.
- 110 Rotate the microscope turret to get the 20× objective in the main position.
- 111 Mark the center of the field of view of the camera using the marker (denoted as M) option on the software control panel (Fig. 13c). Alternatively, any other means (e.g., tape or erasable marker) can be used to mark the center directly on the screen.
- 112 Place the red fluorescent slide on the microscope stage.
- 113 The fluorescence from the slide should be visible on the camera as a bright spot (Fig. 13c). The size of the spot can be controlled by changing frame rate and shutter speed on the camera control panel (Extended Data Fig. 9).

? TROUBLESHOOTING

- 114 Turn the focusing knob up or down until the spot appears brightest and smallest (Supplementary Fig. 13c).
- 115 Move the laser spot toward the mark on the center of the screen using the tilt control knobs of D1 (Fig. 13d).
- 116 Turn off L3 and move the ND filters form rail C to rail B.
- 117 Turn on L2 and repeat Steps 113 and 115 using a green fluorescent slide and D2.
- 118 Turn off L2 and move the ND filters form rail B to rail A.

- 119 Turn on L1 and repeat Steps 113 and 115 using a blue fluorescent slide and D3.
- 120 Turn off L1, remove the markers and change the objective of the microscope to 40×.
- 121 Repeat Steps 111-119 with the 40× objective.
- 122 Change the horizontal gridline spacing to 420 pixels and place one more mark on the screen to represent the detection zone, which is centered at the mark at 420 pixels from the left and 256 pixels from the bottom of the camera window (Fig. 13e).
- 123 Move the tilt control knobs of the dichroic mount D4 to move the fluorescent spot toward the second marker (Fig. 13f).
- 124 Turn off L1 and move the ND filters from rail A to rail B.
- 125 Place the green fluorescent slide on the microscope stage and turn on L2.
- 126 If the fluorescent spot of L2 is not at the second mark, move the tilt knobs of dichroic mount D2 to align the spot with the mark.
- 127 Turn off L2 and move the ND filters from rail B to rail C.
- 128 Turn on L3 and repeat Step 126 using the red fluorescent slide on the microscope stage.
- 129 Turn off L3 and remove the ND filters from rail C.
- 130 This concludes the laser alignment. Cover the optical setup by assembling the black box parts, machined using the provided CAD files as per the assembly map (Fig. 5).
- 131 Place F8a along with the 25 mm filter holder on the diffuser lens under the brightfield lamp and cover the gaps using opaque tape (Extended Data Fig. 10). As the filter F8a is dedicated for transmittance- and fluorescence-activated sorting, it should be replaced with filter F8b if the setup is used for three-color fluorescence sorting.

Computational setup

FPGA card installation • Timing 2 h

▲ CRITICAL The computation power of the workstation to conduct high-speed and real-time calculations comes from the FPGA board (NI PXIe-7856R, Part 45). This FPGA board is installed externally in a chassis (NI PXIe-1073), and it communicates with the PC via a PCIe card (PCIe-8361) that has to be installed on the PC's motherboard. In the following steps, we first install the PCIe card and the FPGA card and then verify the installation:

- 132 Turn off the PC from the main power supply and open the CPU cabinet.
- 133 Locate an empty PCIe slot on the motherboard (Supplementary Fig. 4a-c).
 !CAUTION To prevent electrostatic discharge or electric shock from stray charges, do not touch the exposed metal parts inside the CPU.
- 134 Install the PCIe-8361 card in the empty PCIe slot in the CPU and close the cabinet (Supplementary Fig. 4a-c).
- 135 Connect the PCIe cable (provided with part 47) to its dedicated port on the PCIe card, now situated at the rear panel of the CPU cabinet.
- 136 Turn on the PC and insert the DVD called 'NI PXI Platform Services 19.5' provided with the PCIe card. The NI PXI Platform Services can also be downloaded online from the website www.ni.com.
 !CAUTION The version number (i.e., 19.5) may differ depending on the manufacturing date of the PCIe card.
- 137 Open the DVD contents and double click on file name 'setup' and follow the instructions on screen to install all the available drivers for NI-PXI hardware.
- 138 Insert the USB stick named 'NI System Driver Set 4-2019' provided with the FPGA kit. The NI Service Driver Set can also be downloaded online from the website www.ni.com.
 - **! CAUTION** The version number (i.e., 19.5) may differ depending on the manufacturing date of the PCIe card.
- 139 Double-click on the file name 'setup' and follow the instructions on screen to install all the available drivers for NI services.
- 140 Install the following software with versions 2016 or later on the host PC before installing the hardware for the FPGA setup.
 - LabVIEW (Full or Runtime engine)
 - LabVIEW Real-Time Module
 - LabVIEW FPGA Module
 - NI R series Multifunction RIO Device drivers (Version 19.1)

- ▲ CRITICAL STEP Even though NI PXIe 7856R is compatible with 2016 and later versions of LabVIEW, we suggest the version 2019 as the provided LabVIEW program was developed in LabVIEW 2019 and might not provide complete compatibility with older versions.
- 141 Place the PXI chassis (NI PXIe-1073) close to the CPU and locate its ports to connect the PCIe cable and 68-pin cable (Supplementary Fig. 4d,e)
 - ▲ CRITICAL STEP If the FPGA card (NI PXIe-7856R) is not preinstalled in the PXI Chassis (NI PXIe-1073) refer to the NI user manual (https://www.ni.com/pdf/manuals/378000b.pdf).
- 142 Connect the PCIe-8361 card from the CPU to the port at the backside of the PXI Chassis via the PCIe cable provided with the PCIe card (Supplementary Fig. 4d).
- 143 Connect the SCB-68A to the Connector 0 (RMIO) port of the FPGA module via a shielded 68-pin cable, SHC68-68-RDIO (Supplementary Fig. 4e and Fig. 10).
- 144 Turn on the PXI Chassis and reboot the PC.
- 145 To verify the installation, open NI MAX program in the PC and expand the 'Devices and Interfaces' tab. The PXIe-1073 Chassis should appear in the tab showing PXIe-7856R in its pulldown menu (Supplementary Fig. 4f).
- 146 If the NI Max program is not installed during LabVIEW installation, download and install the NI System Configuration package from NI webpage (version later than 16).

TFADS installation • Timing 5 min

▲ CRITICAL The workstation also requires a user interface to control the droplet sorting operation. For this purpose, we provide a custom-made LabVIEW-based interface termed 'Transmittance and Fluorescence Activated Droplet Sorting' or TFADS (Supplementary Software 1). In the following steps, we install TFADS on the PC. The functions of TFADS are discussed in detail in Box 1 and Supplementary Video 4:

- 147 Open the provided source file (Supplementary Software 1 'TFADS_LabVIEW_Application_2022.zip') and save the contents of the 'TFADS_LabVIEW_Application_2022' folder in the PC hard-drive in a new folder and name it 'TFADS'.
- 148 Right click on the icon 'TFADS_Application_2022' click on send to desktop to make a shortcut path on the desktop.
- 149 Go to desktop and double-click on 'TFADS' icon to open the program. The operation of 'TFADS' is discussed in detail in Box 1.

Workstation setup validation Timing 30 min

▲ CRITICAL Now that the workstation build-up is complete, some quick tests can be conducted to validate that its components are working as desired and that all the wirings and hardware/software installations are correct. We use the workstation to excite a blue florescent slide (that mimics a passing droplet with blue fluorescence) and register its fluorescence through the PMTs. A peak in the fluorescence signal from the PMT1 as seen on TFADS interface indicates that the connection is correct. Similarly, the other PMTs are checked with green and red fluorescence slides. The TFADS initiation is also demonstrated in Box 1 and Supplementary Video 4.

- 150 Turn off the ambient lights and the brightfield lamp of the microscope.
- 151 On TFADS application (opened in Step 148), click on the run button (arrow) in the top left corner of the window to start the application (Box 1).
- 152 The application window should show a live data plot and a control panel along with the 'Assign FPGA ports' tab. The live data plot should be showing random noise, usually in the form of sine waves (Fig. 14a).
- 153 In 'Assign FPGA ports' tab, assign the correct FPGA card as PXI1Slot2 along with the ports for the three PMTs and a high-voltage amplifier as AI/O-0, AI/O-1, AI/O-2 and AO7, respectively.
- 154 Connect the power chord of the PMT power supply to the mains and turn it on.
- 155 Turn on the PMTs one by one using their corresponding switches at the side panel of the black box. The live data should show a fluctuation in the plot every time the corresponding PMT is turned on, indicating that communication is established correctly (Fig. 14a).
 - **! CAUTION** Before turning on the PMTs, make sure that the lights in the room are turned off and the gain values in the control panel are set to a minimum (0.25) for each PMT to avoid PMT saturation. **? TROUBLESHOOTING**
- 156 Turn on laser L1 (405 nm) and wait till it is emitting.
 - !CAUTION Laser safety guidelines must be followed.

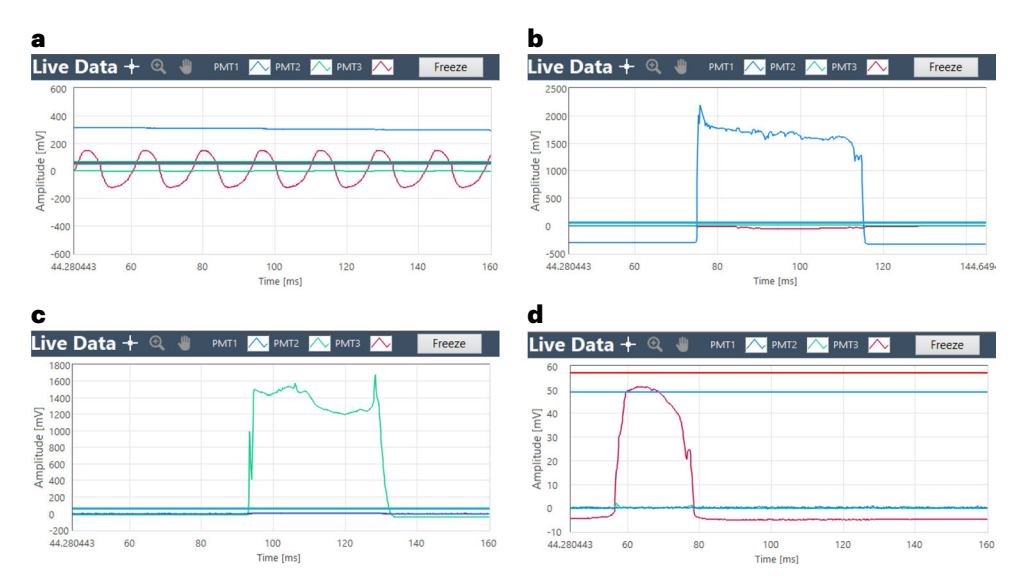


Fig. 14 | Workstation setup validation. a, Live data plot screenshot when PMT1 and PMT2 are just turned on, while the red plot of PMT3 is still showing the sinusoidal noise signal, indicating that PMT3 is not on yet. **b**, Live data plot showing a blue fluorescence peak when the blue fluorescent slide is passed over the objective lens. **c**, Live data plot showing a green fluorescence peak when the green fluorescent slide is passed over the objective lens. **d**, Live data plot showing a red fluorescence peak when the red fluorescent slide is passed over the objective lens.

- 157 Hold a blue fluorescent slide and pass it quickly over the objective lens of the microscope.
- 158 The blue plot in the live data plot, which corresponds to PMT1, should show an irregular-shaped peak each time the slide is passed over indicating a correct connection (Fig. 14b). The other plots (corresponding to PMT2 and PMT3) will also show a fluctuation because of the wide emission spectra of fluorescent slides; however, the peak of the signal detected in PMT1 should be highest in amplitude.

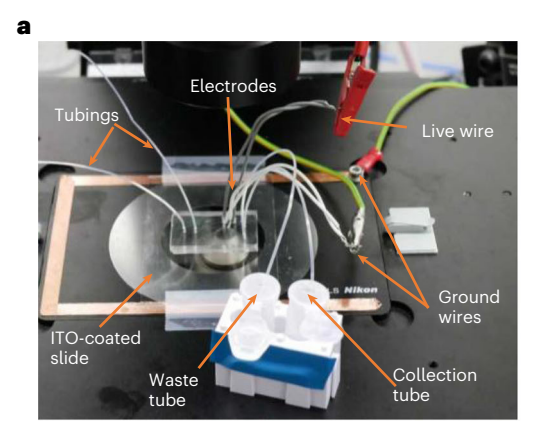
? TROUBLESHOOTING

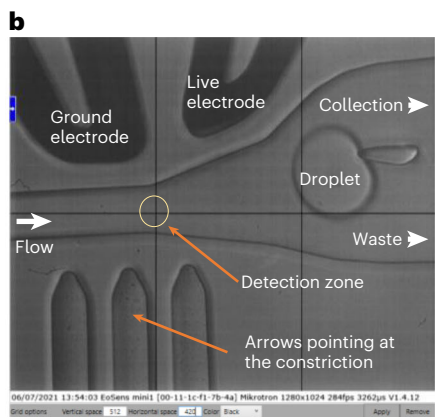
- 159 Repeat Step 157 with green fluorescent slide. The green plot in the live data, corresponding to PMT2, should show a peak as in Step 158, indicating correct connection (Fig. 14c).
- 160 Repeat Step 157 with red fluorescent slide. The red plot in the live data, corresponding to PMT3, should show a peak as in Step 158, indicating correct connection (Fig. 14d).
- 161 Click on the STOP button in the bottom right corner of the application window to stop the TFADS application (Box 1).

Initializing a droplet sorting experiment Timing 3 h

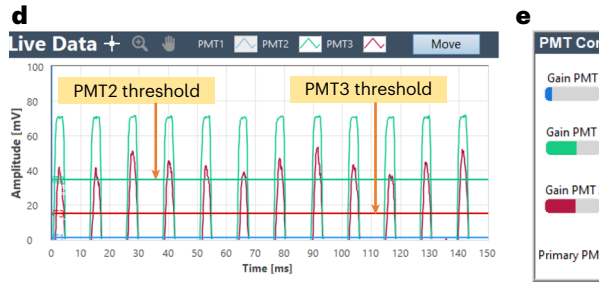
▲ CRITICAL The following steps allow the readers to get familiar with the general practices that are followed in any droplet sorting workflow. These practices include placement of the microfluidic chip, turning on the workstation, initiating the camera and TFADS interface, on-chip droplet generation, optimizing the high-voltage parameters for efficient droplet sorting and testing the sorting efficiency.

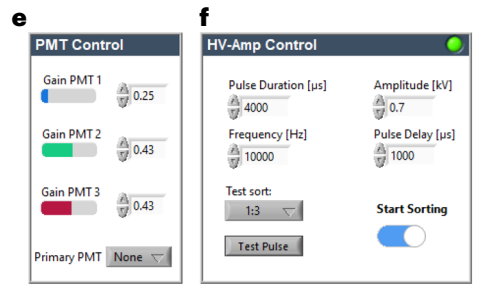
- 162 Prepare the microfluidic chip for droplet sorting as described in Box 2 and place it on the microscope stage such that the ITO-coated glass slide touches the conductive tape on the stage (Fig. 15a). The microfluidic chips can either be fabricated in the clean room (using the CAD files in Supplementary Data 10 and description in Box 2), or can they be ordered from commercial suppliers (e.g., darwin-microfluidics.com, fivephoton.com) using the provided design files.
- 163 Connect the live and ground electrodes to their respective alligator clips (Fig. 15a).
 - ▲ CRITICAL STEP Electrodes must be handled carefully as even a slight twist might make them lose contact with the microfluidic chip.
 - ▲ CRITICAL STEP Before connecting the electrodes to the alligator clips, it is advised to check the electrode's continuity using the multimeter in continuity mode as done in Step 68.
- 164 Turn on the brightfield lamp, the camera and its software (Motion Blitz) and focus the image on the screen (Fig. 15b).
 - **! CAUTION** The brightfield lamp intensity should always be ramped up very slowly when turning it, because it acts with some delay. Carefully monitor the PMT signal while increasing the light intensity in very small increments, as otherwise the PMTs could get burned.

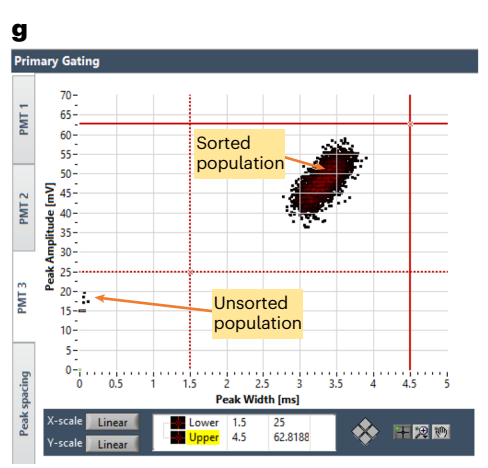


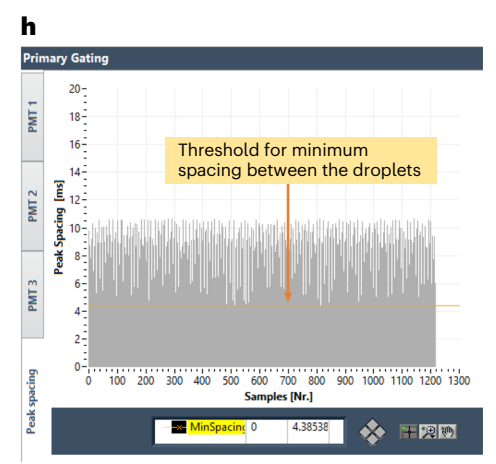












■ Fig. 15 | Droplet sorting initialization. a, Microfluidic chip on the microscope stage with its ITO-coated side (bottom) touching the copper tape. The electrodes from the chip are also connected to their respective alligator clips. b, Camera image of the correct position of the microchannel constriction as defined by the circle (complete chip design is shown in Supplementary Fig. 5). The horizontal and vertical grid spacing is 420 and 512 pixels, respectively. c, The complete droplet sorting experiment setup. d, A typical 'live data' plot in the TFADS program with droplets represented as peaks in PMT2 (green) and PMT3 (red) channels, along with their threshold cursors at 35 mV and 15 mV, respectively (PMT1 is not used here). e, PMT control window with gains set for each PMT. f, High-voltage amplifier parameters set for the sorting experiment, the 'test sort' ratio is set to 1:3 and the 'start sorting' toggle is 'on'. g, Gating performed to define the sorting criteria for droplets detected in PMT3 channel (here, the sorting gates for minimum peak amplitude and peak width for PMT3 are set as 25 mV and 1.5 ms, while the maximum values are set as 63 mV and 4.5 ms, respectively).

h, Threshold placed at 4.5 ms to define the minimum spacing between the droplets to be considered for sorting.

- 165 Mark the camera window using gridlines with horizontal and vertical spacing of 420 and 512 pixels, respectively (Fig. 15b).
- 166 Place a circle mark at 420 pixels from the left and 512 pixels from the bottom of the camera window that defines the droplet detection zone.
- 167 Move the chip such that the constriction in microchannel (as pointed by the arrows in the chip) overlaps the detection zone (Fig. 15b).
 - ▲ CRITICAL The detection zone can be positioned anywhere between the three arrows. However, as this positioning affects the high-voltage parameters (Step 184), we advise to use the same position in every experiment to have consistent and reproducible results.
- 168 Take two 27 G needles and insert ~20 cm tubing onto each of them using a tweezer.
- 169 Mount a syringe filled with the analyte along with the needle and tubing, on the dispersed-phase syringepump (Fig. 15c). The analyte can be a suspension of cells/beads/particles or an emulsion of the droplets.
- 170 Mount another syringe containing the oil phase (e.g., 1% Pico-surf in HFE 7500 oil) on the continuous-phase syringe pump (Fig. 15c).
- 171 Plug the two pieces of tubing from the syringes into their respective inlets on the chip using a tweezer (Fig. 15a).
- 172 Plug two more pieces of tubing at the waste and collection outlet of the chip and place their open end in a 1.5 mL Eppendorf tube (Fig. 15a).
- 173 Turn on the aqueous and oil flow syringe pumps and set the flow rates to generate the droplets. For the provided microfluidic chip design, a range of 500–1,500 μ L/h and 30–100 μ L/h is optimal for the continuous-phase and the dispersed-phase pumps, respectively. Check on the camera and wait until the droplets are generated. The resulting droplet frequency should be ~40–300 Hz.
 - **! CAUTION** When the pumps are running, do not touch the tubing; otherwise, the flow will fluctuate, and a polydisperse emulsion will be produced (Supplementary Fig. 6).

? TROUBLESHOOTING

174 All the generated droplets should be going to the waste channel (Supplementary Video 5). ▲ CRITICAL STEP Before starting the sorting operation, check if the chip is still placed correctly as per Step 162.

? TROUBLESHOOTING

- 175 Open TFADS.
- 176 In 'Assign FPGA ports' tab, assign the correct FPGA card as PXI1Slot2 along with the ports for the three PMTs and a high-voltage amplifier as AI/O-0, AI/O-1, AI/O-2 and AO7, respectively. The PMT not in use for the experiment should be set to 'off' (Box 1).
- 177 Turn on the PMTs using the side switches one by one (only those that are required in the experiment). The live data should show a fluctuation similar to what is described in Step 155.
- 178 Check that the right filter is placed over the brightfield diffuser, i.e., filter F8a if PMT3 is used for transmittance analysis or filter F8b if PMT3 is used for fluorescence analysis (Fig. 16c).
- 179 Turn on the lasers (only those that are required in the experiment) one by one and wait till they are emitting. You should be able to see a faint fluorescent spot in the camera as the droplets pass through the detection zone.
- 180 Increase the gain of the concerned PMTs until the respective droplet signals appear as discernible peaks in the LIVE data window (Fig. 16d and Box 1). Usually, a gain of 0.35 V to 0.5 V is sufficient to get the droplet signals with a peak amplitude of 50-100 mV.
- 181 Once the droplet signals are discernible for every channel, the cursors of the corresponding signals are moved to define the droplet threshold (Fig. 16d and Box 1). The default threshold value for each PMT is fixed at 0 mV. If any channel has low signal-to-noise ratio that is preventing a clear threshold, the channel with consistent signal is set as primary PMT, using the dropdown menu in control panel. The threshold of primary PMT will define the droplet detection irrespective of the

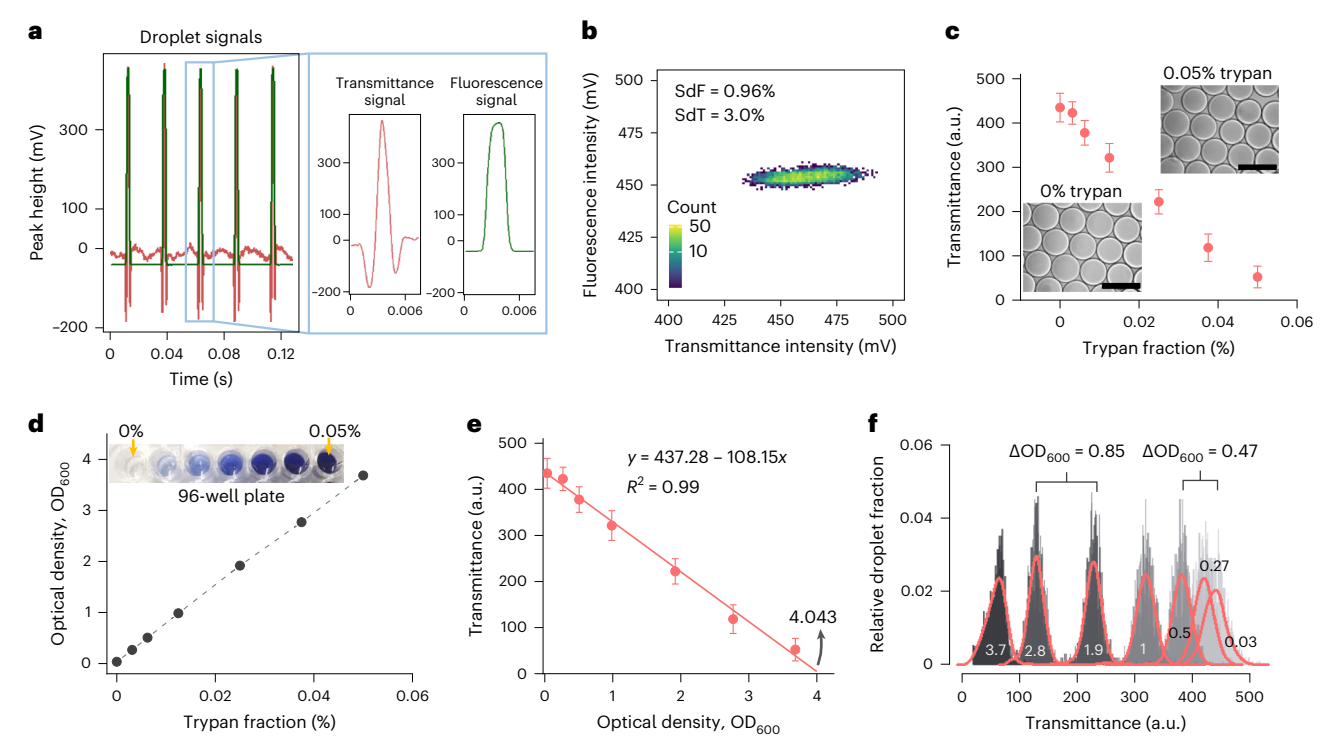


Fig. 16 | Transmittance and fluorescence signals. a, Droplet signals simultaneously acquired using transmittance and fluorescence of the droplets. **b**, Droplet signal peak height distribution as acquired using fluorescence and transmittance signals. **c**, Droplet transmittance mean peak height generated with a range of trypan blue concentrations diluted in PBS. Each point represents the mean transmittance peak height of more than 2,000 droplets and error bars represent the corresponding standard deviation. Inset shows the images of monodisperse droplets with 0% and 0.05% trypan. Scale bars, 100 μm. **d**, $OD_{600 \text{ nm}}$ curve obtained with a spectrophotometer for the different trypan blue concentrations in a 96-well microtiter plate. **e**, Transmittance values corresponding to the $OD_{600 \text{ nm}}$ curve. The equation represents the linear fit with the *x*-axis intercept at 4.043 denoting limit of detection. Each point represent the mean transmittance peak height of more than 2,000 droplets, and error bars represent the corresponding standard deviation. **f**,Transmittance intensity distribution of populations containing 2,000 droplets each with different OD_{600} (exact values are shown as numbers in the plot). The minimum difference in OD_{600} for which the populations do not overlap is 0.85.

values in other channels. The peak amplitude, peak width and peak area calculations will be conducted for individual channels in accordance with the threshold defined by primary PMT.

- 182 Click on the 'Sorting criteria tab' and gate all the droplets by defining minimum and maximum values of peak amplitude and peak width using cursors for each PMT in their corresponding tab in the primary gating section (Fig. 15g and Box 1).
 - In this step, all the droplets are gated for testing the sorting operation. Once the testing is successful, the sorting criteria will be redefined to gate only the droplets of interest (Step 195)
 - The default minimum and maximum value for each cursor is fixed at 0 and 50, respectively
 - The solid line cursor defines the upper limits while the dotted line cursor defines the lower limits
- 183 Define the minimum peak spacing in the fourth tab using the cursor (Fig. 15h and Box 1). The default minimum peak spacing value is fixed at 0 ms.
- 184 In the HV-amp control section, feed the values for the displayed parameters, i.e., pulse delay, pulse duration, amplitude and frequency. For the design provided in the Supplementary Data 10, these values have a range of 0–2 ms, 3–7 ms, 0.5–0.8 kV and 10–20 kHz for pulse delay, pulse duration, amplitude and frequency, respectively.
- 185 Turn on the high-voltage amplifier.
 - **!CAUTION** Never switch on the high-voltage amplifier without checking the proper grounding as per Step 68.
 - **! CAUTION** Always turn off the high-voltage amplifier before touching any exposed metal part of the workstation.
- 186 To optimize high-voltage parameters, first set the voltage as 0.5 kV and click on 'test pulse' to generate a continuous high-voltage pulse that should pull all droplets toward the sorting channel (Fig. 15f and Box 1). This step also confirms that the high-voltage connection is working as desired.
- 187 If the droplets are not pulled toward the collection channel while pressing 'test pulse', increase the high-voltage amplitude by 0.1 kV (Supplementary Video 6).

188 If the droplets are deforming too much (either stretching so much that they break or merge with other droplets), reduce the voltage amplitude (Supplementary Video 6).

- 189 Repeat Steps 186–188 till all the droplets start to go toward the collection channel without notable deformation when 'test pulse' is pressed, like shown in Supplementary Video 6.
- 190 To further tune the high-voltage parameters, set the pulse delay and duration as 0 ms and 1,000 ms, respectively, and fix the 'test sort' ratio to 1:3.
- 191 Turn on the 'start sorting' toggle. Make sure that all the droplets are gated as positive.
- 192 Check if every third droplet is going to the collection channel. You may record a video at a high frame rate to check the sorting efficiency (Supplementary Video 7 and Box 1).
- 193 If the sorting is not efficient, change the high-voltage pulse duration and/or delay by increments of 500 ms and repeat Steps 190 and 192.
- 194 Once the optimum high-voltage parameters are found, turn off 'start sorting' and change the 'test sort' ratio to 1:1 (Fig. 15f and Box 1).
- 195 Change the gating in the sorting criteria to gate the droplets of interest as per the experiment requirements. In common practice, the gating is manually set by the user where a separation between the two populations can be observed.
- 196 If secondary gating is required, turn on the 'secondary gating' switch and select the axis from the drop-down menu (Box 1).
- 197 Define the minimum and maximum allowed values for peak area in secondary gating plot by performing the actions described in Step 182.
- 198 Turn off the high-voltage amplifier.
- 199 Replace the collection tube and collection vial to avoid contamination from the previous tests.
- 200 Adjust the microfluidic chip placement on the stage again as the tube replacement might have displaced it a little (Fig. 15b and Box 1). For future reference and to save time in subsequent experiments, you can save the metadata to preserve the configuration of high-voltage parameters as well as gating parameters that provided efficient droplet sorting. Similar parameters can be used again with some fine tuning if the experiment conditions (e.g., droplet size, flow rates and channel dimensions) stay the same (Box 1).
- 201 Turn on the high-voltage amplifier and press 'Start sorting' to initiate the droplet sorting.

Troubleshooting

Troubleshooting advice can be found in Table 4.

Table	Table 4 Troubleshooting table								
Step	Problem	Possible reason	Solution						
29	Camera does not show any image or light	Incorrect microscope settings	Make sure the output port is set to the prism mode. Check the trinocular port is set for the camera and not for the eyepiece. Refer to the microscope manual						
		Low light intensity	Check the light button and the light knob intensity on microscope						
		Device is not recognized	Check the cable connection with the computer. Refer to camera manual as well						
		Incorrect camera settings	Check and put the shutter and frame rate speed on appropriate value						
68	No beep sound on multimeter	Incorrect multimeter setting	Put the multimeter in continuity mode with sound. Check the user manual of the multimeter for details						
		Faulty continuity mode on multimeter	For multimeters that do not have a contact mode, or when contact mode is not working properly, a resistance value of <50 Ω between the terminals can also confirm continuity						
		Grounding is not correct	Verify the wire connection with the high-voltage amplifier, breadboard and the microscope platform						
70	Brightfield light is not coming from the left side port of microscope	Incorrect microscope setting	Make sure the output port is set to the prism mode so that the brightfield light is coming out from the left side port of the microscope (toward the PMTs)						
			Table continued						

Table	4 (continued)		
Step	Problem	Possible reason	Solution
71	No light is visible downstream of the filter	Low brightfield light intensity	Check if shutters for brightfield are open or if any other obstacles are in the path of the light
		Ambient lights are on	The beam intensity is weak and is best visible when the ambient lights are off
81	No visible projection on target disc	Microscope is not aligned	The microscope is tilted so that the projection is not falling on the target. Adjust/straighten the microscope so it makes a 90° angle to rail D (Step 23)
113	Fluorescence spot is very dim	Fluorescent slide is photobleached	Move the slide to a new position
		Incorrect camera settings	Reduce the frame rate of the camera
154	No signal change observed on screen when PMT is turned on	Wrong cable connection	Double check correct execution of Steps 41–53 with the corresponding Figs. 9 and 10 and Table 3 $$
157	The fluorescence	Ambient light interference	Turn off the ambient lights
	baseline is noisy	Brightfield light interference	Check the position of the brightfield filter from Step 131
173	Droplets not generated	Wetting	Improper or no hydrophobic coating in microchannels ²² . Perform Aquapel treatment as per Box 2
174	Droplets not going in waste channel	Flow resistance	Increase the height of collection channel tube or decrease the height of waste tube, just enough that the droplets start going to the waste channel as shown in Supplementary Fig. 7

Timing

Assembly layout

Steps 1-8, breadboard installation: 1 h

Steps 9-12, mounting filters: 30 min

Steps 13-16, mounting dichroic mirrors: 24 h

Steps 17-21, mounting PMTs: 30 min

Steps 22-29, mounting microscope: 1 h

Electrical connections

Steps 30-42, power supply: 1 h

Steps 43-47, PMT connections: 30 min

Steps 48-55, FPGA I/O connections: 1 h

Steps 56–61, high-voltage amplifier connections: 30 \min

Steps 62-68, electrical grounding: 30 min

Optical alignment

Steps 69-89, emission light alignment: 1 h

Steps 90-131, laser alignment: 3 h

Computational setup

Steps 132-146, FPGA card installation: 2 h

Steps 147-149, TFADS installation: 5 min

Finalizing workstation setup

Steps 150-161, workstation setup validation: 30 min

Steps 162-201, initializing a droplet sorting experiment: 3 h

Anticipated results

The microfluidics workstation constructed by following the aforementioned protocol should now be ready to conduct high-throughput, fluorescence-activated droplet sorting experiments. To demonstrate its capability and expected results, we conducted a series of experiments.

Characterization of the system by acquiring transmittance and fluorescence signals of droplets

First, to demonstrate the suitability of transmittance signals for droplet detection, we simultaneously measured the transmittance and the fluorescence signals from the same monodispersed droplet population and compared them. We generated droplets containing 1 μM fluorescein and passed them through the detection zone of the microfluidic chip as described in Steps 162-201 (Fig. 16a and Supplementary Fig. 3). We turned on PMT2 and PMT3 to acquire green fluorescence and transmittance, respectively, with a gain of 0.42 V each, and saved the acquired data for analysis. We plotted the amplitudes of the peaks representing the droplet transmittance and fluorescence signals (raw data in Source Data Fig. 16). We observed a one-to-one mapping between the two signals indicating that the transmittance signals can be used as an alternative to droplet fluorescence signals for label-free droplet detection (Fig. 16b). However, the standard deviation of transmittance signals (3.0%) is found to be greater than that of the fluorescence signals (0.96%). This is because the bigger droplets tend to converge more light on to the sensor, which is not the case for fluorescence intensity measurements, in which only a fraction of the focal volume generates the signal (meaning different droplet sizes translate into different droplet widths rather than intensities, as long as the droplets completely fill the channels⁴⁷). To verify this, we generated a polydisperse droplet population by constantly flicking the aqueous phase tubing during the droplet generation procedure described in Step 173. We acquired the transmittance signals from this polydisperse droplet population and found that the standard deviation was larger (as compared with the signals of the monodisperse population): 13.06% versus 3.0% (Supplementary Fig. 6 and Box 3). More importantly, transmittance measurements confirmed that there were two dominating droplet sizes, as also observed by microscopic imaging. Taken together, we believe transmittance measurements provide a useful label-free alternative to the use of fluorescent markers for droplet detection.

Sensitivity and limit of transmittance detection

To determine the limit of detection and sensitivity of transmittance analysis, we measured the transmittance signals from seven distinct droplet populations containing different amounts of trypan blue ranging from 0% to 0.05%, corresponding to an optical density at 600 nm (OD_{600}) range of 0.035–3.68 (Fig. 16c,d and Box 3). We observed an excellent linearity between the transmittance signals and the OD_{600} values with a linear fit showing a coefficient of determination (R^2) of 0.99. The x-axis intercept of this linear fit provided the limit of detection at OD_{600} of 4.043 (Fig. 16e). Moreover, the same transmittance signal distribution can be used to deduce the sensitivity of our transmittance analysis method by identifying the minimum difference in OD_{600} of two droplet populations where they can be still seen as distinct populations. We observed that populations that are separated by an OD_{600} of 0.85 appear distinct, while a separation of less than 0.47 results in overlapping populations (Fig. 16f).

Sorting droplets containing fluorescent beads

The second type of experiment to check that the system works involves sorting of droplets that contain fluorescent beads; this experiment is also a very useful hands-on exercise to train the user on the basics of a droplet sorting workflow, before moving on to a more in-depth biological experiment. This experiment was done as follows:

- 1 We encapsulated blue and green fluorescent beads in a 1:3 ratio into droplets, following Poisson distribution with an average occupancy (λ) of ~0.1 for the droplets with a volume of ~140 pL (or ~65 µm diameter)²². The sample preparation for this exercise is discussed in detail in Box 3.
- 2 The droplets were generated at a frequency of ~200 Hz using a flow-focusing junction upstream the detection zone, where their transmittance and fluorescence signals were acquired as per Steps 159–176 (Fig. 17a,b).
- 3 We fixed the gain of PMT1, PMT2 and PMT3 as 0.42 V, 0.46 V and 0.49 V, respectively, and set PMT3 as the primary PMT with a threshold at 50 mV.
- 4 We applied the primary gating for each PMT (PMT1: 42 to 10,000 mV, to include high blue fluorescence; PMT2: -21 to 200 mV, to exclude high green fluorescence; PMT3: 0 to 300 mV, to include all the droplets) to identify and sort the droplets that are containing only blue fluorescent beads (Fig. 17c,d and raw data in Source Data Fig. 17).
- 5 The sorting was then initiated with a pulse amplitude, duration, delay and frequency of 0.9 kV, 1.5 ms, 0.1 ms and 10 kHz, respectively (Supplementary Video 8).

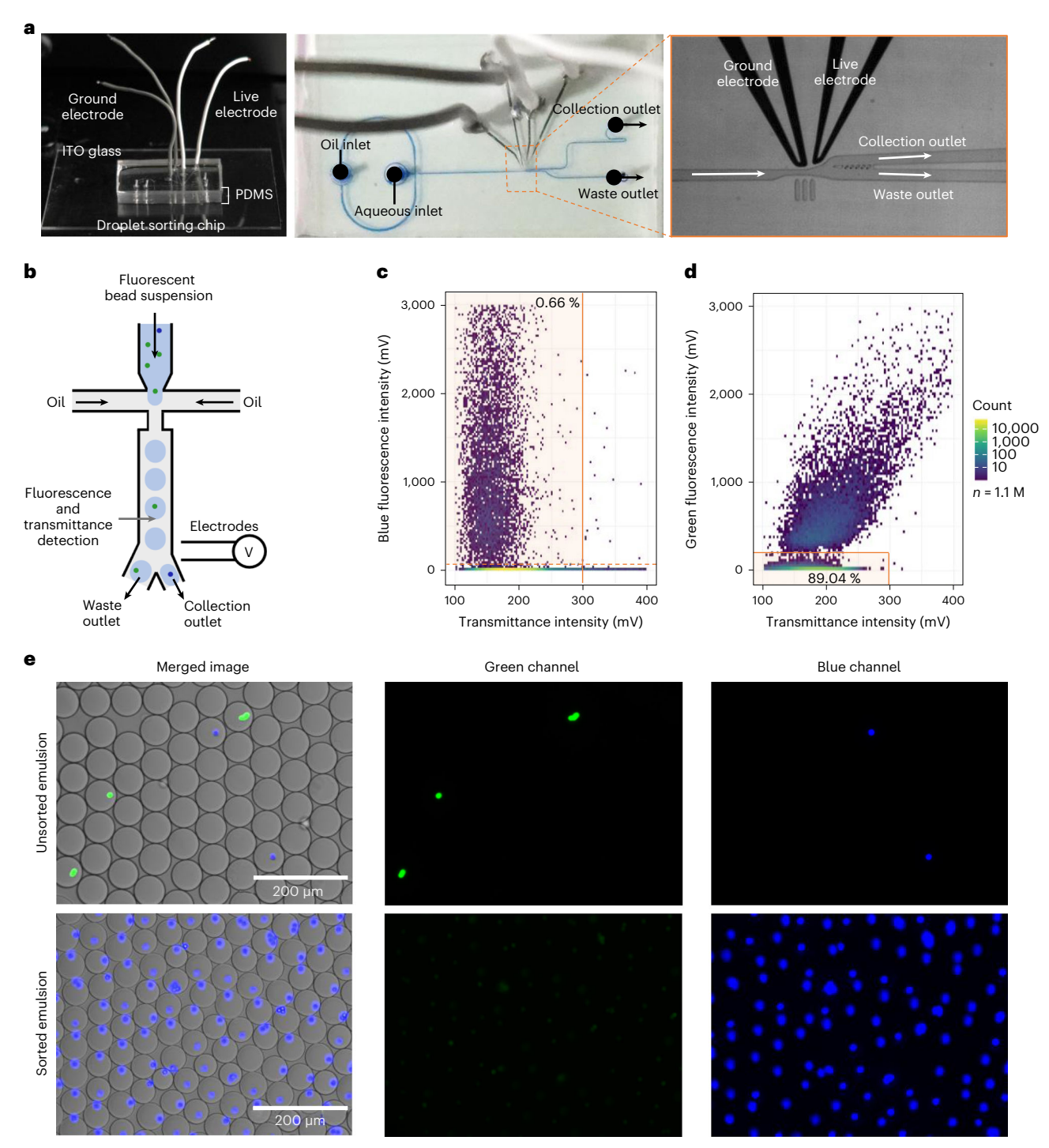


Fig. 17 | Fluorescent beads sorting experiment. a, Sorting chip with a zoom-in of the sorting junction (the channels are filled with trypan blue dye for better visualization). **b**, Schematic of the experiment where two types of fluorescent bead (blue and green emission) are encapsulated and sorted. **c**, Scatter plot showing amplitude of blue fluorescence and transmittance peaks from droplets. The orange-shaded area shows the population of droplets with high blue fluorescence that was gated for sorting (0.67% of the total population). The solid and dashed orange lines represent upper and lower gates, respectively. The remaining 99.33% of droplets do not fall into the gated population, because they are either empty or only host green beads. **d**, Scatter plot showing amplitude of green fluorescence and transmittance peaks from droplets. The orange-shaded area shows gated population of droplets with low green fluorescence (89.04% of the total population). A droplet is sorted only if it falls in both gates, i.e., high blue and low green fluorescence. The details of gates and sorting parameters can be found in metadata in Source Data Fig. 17. **e**, Microscope images of the unsorted emulsion and of the emulsion enriched with blue beads after sorting.

We screened ~0.3 million droplets and observed an enrichment of droplets containing only blue beads from 2.28% to 99.43% in the sorted droplet population, as determined by imaging ~500 droplets each in the sorted and unsorted population (Table 5 and Fig. 17e). The remaining fraction of the sorted droplets consists of empty droplets (0.57%) that accounts for the sorting error. These errors arise primarily from inherent issues in microfluidics such as pulsating pumps⁴⁸, clogging of the microchannels⁴⁹ and pressure changes in the channel while unplugging the collection tube, perturbing the flow properties in the microchannel that eventually result in one or more droplets going to collection channel without activation. The sorting errors are more severe when the droplets are reinjected into the microfluidic channel for sorting after off-chip incubation, due to the additional contribution from the droplets that are either merged or are broken into smaller droplets during transportation. This results in non-uniform droplet sizes and spacing, which in turn may attenuate the sorting efficiency²². An example of droplet sorting after off-chip incubation and reinjection can be seen in the next experiment.

Sorting droplets containing single cells

The third experiment shows a single-cell enzymatic assay to demonstrate a 'microfluidic droplet sorting workflow' that is usually followed in droplet-based single-cell studies^{8–12,14,19,22}. This experiment aims to sort and enrich cells with high matrix metalloproteinase (MMP) enzyme activity^{50,51}, which is typical for cancer cells with a metastatic phenotype. Note that MMPs are usually secreted or surface anchored, for which reason their activity cannot be measured easily by FACS, but rather requires compartmentalization techniques as described here. Similar workflows could also be used to select cells expressing enzyme variants with increased or altered catalytic activities from a pool of large genetic libraries, e.g., using surface-displayed enzyme libraries generated by mutagenesis. This is the overview of the workflow used for Fig. 18:

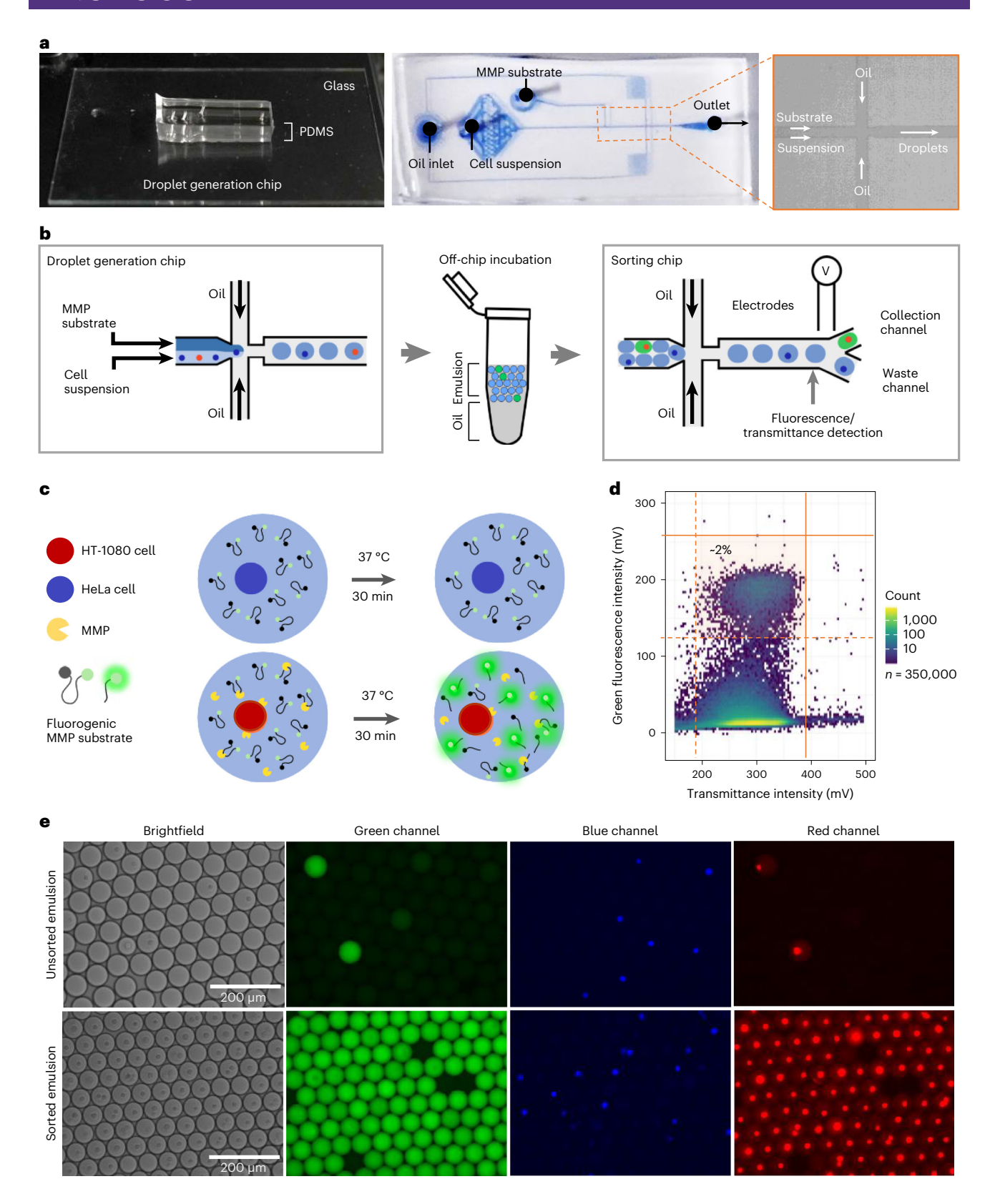
- 1 We encapsulated two types of cell lines—fibrosarcoma (HT-1080) and cervical carcinoma (HeLa) cells—at a ratio of 1:5, along with 2.5 μ M fluorogenic MMP-FRET substrate to reach an average occupancy (λ) of ~0.1 cells per droplet, as discussed in Box 3 (Fig. 18a,b and Supplementary Video 9). The HT-1080 cells exhibit higher MMP activity than HeLa cells^{52,53}, resulting in higher amounts of the fluorescent product and hence stronger fluorescent intensities (Fig. 18c).
- 2 The HT 1080 and HeLa cells were also stained with red and blue marker dyes, respectively, for fluorescence imaging post sorting, which allows to validate enrichment of cells with the desired enzymatic activity.
- 3 After an incubation of 30 min at 37 °C, the droplet emulsion was reinjected into the droplet sorting chip to sort the droplets with high green fluorescence intensities (Supplementary Video 10).
- 4 In similar manner to the first experiment, we used PMT2 with a gain of 0.46 V to acquire green fluorescence and the PMT3 with a gain of 0.51 V to acquire the transmittance signals. The PMT3 was also assigned as the primary PMT with a threshold at 113 mV to detect all the droplets.
- 5 We gated for the droplet population that had a green fluorescence amplitude between 122 mV and 257 mV to exclude droplets with low green fluorescence produced by residual MMP activity from HeLa cells⁵³ (<122 mV, lower gate) and droplets that may contain multiple HT-1080 cells producing very high green fluorescence (>257 mV, upper gate) (Fig. 18d, Source Data Fig. 18 and Supplementary Video 11).
- 6 The gated droplet population was then sorted with a high-voltage pulse amplitude, duration, delay and frequency of 0.8 kV, 1.8 ms, 0 ms and 10 kHz, respectively.
- 7 We screened ~1.1 million droplets and optically determined the fraction of droplets with strong green fluorescence in the sorted and unsorted population, including ~500 droplets in each pool (Table 5).

We observed 95.93% green fluorescence droplets in the sorted population against \sim 3.4% of such droplets in the unsorted population (Fig. 18e). Among the sorted population with green fluorescence, 98.3% contained red HT-1080 cells and the remaining population were either aggregates of blue HeLa cells that may have accumulation of residual MMP expression⁵³ or dying HeLa cells releasing proteases that also convert the MMP substrate (Fig. 18e).

The results summarized in Table 5 validate that the workstation constructed using the presented protocol can conduct high-throughput multi-wavelength fluorescence and transmittance activated droplet analysis and sorting, optionally at the single-cell level. This protocol, along with the provided resources, can therefore serve as a blueprint to bring state-of-art droplet microfluidic technology into any life-science laboratory, making ultrahigh-throughput phenotypic assays similarly accessible as already widely distributed single-cell transcriptomic methods and workflows.

Table 5 R	Table 5 Results summary								
Droplet generation	PMT1	PMT2	PMT3	Sorted for	Sorting frequency	Total no. of droplets	Total no. of No. of droplets corted	Composition of the Accuracy ^a sorted population ^a	Accuracy ^a
Sorting of dr	Sorting of droplets containing only blue fluorescent beads	olue fluorescent beads							
On-chip	Blue fluorescent beads	Green fluorescent beads	Droplet detection by transmittance	Blue fluorescence with no green	~200 Hz	1,198,280	9,175	92.8% with one blue 99.43% bead ^b	99.43%
				fluorescence				6.6% multiple blue beads ^b	
								0.5% empty droplets	
Sorting of dr	Sorting of droplets with cells showing enzymatic activity	enzymatic activity						0% green beads	
	1 1 2	Section of the Sectio	10000	J	-	751 750	7007	4ti /0 / 00	7000
reinjection	nase nase	fluorescence)	by transmittance	סו פפון וומסו פאכפון כפ	7∐ 00I _~	667,166	,,024	HT-1080 cell ^b	93.9370
•			•					4.6% with multiple	
								HT-1080 cells ^b	
								1.6% with only	
								HeLa cells	
								4.06% empty	
								droplets	

Description of the droplet sorting experiments and their outputs. *Composition and accuracy are measured optically using microscope images by counting -500 droplets in sorted and unsorted populations and determining the color of droplets, braction corresponds to the true positives in the sorted population.



■ Fig. 18 | Single-cell enzymatic droplet assay and sorting experiment. a, Droplet generation chip with two aqueous inlets, one for the cell suspension and one for the enzymatic substrate (the channels are filled with trypan blue dye for better visualization). b, Schematic workflow. HeLa cells stained with a blue fluorescent dye and HT-1080 cells stained with red fluorescent dye are encapsulated into droplets using the first chip, together with a substrate. Subsequently, droplets are collected and incubated for 30 min at 37 °C. The emulsion is then injected into the sorting device and the droplets are sorted on the basis of MMP activity, visualized in the green channel. c, Illustration of droplets containing HeLa and HT-1080 cells, along with the MMP-FRET substrate. The droplets are incubated off-chip to allow the conversion of the MMP-FRET substrate by MMPs, secreted from the HT-1080 cells, giving rise to green fluorescence. d, Scatter plot showing amplitude of green fluorescence and transmittance peaks from droplets. The orange-shaded area shows gated population of droplets with high green fluorescence (-2% of the total population). The details of gates and sorting parameters can be found in metadata in Source Data Fig. 18. e, Microscope images of the unsorted emulsion (top) and the sorted emulsion (bottom), enriched with green fluorescence (indicating MMP activity).

Reporting summary

Further information on research design is available in the Nature Portfolio Reporting Summary linked to this article.

Data availability

The custom-made software for droplet analysis and sorting is provided in Supplementary Software 1 and 2 and can also be checked for updates at www.epfl.ch/labs/lbmm/downloads/ or at https://doi.org/10.5281/zenodo.6399980. The design files for all the machined parts, 3D printed parts and microfluidic chips are provided in Supplementary Data 1–10 or at https://doi.org/10.5281/zenodo.6399971. Numeric data for all the experiments are in Source Data Figs. 16–18 and Supplementary Data 11. Raw data can be found at https://doi.org/10.5281/zenodo.6392149. Source data are provided with this paper.

References

- 1. Papalexi, E. & Satija, R. Single-cell RNA sequencing to explore immune cell heterogeneity. *Nat. Rev. Immunol.* 18, 35–45 (2018).
- Zhang, X. et al. Comparative analysis of droplet-based ultra-high-throughput single-cell RNA-seq systems. Mol. Cell 73, 130–142.e5 (2019).
- Matuła, K., Rivello, F. & Huck, W. T. S. Single-cell analysis using droplet microfluidics. Adv. Biosyst. 4, 1900188 (2020).
- 4. Leman, M., Abouakil, F., Griffiths, A. D. & Tabeling, P. Droplet-based microfluidics at the femtolitre scale. *Lab Chip* 15, 753–765 (2015).
- Collins, D. J., Neild, A., deMello, A., Liu, A. Q. & Ai, Y. The Poisson distribution and beyond: methods for microfluidic droplet production and single cell encapsulation. *Lab Chip* 15, 3439–3459 (2015).
- Shembekar, N., Chaipan, C., Utharala, R. & Merten, C. A. Droplet-based microfluidics in drug discovery, transcriptomics and high-throughput molecular genetics. *Lab Chip* 16, 1314–1331 (2016).
- Seah, Y. F. S., Hu, H. & Merten, C. A. Microfluidic single-cell technology in immunology and antibody screening. Mol. Asp. Med. 59, 47–61 (2018).
- 8. El Debs, B., Utharala, R., Balyasnikova, I. V., Griffiths, A. D. & Merten, C. A. Functional single-cell hybridoma screening using droplet-based microfluidics. *Proc. Natl Acad. Sci. USA* **109**, 11570–11575 (2012).
- 9. Hu, H., Eustace, D. & Merten, C. A. Efficient cell pairing in droplets using dual-color sorting. *Lab Chip* 15, 3989–3993 (2015).
- Shembekar, N., Hu, H., Eustace, D. & Merten, C. A. Single-cell droplet microfluidic screening for antibodies specifically binding to target cells. Cell Rep. 22, 2206–2215 (2018).
- Gérard, A. et al. High-throughput single-cell activity-based screening and sequencing of antibodies using droplet microfluidics. Nat. Biotechnol. 38, 715–721 (2020).
- 12. Wang, Y. et al. High-throughput functional screening for next-generation cancer immunotherapy using droplet-based microfluidics. Sci. Adv. 7, eabe3839 (2021).
- 13. Chokkalingam, V. et al. Probing cellular heterogeneity in cytokine-secreting immune cells using droplet-based microfluidics. *Lab Chip* **13**, 4740–4744 (2013).
- 14. Obexer, R. et al. Emergence of a catalytic tetrad during evolution of a highly active artificial aldolase. *Nat. Chem.* **9**, 50–56 (2017).
- 15. Autour, A. et al. Fluorogenic RNA Mango aptamers for imaging small non-coding RNAs in mammalian cells. *Nat. Commun.* **9**, 656 (2018).
- Bouhedda, F. et al. A dimerization-based fluorogenic dye-aptamer module for RNA imaging in live cells. Nat. Chem. Biol. 16, 69–76 (2020).
- 17. Lim, S. W., Tran, T. M. & Abate, A. R. PCR-activated cell sorting for cultivation-free enrichment and sequencing of rare microbes. *PLoS ONE* **10**, 1–16 (2015).
- 18. Pryszlak, A. et al. Enrichment of gut microbiome strains for cultivation-free genome sequencing using droplet microfluidics. *Cell Rep. Methods* 2, 100137 (2022).

19. Colin, P. Y. et al. Ultrahigh-throughput discovery of promiscuous enzymes by picodroplet functional metagenomics. *Nat. Commun.* **6**, 10008 (2015).

- 20. Zhu, Y. & Fang, Q. Analytical detection techniques for droplet microfluidics—a review. *Anal. Chim. Acta* 787, 24–35 (2013).
- 21. Xi, H. D. et al. Active droplet sorting in microfluidics: a review. Lab Chip 17, 751-771 (2017).
- Mazutis, L. et al. Single-cell analysis and sorting using droplet-based microfluidics. Nat. Protoc. 8, 870–891 (2013).
- 23. Ryckelynck, M. et al. Using droplet-based microfluidics to improve the catalytic properties of RNA under multiple-turnover conditions. RNA 21, 458–469 (2015).
- 24. Gielen, F. et al. Ultrahigh-throughput-directed enzyme evolution by absorbance-activated droplet sorting (AADS). *Proc. Natl Acad. Sci. USA* 113, E7383–E7389 (2016).
- 25. Siltanen, C. A. et al. An oil-free picodrop bioassay platform for synthetic biology. Sci. Rep. 8, 1-7 (2018).
- Herzenberg, L. A., Sweet, R. G. & Herzenberg, L. A. Fluorescence-activated cell sorting. Sci. Am. 234, 108–117 (1976).
- Piyasena, M. E. & Graves, S. W. The intersection of flow cytometry with microfluidics and microfabrication. *Lab Chip* 14, 1044–1059 (2014).
- 28. Zinchenko, A. et al. One in a million: flow cytometric sorting of single cell-lysate assays in monodisperse picolitre double emulsion droplets for directed evolution. *Anal. Chem.* **86**, 2526–2533 (2014).
- 29. Zhu, Z. & Yang, C. J. Hydrogel droplet microfluidics for high-throughput single molecule/cell analysis. *Acc. Chem. Res.* **50**, 22–31 (2017).
- 30. Fischlechner, M. et al. Evolution of enzyme catalysts caged in biomimetic gel-shell beads. *Nat. Chem.* **6**, 791–796 (2014).
- 31. Lim, S. W. & Abate, A. R. Ultrahigh-throughput sorting of microfluidic drops with flow cytometry. *Lab Chip* 13, 4563–4572 (2013).
- 32. Akbari, S. & Pirbodaghi, T. A droplet-based heterogeneous immunoassay for screening single cells secreting antigen-specific antibodies. *Lab Chip* 14, 3275–3280 (2014).
- 33. Josephides, D. et al. Cyto-Mine: an integrated, picodroplet system for high-throughput single-cell analysis, sorting, dispensing, and monoclonality assurance. *SLAS Technol.* **25**, 177–189 (2020).
- 34. Yang, T., Stavrakis, S. & DeMello, A. A high-sensitivity, integrated absorbance and fluorescence detection scheme for probing picoliter-volume droplets in segmented flows. *Anal. Chem.* 89, 12880–12887 (2017).
- 35. Baret, J.-C. et al. Fluorescence-activated droplet sorting (FADS): efficient microfluidic cell sorting based on enzymatic activity. *Lab Chip* **9**, 1850–1858 (2009).
- 36. Gruner, P. et al. Controlling molecular transport in minimal emulsions. Nat. Commun. 7, 10392 (2016).
- 37. Vermeir, L. et al. Effect of molecular exchange on water droplet size analysis as determined by diffusion NMR: the W/O/W double emulsion case. *J. Colloid Interface Sci.* 475, 57–65 (2016).
- 38. Skhiri, Y. et al. Dynamics of molecular transport by surfactants in emulsions. *Soft Matter* **8**, 10618–10627 (2012).
- 39. Baret, J.-C. C. Surfactants in droplet-based microfluidics. Lab Chip 12, 422-433 (2012).
- 40. Arppe, R., Carro-Temboury, M. R., Hempel, C., Vosch, T. & Sørensen, T. J. Investigating dye performance and crosstalk in fluorescence enabled bioimaging using a model system. *PLoS ONE* **12**, 1–17 (2017).
- 41. Waters, J. C. Accuracy and precision in quantitative fluorescence microscopy. J. Cell Biol. 185, 1135–1148 (2009).
- 42. Schütz, S. S., Beneyton, T., Baret, J. C. & Schneider, T. M. Rational design of a high-throughput droplet sorter. *Lab Chip* **19**, 2220–2232 (2019).
- 43. Kim, M.-S. et al. Refraction limit of miniaturized optical systems: a ball-lens example. *Opt. Express* 24, 6996–7005 (2016).
- 44. Sciambi, A. & Abate, A. R. Accurate microfluidic sorting of droplets at 30 kHz. Lab Chip 15, 47-51 (2014).
- 45. Clark, I. C., Thakur, R. & Abate, A. R. Concentric electrodes improve microfluidic droplet sorting. *Lab Chip* 18, 710–713 (2018).
- 46. Pohl, H. A. Some effects of nonuniform fields on dielectrics. J. Appl. Phys. 29, 1182-1188 (1958).
- Srisa-Art, M., deMello, A. J. & Edel, J. B. High-throughput DNA droplet assays using picoliter reactor volumes. Anal. Chem. 79, 6682–6689 (2007).
- 48. Li, Z., Yi Mak, S., Sauret, A. & Cheung Shum, H. Syringe-pump-induced fluctuation in all-aqueous microfluidic system implications for flow rate accuracy. *Lab Chip* 14, 744–749 (2014).
- 49. Dressaire, E. & Sauret, A. Clogging of microfluidic systems. Soft Matter 13, 37-48 (2017).
- 50. Birkedal-Hansen, H. et al. Matrix metalloproteinases: a review. Crit. Rev. Oral. Biol. Med. 4, 197-250 (1993).
- Bourboulia, D. & Stetler-Stevenson, W. G. Matrix metalloproteinases (MMPs) and tissue inhibitors of metalloproteinases (TIMPs): positive and negative regulators in tumor cell adhesion. Semin. Cancer Biol. 20, 161–168 (2010).
- 52. Stanton, H. et al. The activation of ProMMP-2 (gelatinase A) by HT1080 fibrosarcoma cells is promoted by culture on a fibronectin substrate and is concomitant with an increase in processing of MT1-MMP (MMP-14) to a 45 kDa form. *J. Cell Sci.* 111, 2789–2798 (1998).
- Schröpfer, A. et al. Expression pattern of matrix metalloproteinases in human gynecological cancer cell lines. BMC Cancer 10, 553 (2010).
- 54. Singh, P. & Aubry, N. Transport and deformation of droplets in a microdevice using dielectrophoresis. *Electrophoresis* **28**, 644–657 (2007).

Acknowledgements

Parts of this work were supported by DFG-Grant ME 3536/9-1 and the DFG-funded part of the transnational JPIAMR Grant 01KI1822 ("DISRUPT").

Author contributions

C.A.M. conceived the project and supervised the experimental work. J.P. and A.A. introduced the transmittance-based sorting mode. J.P. wrote the LabVIEW code for droplet sorting software. A.A. performed all cell-based assays. All authors contributed to the writing of the manuscript.

Competing interests

C.A.M. is a cofounder of Veraxa Biotech and head of the TheraMe! consortium, both exploiting droplet microfluidic technology. However, the instrument described in this protocol is not offered commercially by any of these two entities.

Additional information

Extended data is available for this paper at https://doi.org/10.1038/s41596-022-00796-2.

 $\textbf{Supplementary information} \ The \ online \ version \ contains \ supplementary \ material \ available \ at \ https://doi.org/10.1038/s41596-022-00796-2.$

Correspondence and requests for materials should be addressed to Christoph A. Merten.

Peer review information Nature Protocols thanks Han Zhang and the other, anonymous, reviewer(s) for their contribution to the peer review of this work.

Reprints and permissions information is available at www.nature.com/reprints.

Publisher's note Springer Nature remains neutral with regard to jurisdictional claims in published maps and institutional affiliations.

Springer Nature or its licensor (e.g. a society or other partner) holds exclusive rights to this article under a publishing agreement with the author(s) or other rightsholder(s); author self-archiving of the accepted manuscript version of this article is solely governed by the terms of such publishing agreement and applicable law.

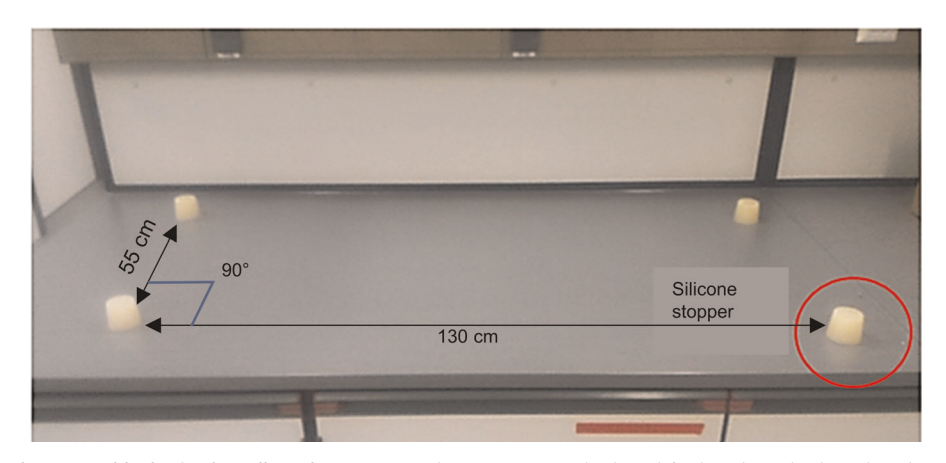
Received: 18 August 2021; Accepted: 9 November 2022;

Published online: 27 January 2023

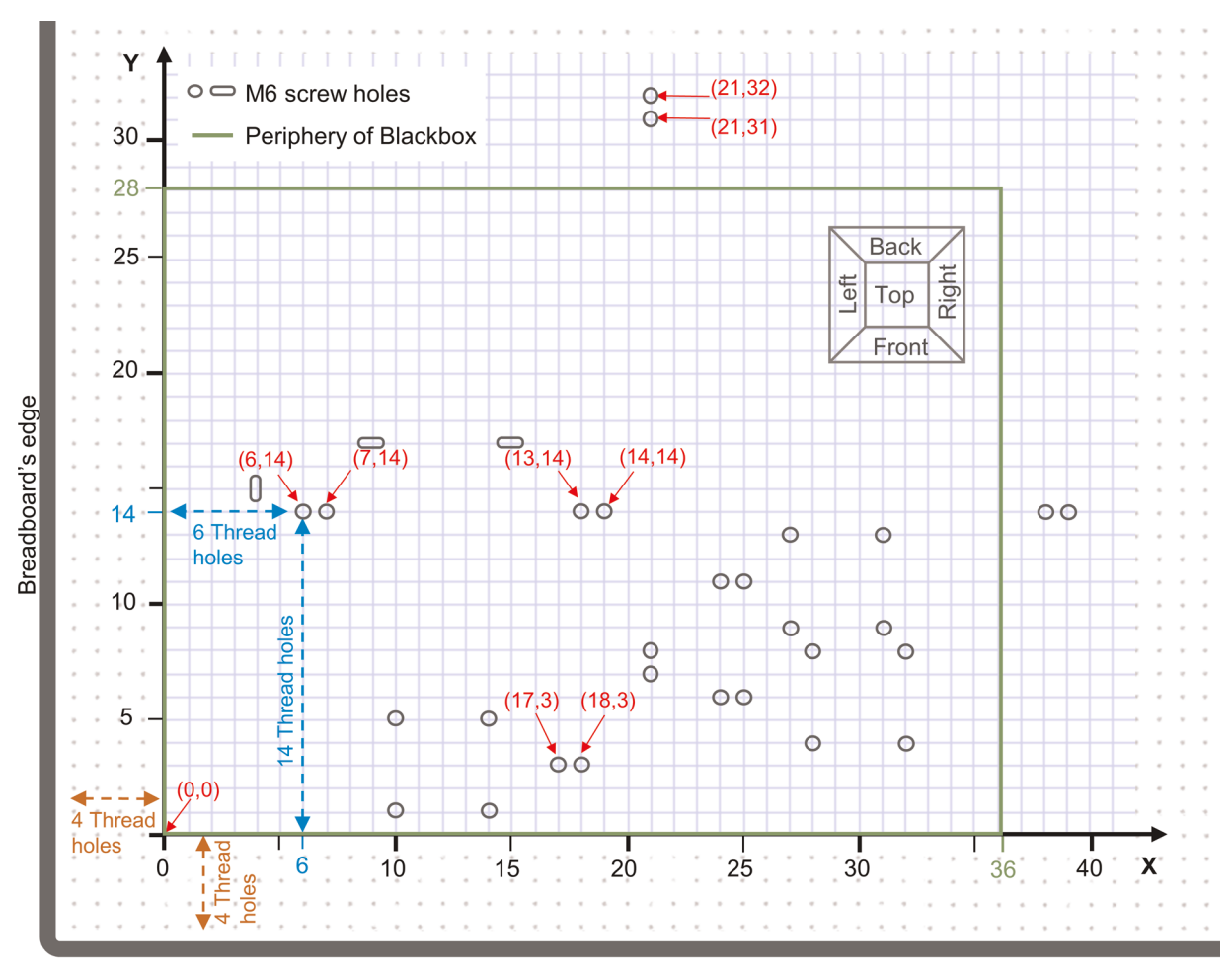
Related links

Key references using this protocol

El Debs, B. et al. *Proc. Natl Acad. Sci. USA* **109**, 11570–11575 (2012): https://doi.org/10.1073/pnas.1204514109 Shembekar, N. et al. *Cell Rep.* **22**, 2206–2215 (2018): https://doi.org/10.1016/j.celrep.2018.01.071 Hu, H. et al. *Lab Chip* **15**, 3989–3993 (2015): https://doi.org/10.1039/C5LC00686D

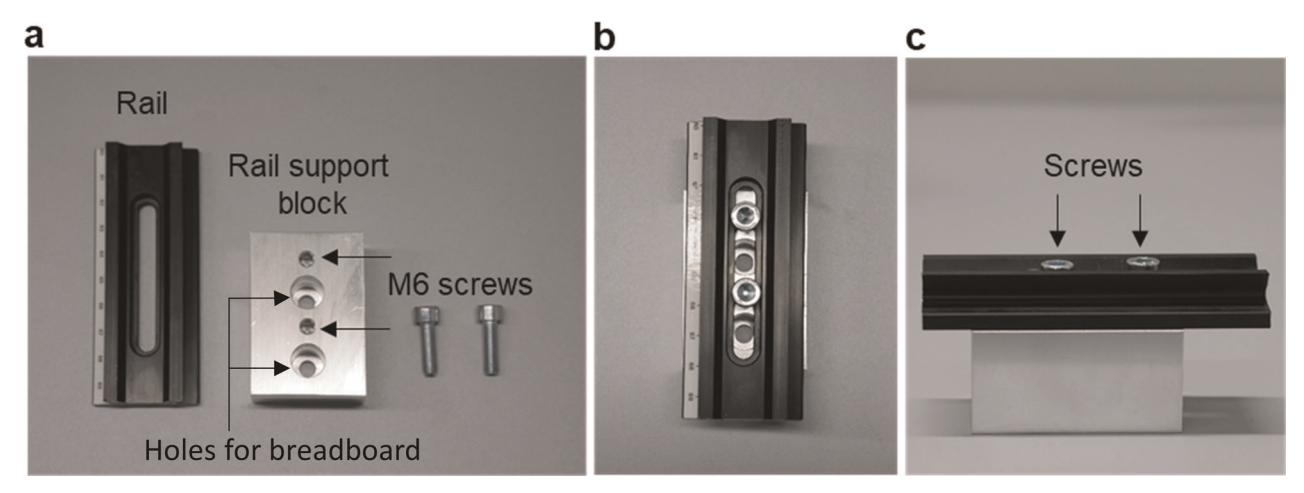


Extended Data Fig. 1 | Support blocks for breadboard mounting. Silicone stoppers (red circle) placed on the host bench to provide support and passive vibration isolation to the breadboard. The relative distance between the silicone stoppers ensure their alignment to the four corners of the breadboard.

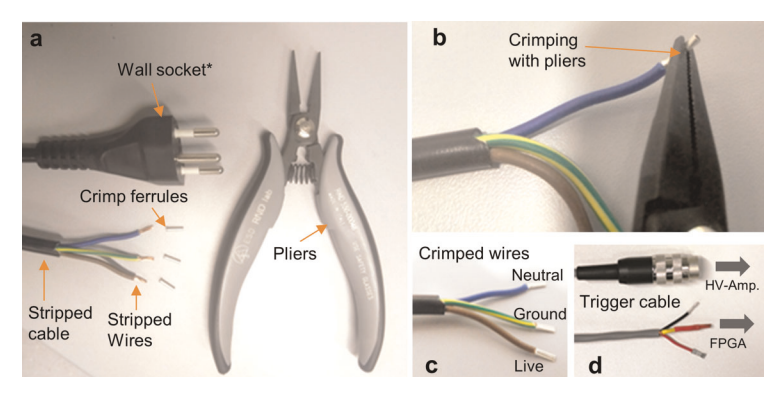


*1 unit = distance between two consecutive holes on the breadboard = 2.5 cm

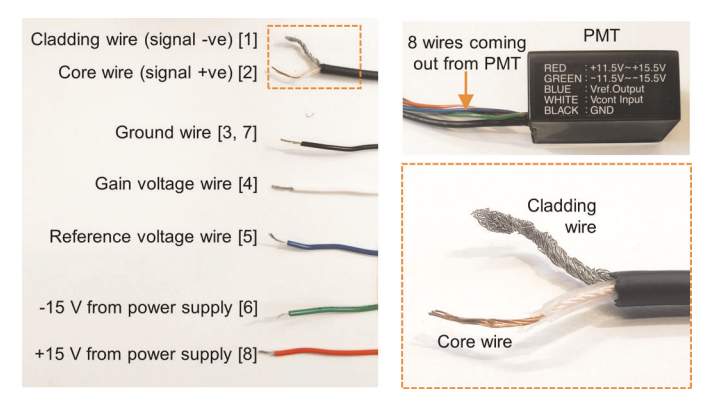
Extended Data Fig. 2 | Map with screw coordinates. Map depicting the coordinates for the screw positions to be marked before the breadboard assembly as per Fig. 5. The coordinate system has the origin at the left bottom side of the breadboard with a distance of 1 hole from the left edge. The screw positions follow the coordinates described in Table 2. As example, some screw coordinated are labelled.



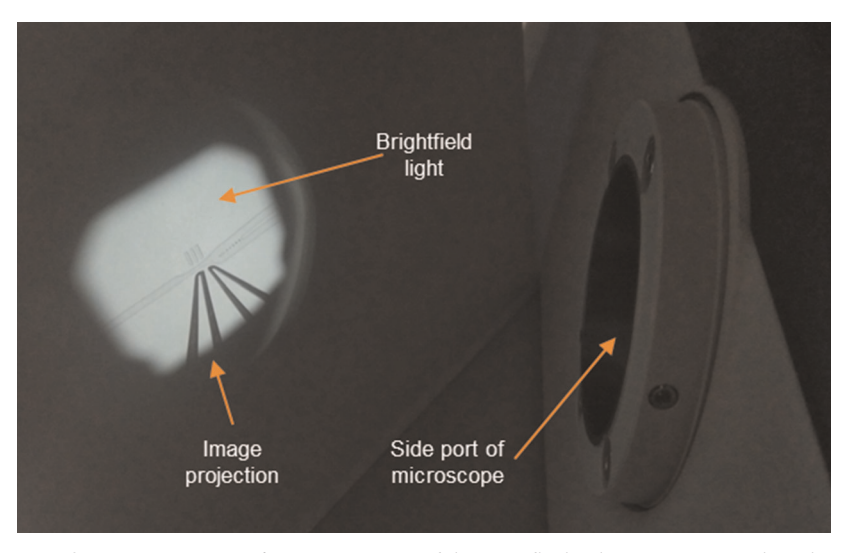
Extended Data Fig. 3 | Rail mounting on rail support blocks. a) Essential pieces to assemble a small rail (e.g. rail A to E) on a rail support block. The black arrows point to the corresponding holes for the two M6 screws. Note that prior to mounting rails on the blocks, the block should already be screwed on the breadboard at its position as per Fig. 5.) through the depicted holes for breadboard **b)** Top view of the assembly. **c)** Side view of the assembly. The two screws allow to attach the rail to the block.



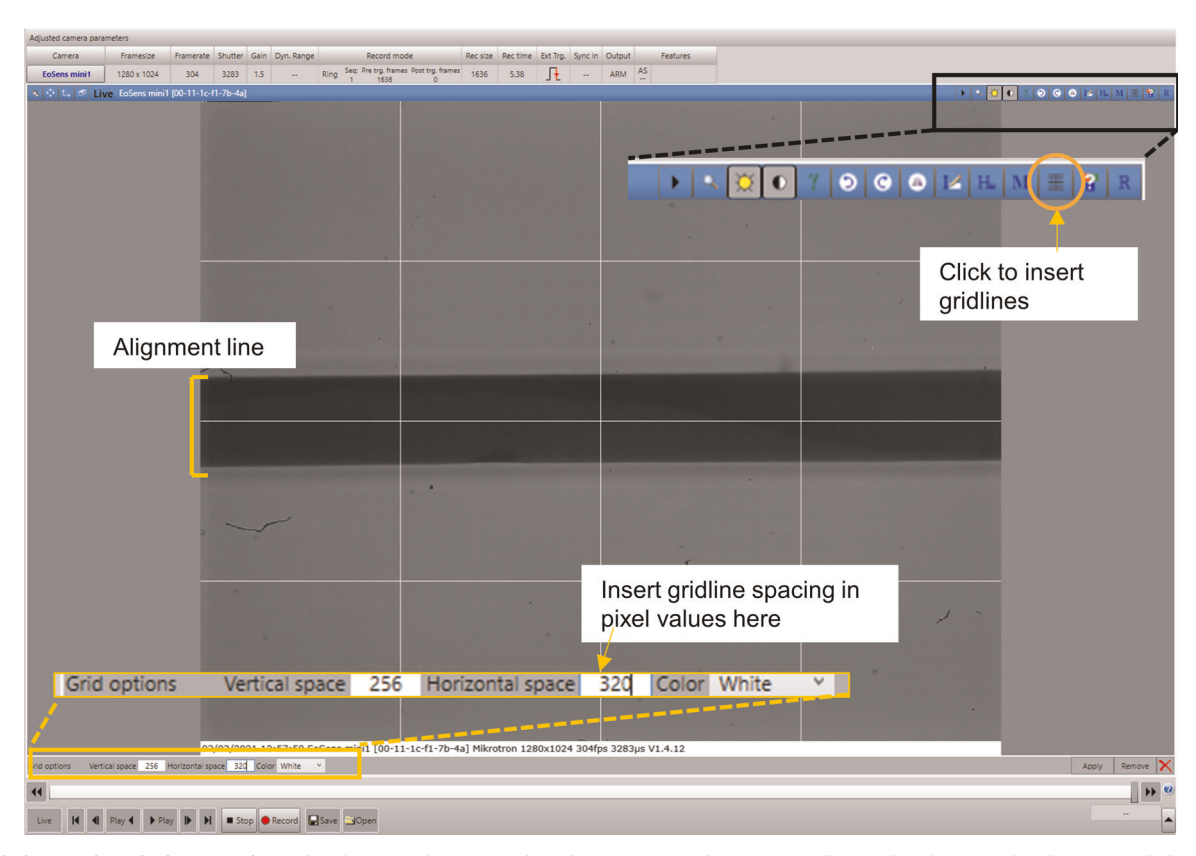
Extended Data Fig. 4 | Wire crimping. a) Power cable for PMT power supply with its rear end cut and stripped along with crimp ferrules and pliers for wire crimping. *The wall socket plug is country specific. **b)** Pliers crimping the wire with a crimp ferrule on its stripped end. **c)** Crimped wires of the power supply depicting neutral, live and ground wires (note that the color convention is country specific). **d)** Crimped end of the high-voltage amplifier's trigger cable. The crimped wires will be connected to FPGA in later steps (57-59).



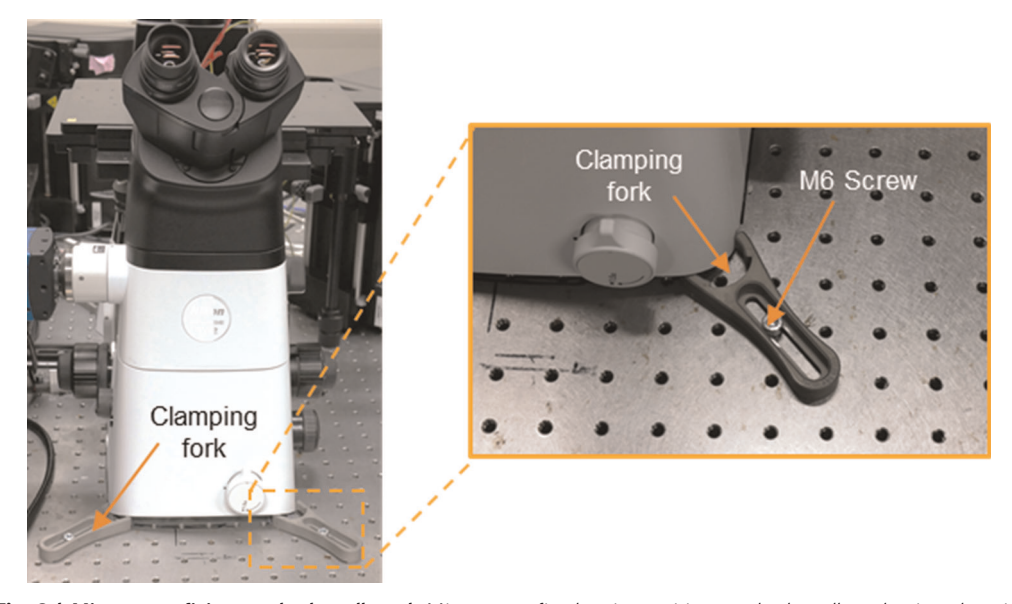
Extended Data Fig. 5 | PMT wires. The wires coming out of the PMT are assigned their function and pin number (in brackets) of the eight-pin connector. The cladding and core wire of the thick black cable are shown in zoom.



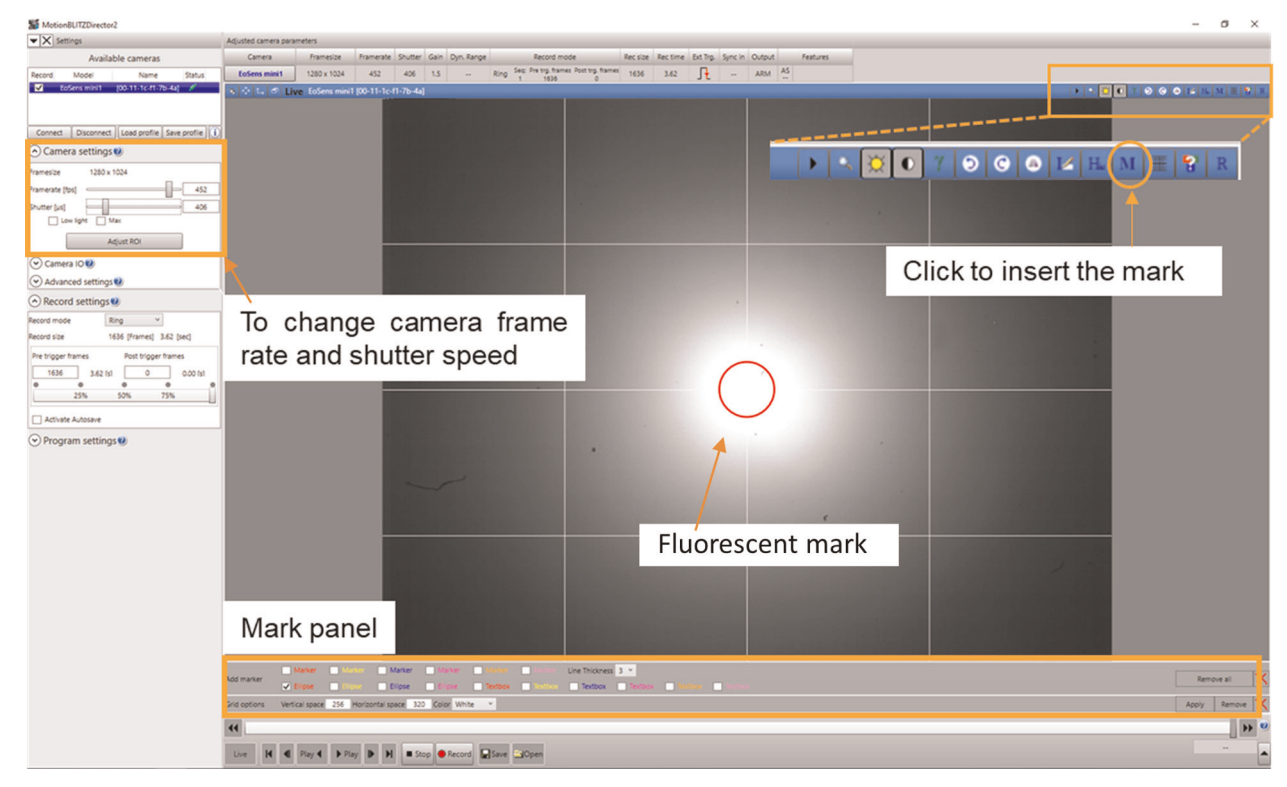
Extended Data Fig. 6 | Projection from microscope's side port. Projection of the microfluidic chip's image on a white sheet of paper, held close to the focal plane of the objective lens near the (left) side port of the microscope.



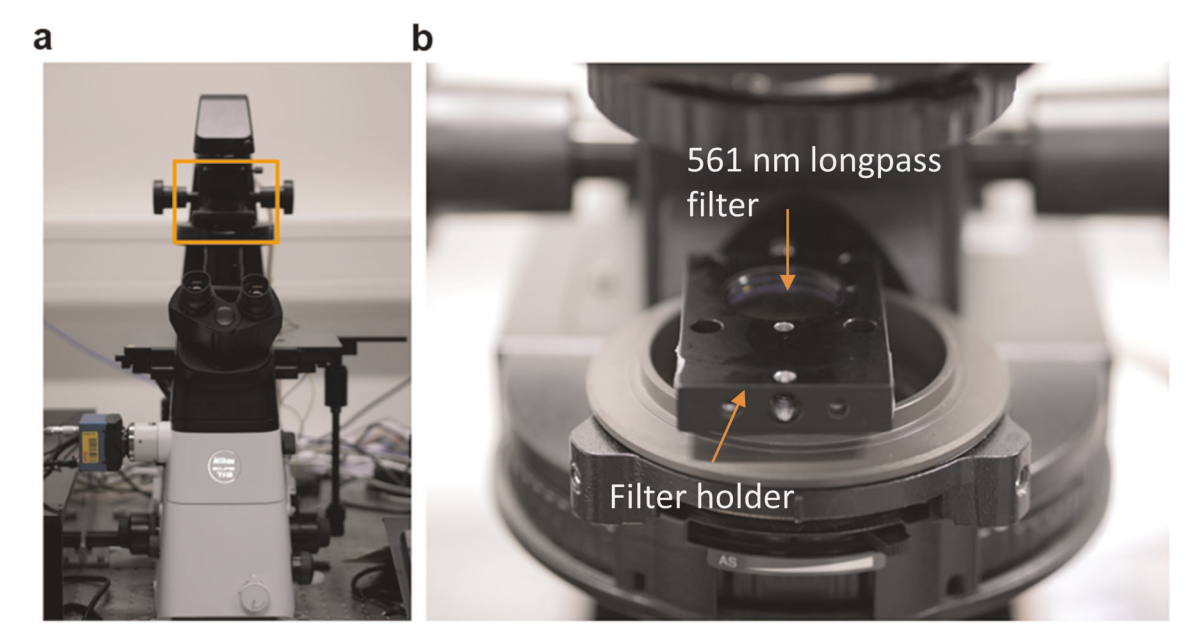
Extended Data Fig. 7 | Alignment line. The alignment line centred on the camera window using gridlines. The alignment line here is made by flowing molten Indium alloy into a straight (100 micron wide) microfluidic channel to achieve a good contrast between the line and the background. The projection of this alignment line is used for emission light alignment. The essential buttons in "MotionBLITZdirector2" software are highlighted in the picture.



Extended Data Fig. 8 | Microscope fixing on the breadboard. Microscope fixed at its position on the breadboard using clamping forks after the emission light alignment process.



Extended Data Fig. 9 | Camera software controls. Camera settings for the MotionBLITZdirector2 software to change the frame rate and for inserting a mark for alignment process on the camera window.



Extended Data Fig. 10 | Brightfield filter positioning. a) The full microscope is shown with the condenser for the brightfield lamp, located above of the microscope stage (orange box). **b)** A 561 nm longpass filter on a 25mm filter holder is placed over the condenser. This filter only allows the wavelengths that are not detected by any PMT to pass, enabling imaging by camera while simultaneously measuring fluorescence signals.

nature portfolio

Corresponding author(s):	
Last updated by author(s):	2022-11-01

Christoph A. Merten

Reporting Summary

Nature Portfolio wishes to improve the reproducibility of the work that we publish. This form provides structure for consistency and transparency in reporting. For further information on Nature Portfolio policies, see our Editorial Policies and the Editorial Policy Checklist.

Please do not complete any field with "not applicable" or n/a. Refer to the help text for what text to use if an item is not relevant to your study. For final submission: please carefully check your responses for accuracy; you will not be able to make changes later.

Statistics

L~~	oll statistical an	al.,,,,,,,,	aanfirm that t	ha fallawing	itamas ara	nracant in that	iaura laaand	l +abla lagand	manin taxt	, or Methods secti	
F()[ali StatiSticai ati	オルスピス	. commun mai i	ne ioliowins	nems are	oreseni in ine i	181116 1686110	i. Table legend	. main iexi	OF IVIETHOUS SECT	acorn.

n/a Confirmed

- To The exact sample size (n) for each experimental group/condition, given as a discrete number and unit of measurement
- 🔟 A statement on whether measurements were taken from distinct samples or whether the same sample was measured repeatedly
- The statistical test(s) used AND whether they are one- or two-sided
 - Only common tests should be described solely by name; describe more complex techniques in the Methods section.
- A description of all covariates tested
- (C) A description of any assumptions or corrections, such as tests of normality and adjustment for multiple comparisons
- 0
- A full description of the statistical parameters including central tendency (e.g. means) or other basic estimates (e.g. regression coefficient) AND variation (e.g. standard deviation) or associated estimates of uncertainty (e.g. confidence intervals)
 - For null hypothesis testing, the test statistic (e.g. *F*, *t*, *r*) with confidence intervals, effect sizes, degrees of freedom and *P* value noted *Give P values as exact values whenever suitable.*
 - To For Bayesian analysis, information on the choice of priors and Markov chain Monte Carlo settings
 - For hierarchical and complex designs, identification of the appropriate level for tests and full reporting of outcomes
 - Entimates of effect sizes (e.g. Cohen's d, Pearson's r), indicating how they were calculated

Our web collection on statistics for biologists contains articles on many of the points above.

Software and code

Policy information about availability of computer code

Data collection Data collection was done by custom code written in LabVIEW 2019

Data analysis Data analysis was performed in real-time in custom code written in LabVIEW 2019 and some plots were plotted using R-Studio or Origin 2020b

For manuscripts utilizing custom algorithms or software that are central to the research but not yet described in published literature, software must be made available to editors and reviewers. We strongly encourage code deposition in a community repository (e.g. GitHub). See the Nature Portfolio guidelines for submitting code & software for further information.

Data

Policy information about availability of data

All manuscripts must include a data availability statement. This statement should provide the following information, where applicable:

- Accession codes, unique identifiers, or web links for publicly available datasets
- A description of any restrictions on data availability
- For clinical datasets or third party data, please ensure that the statement adheres to our policy

The custom-made software for droplet analysis and sorting is provided in Supplementary Software 1 and 2 and can also be checked for updates on www.epfl.ch/labs /lbmm/downloads/ or on https://doi.org/10.5281/zenodo.6399980. The design files for all the machined parts, 3D printed parts and microfluidic chips are provided in Supplementary Data 1 to 10 or on https://doi.org/10.5281/zenodo.6399971. Numeric data for all the experiments is Source Data 1 to 3, and Supplementary Data 11. Raw data can be found on https://doi.org/10.5281/zenodo.6392149. Human research participants Policy information about studies involving human research participants and Sex and Gender in Research. n/a Reporting on sex and gender n/a Population characteristics Recruitment Ethics oversight n/a Note that full information on the approval of the study protocol must also be provided in the manuscript. Field-specific reporting Please select the one below that is the best fit for your research. If you are not sure, read the appropriate sections before making your selection. OLife sciences OBehavioural & social sciences Ecological, evolutionary & environmental sciences Life sciences study design All studies must disclose on these points even when the disclosure is negative. Sample size was determined by the number of individual droplets analyzed during the experiment and is reported appropriately in the Sample size Data exclusions n/a Replication n/a Randomization Blinding n/a Behavioural & social sciences study design All studies must disclose on these points even when the disclosure is negative. Study description Research sample Sampling strategy Data collection Timing Data exclusions Non-participation Randomization Ecological, evolutionary & environmental sciences study design All studies must disclose on these points even when the disclosure is negative. Study description Research sample Sampling strategy

Data collection

Timing and spatial scale

Data exclusions								
Reproducibility								
Randomization								
Blinding								
Did the study involve field work	? Oyes Ono							
Field work, collection	and transport							
	·							
Field conditions								
Location								
Access & import/export								
Disturbance								
Disturbance								
Danautina fama	a a sifi a ma atamia la cavata ma a amad ma atha a da							
Reporting for sp	pecific materials, systems and methods							
	about some types of materials, experimental systems and methods used in many studies. Here, indicate whether each material,							
system of method listed is relevant to	your study. If you are not sure if a list item applies to your research, read the appropriate section before selecting a response.							
Materials & experimental s	ystems Methods							
n/a Involved in the study	n/a Involved in the study							
Antibodies	ChIP-seq							
Eukaryotic cell lines	Flow cytometry							
Palaeontology and archaeology MRI-based neuroimaging								
Animals and other organisms								
Clinical data								
Dual use research of concerr								
Antibodies								
Antibodies used								
Validation								
Eukaryotic cell lines								
Lakaryotic cen inies								
,	and Sex and Gender in Research							
,	and Sex and Gender in Research HT-1080 fibrosarcoma cell line (DSMZ, cat. no. ACC 315, RRID: CVCL_0317)							
Policy information about cell lines								
Policy information about cell lines Cell line source(s)	HT-1080 fibrosarcoma cell line (DSMZ, cat. no. ACC 315. RRID: CVCL 0317)							
Policy information about cell lines Cell line source(s) Authentication	HT-1080 fibrosarcoma cell line (DSMZ, cat. no. ACC 315, RRID: CVCL 0317) cell lines were not authenticated							
Policy information about cell lines Cell line source(s) Authentication Mycoplasma contamination	HT-1080 fibrosarcoma cell line (DSMZ, cat. no. ACC 315, RRID: CVCL 0317) cell lines were not authenticated cell lines were not tested for mycoplasma contamination.							
Policy information about cell lines Cell line source(s) Authentication Mvcoplasma contamination Commonly misidentified lines (See ICLAC register)	HT-1080 fibrosarcoma cell line (DSMZ, cat. no. ACC 315, RRID: CVCL 0317) cell lines were not authenticated cell lines were not tested for mycoplasma contamination. n/a							
Policy information about cell lines Cell line source(s) Authentication Mvcoplasma contamination Commonly misidentified lines (See ICLAC register)	HT-1080 fibrosarcoma cell line (DSMZ, cat. no. ACC 315, RRID: CVCL 0317) cell lines were not authenticated cell lines were not tested for mycoplasma contamination. n/a							
Policy information about cell lines Cell line source(s) Authentication Mvcoplasma contamination Commonly misidentified lines (See ICLAC register)	HT-1080 fibrosarcoma cell line (DSMZ, cat. no. ACC 315, RRID: CVCL 0317) cell lines were not authenticated cell lines were not tested for mycoplasma contamination. n/a							
Policy information about cell lines Cell line source(s) Authentication Mycoplasma contamination Commonly misidentified lines (See ICLAC register) Palaeontology and Ar	HT-1080 fibrosarcoma cell line (DSMZ, cat. no. ACC 315, RRID: CVCL 0317) cell lines were not authenticated cell lines were not tested for mycoplasma contamination. n/a							
Policy information about cell lines Cell line source(s) Authentication Mycoplasma contamination Commonly misidentified lines (See ICLAC register) Palaeontology and Ar Specimen provenance	HT-1080 fibrosarcoma cell line (DSMZ, cat. no. ACC 315, RRID: CVCL 0317) cell lines were not authenticated cell lines were not tested for mycoplasma contamination. n/a							
Policy information about cell lines Cell line source(s) Authentication Mycoplasma contamination Commonly misidentified lines (See ICLAC register) Palaeontology and Ar Specimen provenance Specimen deposition Dating methods	HT-1080 fibrosarcoma cell line (DSMZ, cat. no. ACC 315, RRID: CVCL 0317) cell lines were not authenticated cell lines were not tested for mycoplasma contamination. n/a							

Animals and other research organisms Policy information about studies involving animals; ARRIVE guidelines recommended for reporting animal research, and Sex and Gender in Research Laboratory animals Wild animals Reporting on sex Field-collected samples Ethics oversight Note that full information on the approval of the study protocol must also be provided in the manuscript. Clinical data Policy information about clinical studies All manuscripts should comply with the ICMJE guidelines for publication of clinical research and a completed CONSORT checklist must be included with all submissions. Clinical trial registration Study protocol Data collection Outcomes Dual use research of concern Policy information about dual use research of concern Hazards Could the accidental, deliberate or reckless misuse of agents or technologies generated in the work, or the application of information presented in the manuscript, pose a threat to: No Yes OPublic health ONational security OCrops and/or livestock OEcosystems OAny other significant area Experiments of concern Does the work involve any of these experiments of concern: No ODemonstrate how to render a vaccine ineffective O OConfer resistance to therapeutically useful antibiotics or antiviral agents OEnhance the virulence of a pathogen or render a nonpathogen virulent Oincrease transmissibility of a pathogen OAlter the host range of a pathogen OEnable evasion of diagnostic/detection modalities OEnable the weaponization of a biological agent or toxin OAny other potentially harmful combination of experiments and agents ChIP-sea Data deposition Confirm that both raw and final processed data have been deposited in a public database such as GEO. Confirm that you have deposited or provided access to graph files (e.g. BED files) for the called peaks.

Data access links

May remain nrivate hefore nuhlication

Files in database submission	
Genome browser session (e.g. UCSC)	
Methodology	
Replicates Sequencing depth	
Antibodies Peak calling parameters	
Data quality	
Software	
Flow Cytometry	
Plots Confirm that:	
☐The axis labels state the mark	ker and fluorochrome used (e.g. CD4-FITC).
_	ible. Include numbers along axes only for bottom left plot of group (a 'group' is an analysis of identical markers).
■All plots are contour plots wit	
	r of cells or percentage (with statistics) is provided.
Methodology	
Sample preparation	
Instrument	
Software	
Cell population abundance	
Gating strategy	
Tick this box to confirm that a	a figure exemplifying the gating strategy is provided in the Supplementary Information.
Magnetic resonance i	maging
Wagnetic resonance i	
Experimental design Design type	
Design specifications	
Behavioral performance measur	res
Acquisition	
Imaging type(s)	
Field strength	
Sequence & imaging parameters	s
Area of acquisition	
Diffusion MRI OUsed	ONot used
Preprocessing	
Preprocessing software	
Normalization	
Normalization template	
Noise and artifact removal	
Volume censoring	
Statistical modeling & inference	ence
Model type and settings	
Effect(s) tested	
Specify type of analysis:	

OWhole brain	OROI-based	OBoth			
Statistic type fo (See Eklund et					
Correction					
Function Graph a	ed in the study al and/or effective o	,			
Functional and	or effective conn	ectivitv			
Graph analysis					
Multivariate m	ndeling and predic	tive analysis			